

**Dehydration of Boric Acid for Thermochemical Energy
Storage purpose**

Catarina Maria Castilho Godinho

Thesis to obtain the Master of Science Degree in

Chemical Engineering

Supervisors: Prof. Franz Winter

Prof. Carlos Henriques

Examination Committee

Chairperson: Prof. Carla Isabel Costa Pinheiro

Supervisor: Prof. Carlos Manuel Faria de Barros Henriques

Members of Committee: Prof. José Manuel Félix Madeira Lopes

June 2018

Acknowledgements

I would like to start by expressing my profound acknowledgement to Professor Franz Winter for having received and welcomed me so well in his research group and especially for giving me the opportunity to develop my master thesis on such an important topic for the future.

I would also like to thank Saman Jahromy, Clemens Huber and Mudassar Azam for helping and supporting me whenever I had to, for the time and effort they had put into following the progress of my work, helping me with technical support, critics and suggestions.

To Florian Reschehofer for helping me in the experimental work with the TGA and Christoph Gasser for having helped me in all the research for an adequate analytical method, which was quite tricky, and in all the theories made to justify the results.

To my friend Joana Reis for having been on this trip with me and for being my support and family outside of Portugal.

To Carlos Henriques for accepting to guide this thesis and for helping me in the most challenging part that is writing all the ideas.

To my colleagues and friends that accompanied me throughout my journey at IST through the good and bad moments: Joana Silva, Marta Ferreira, Maria Naughton, Maria Dias, Mafalda Rodrigues, Susana Bento and Teresa Videira.

To my family, a big thank you for all the help and support, even being away, especially to my parents, Filomena e João Godinho, and my brother Pedro for having given me the opportunity to do my thesis outside Portugal.

Finally, I would like to thank my boyfriend Hugo for all the support, help and affection he gave me every day and mainly for always believing in me and not let me give up even in the most challenging times.

Abstract

Nowadays, energy storage is essential to cope with periods where the demand is bigger than supply. In this work, the impact of different parameters of the boric acid/boron oxide reverse reaction, especially the dehydration reaction, using pure and generated boric acid is studied. The goal is to determine the optimum temperature/time conditions that can be used in the dehydration reaction to achieve a conversion above 90%.

Simultaneous thermal analysis showed that the reaction occurs between 90°C and 400°C and that it can be divided into two parts. For the 1^o region, the activation energy and frequency factor are 132,2 kJ/mol and $1,89 \times 10^{15} \text{ s}^{-1}$, respectively.

Temperature, time, particle size and final appearance of the dehydration product were studied at two different pressures: At atmospheric pressure, the best results were achieved using 250°C, 10 minutes obtaining a conversion of $94,08 \pm 0,02\%$ and $91,57 \pm 0,02\%$ using pure and generated boric acid, respectively. At 175 mbar the best results were found at 250°C, 30 minutes obtaining a conversion of 96,2% and 90,2%, respectively. The results were confirmed with a quick rehydration test and Raman spectroscopy.

The main difference in using different pressures is in the final appearance of the product: a glassy solid at atmospheric pressure whereas at 175 mbar is a hard powder.

Although the conversion results do not appear to be influenced by the pressure, it has been found that during the rehydration tests the appearance of the dehydration product influences the reverse reaction. Concluding, the best results were found below atmospheric pressure.

Keywords

TCES, Dehydration, Boric acid, STA, Muffle Furnace, Evaporation device.

Resumo

Atualmente, o armazenamento de energia é essencial para lidar com períodos onde a procura é maior que a oferta. Neste trabalho, o impacto de diferentes parâmetros na reação reversível de ácido bórico/óxido de boro, especialmente na reação de desidratação, usando quer ácido bórico puro quer gerado, é estudado. O objetivo é determinar as condições ótimas de temperatura e tempo que podem ser usadas na reação de desidratação para obter uma conversão acima de 90%.

A análise térmica simultânea mostrou que a reação ocorre entre 90°C e 400°C e pode ser dividida em duas partes. Para a 1ª região, a energia de ativação e o fator de frequência são 132,2 kJ/mol and $1,89 \times 10^{15} s^{-1}$, respetivamente.

A temperatura, tempo de desidratação, tamanho de partícula e aparência final do produto da reação foram estudados a 2 pressões diferentes: À pressão atmosférica os melhores resultados foram obtidos a 250°C, 10 minutos, obtendo-se uma conversão de $94,08 \pm 0,02\%$ e $91,57 \pm 0,02\%$ usando ácido bórico puro e gerado, respetivamente. A 175 mbar os melhores resultados foram obtidos a 250°C, 30 minutos, obtendo-se uma conversão de 96,2% e 90,2%, respetivamente. Os resultados da conversão foram confirmados com um teste de hidratação e espectroscopia Raman.

A principal diferença em usar diferentes pressões está na aparência final do produto: um sólido vítreo à pressão atmosférica, enquanto que a 175 mbar se obtém um pó.

Embora os resultados de conversão não pareçam ser influenciados pela pressão, verificou-se que durante os testes de hidratação a aparência do produto de desidratação influencia a reação inversa. Assim, concluiu-se que os melhores resultados foram encontrados a 175 mbar.

Palavras-chave

TCES, Dehydration, Boric acid, STA, Muffle Furnace, Evaporation device.

Table of Contents

| | |
|--|-----------|
| Acknowledgements | v |
| Abstract..... | vii |
| Resumo | viii |
| Table of Contents..... | ix |
| List of Figures | xi |
| List of Tables..... | xiii |
| List of Acronyms | xiv |
| List of Symbols..... | xv |
| 1 Introduction | 1 |
| 1.1 Overview..... | 2 |
| 1.1.1 Energy | 2 |
| 1.1.2 Thermal energy storage | 3 |
| 1.2 Motivation and Contents | 7 |
| 2 Background and concepts about TCES..... | 9 |
| 2.1 TCES..... | 10 |
| 2.1.1 General introduction | 10 |
| 2.2 System boric acid/boron oxide..... | 11 |
| 2.2.1 Thermodynamic concepts | 11 |
| 2.2.2 Dehydration | 14 |
| 2.2.3 Boric acid properties | 16 |
| 2.2.4 Boron oxide properties | 19 |
| 2.3 State-of-the-art | 20 |
| 2.3.1 Introduction | 20 |
| 2.3.2 Problematics | 23 |
| 2.3.3 Reactors type..... | 23 |
| 3 Experimental set-up | 27 |

| | | |
|-------|-------------------------------------|----|
| 3.1 | Aim | 28 |
| 3.2 | Test Rigs | 28 |
| 3.2.1 | Methodology | 28 |
| 3.2.2 | Macroscopic TGA | 29 |
| 3.2.3 | Simultaneous thermal analyser | 33 |
| 3.2.4 | Muffle furnace | 34 |
| 3.2.5 | Evaporation device | 35 |
| 4 | Test results and discussion | 37 |
| 4.1 | Experiments and results | 38 |
| 4.1.1 | Macroscopic TGA | 39 |
| 4.1.2 | Simultaneous thermal analyser | 43 |
| 4.1.3 | Muffle furnace | 49 |
| 4.1.4 | Evaporation device | 56 |
| 5 | Analysis methods | 61 |
| 5.1 | Introduction | 62 |
| 5.1.1 | Rehydration tests | 62 |
| 5.1.2 | Chemical analysis methods | 67 |
| 6 | Conclusions | 75 |
| 6.1 | Conclusions | 76 |
| 6.2 | Future work | 79 |
| | Annex A. | 81 |
| | References | 94 |

List of Figures

| | |
|--|----|
| Figure 1.1: World total primary energy consumption from 1980-2015..... | 2 |
| Figure 1.2: World's energy consumption in 2016 by source. | 3 |
| Figure 1.3: Classification of thermal energy storage systems (Adapted from [10]). | 3 |
| Figure 1.4: Processes involved in a thermochemical energy storage cycle. (Adapted from [7]) .. | 5 |
| Figure 2.1: Simplified scheme of TCES based on chemical reactions[4]. | 10 |
| Figure 2.2: B_2O_3 -water system [34]. | 16 |
| Figure 2.3: Solubility of boric acid in water..... | 17 |
| Figure 2.4: Boric acid >99,8% from <i>Carl Roth</i> | 18 |
| Figure 2.5: Solubility of Boron oxide [30]..... | 19 |
| Figure 3.1: Methodology..... | 29 |
| Figure 3.2: TGA apparatus..... | 30 |
| Figure 3.3: Reactor used in the TGA apparatus..... | 30 |
| Figure 3.4: Buoyancy effect..... | 31 |
| Figure 3.5: Simultaneous thermal analyser used (left) and a detail of its scale (right). | 34 |
| Figure 3.6: Temperature program controller (left) and muffle furnace (right)..... | 35 |
| Figure 3.7: Evaporation device..... | 36 |
| Figure 4.1: Mass and temperature variation over time in experiment 1. | 40 |
| Figure 4.2: Mass loss over temperature for experiment 1..... | 40 |
| Figure 4.3: Mass and temperature variation over time in experiment 2..... | 41 |
| Figure 4.4: Mass loss over temperature inside the reactor for experiment 2..... | 41 |
| Figure 4.5: Appearance of the final product..... | 42 |
| Figure 4.6: TGA and DTG for a heating rate of 2 K/min..... | 44 |
| Figure 4.7: DSC signal for a heating rate of 2 K/min..... | 44 |
| Figure 4.8: Coats-Redfern method used for the dehydration of boric acid..... | 47 |
| Figure 4.9: Conversion evolution over temperature, using the same dehydration time..... | 49 |
| Figure 4.10: Conversion over time at different temperatures and dehydration time..... | 50 |
| Figure 4.11: Ceramic crucible after the dehydration reaction..... | 51 |
| Figure 4.12: Heating rate for the experiment between 160°C and 250°C..... | 51 |
| Figure 4.13: the General look at the product after dehydration below 300°C..... | 53 |
| Figure 4.14: Dehydration for 10 min at 350°C..... | 53 |
| Figure 4.15: Generated BA after drying process..... | 54 |
| Figure 4.16: BO after dehydration reaction, using generated BA..... | 54 |
| Figure 4.17: Results of the dehydration reaction below atmospheric pressure..... | 58 |
| Figure 4.18: Difference between sheer boric acid(left) and generated boron oxide (right)..... | 58 |
| Figure 4.19: Boron oxide after dehydration with generated boric acid..... | 59 |
| Figure 5.1: Methodology used for the analysis methods..... | 62 |
| Figure 5.2: Rehydration test rig..... | 63 |
| Figure 5.3: Calibration line for 7 mL of water, at 23,9°C ($\alpha\% = 0,5876Q + 0,3780$, $R_2 = 1$) | 64 |
| Figure 5.4: Water temperature variation over time..... | 65 |
| Figure 5.5: Water temperature variation during the 60 seconds of the experiment..... | 65 |
| Figure 5.6: Rehydration of boron oxide produced in the muffle furnace (left) and in the evaporation | |

| | |
|---|----|
| device (right) using 7 mL of water..... | 66 |
| Figure 5.7: Rehydration of boron oxide produced with pure boric acid..... | 66 |
| Figure 5.8: Rehydration of boron oxide produced with generated boric acid..... | 67 |
| Figure 5.9: Comparison between pure boric acid, pure metaboric acid and pure boron oxide. . | 70 |
| Figure 5.10: Generated boric acid dried under different drying conditions. | 70 |
| Figure 5.11: Final product from muffle furnace, produced with pure boric acid. | 71 |
| Figure 5.12: Final product from muffle furnace, produced with generated boric acid. | 71 |
| Figure 5.13: Final product from evaporation device, produced with pure boric acid. | 72 |
| Figure 5.14: Final product from evaporation device, produced with generated boric acid. | 73 |
| Figure 7.1: Boric acid/boron oxide enthalpy of reaction at atmospheric pressure. | 82 |
| Figure 7.2: Relative humidity at the inlet and outlet over time for experiment 1. | 85 |
| Figure 7.3: Relative humidity at the inlet and outlet over temperature for experiment 1. | 85 |
| Figure 7.4: Relative humidity at the inlet and outlet over time for experiment 2. | 86 |
| Figure 7.5: Relative humidity at the inlet and outlet over temperature for experiment 2. | 86 |
| Figure 7.6: TG and DTG for a heating rate of 4 K/min (mass loss of -41,89%). | 87 |
| Figure 7.7: DSC signal for a heating rate of 4 K/min..... | 87 |
| Figure 7.8: TG and DTG for a heating rate of 8K/min (mass loss of -44,04%). | 88 |
| Figure 7.9: DSC signal for a heating rate of 8 K/min..... | 88 |
| Figure 7.10: Differential granulometric composition curve. | 93 |

List of Tables

| | |
|--|----|
| Table 1.1: Comparison of thermal energy storage systems [4], [7], [18], [19]. | 6 |
| Table 2.1: Comparison between TCES systems. | 11 |
| Table 2.2: Data used in reaction enthalpy calculation, at different temperatures [28],[31]. | 13 |
| Table 2.3: Melting temperatures of crystalline boric acid, metaboric acid and boron oxide [34]. | 15 |
| Table 2.4: Solubility of boric acid in other compounds. | 17 |
| Table 2.5: Properties of H_3BO_3 . | 18 |
| Table 2.6: Properties of B_2O_3 . | 19 |
| Table 2.7: Comparison between the fluidised bed and rotary kiln reactor [57]. | 25 |
| Table 4.1: Data used in STA. | 43 |
| Table 4.2: R^2 values for different reaction orders using the C-R method. | 47 |
| Table 4.3: Results of kinetic analysis using the C-R method. | 48 |
| Table 4.4: Dehydration results in the optimum conditions of temperature and dehydration time. | 51 |
| Table 4.5: Conditions used to dry generated BA. | 54 |
| Table 4.6: Dehydration conversion for the optimum conditions using generated BA. | 54 |
| Table 4.7: Energy density values the bests temperature/time conditions. | 56 |
| Table 4.8: Dehydration results in the optimum conditions of temperature and dehydration time. | 57 |
| Table 4.9: Dehydration results in the optimum conditions using generated boric acid. | 59 |
| Table 4.10: energy density values the bests temperature/time conditions. | 60 |
| Table 5.1: Rehydration tests of pure boron oxide. | 63 |
| Table 7.1: Enthalpy variation from atmospheric pressure to 175 mbar. [77] | 82 |
| Table 7.2: Propagation of uncertainty. | 83 |
| Table 7.3: Dehydration conversion relative error, calculated for the best temperature and time conditions found. | 83 |
| Table 7.4: Rehydration conversion relative error, calculated for the best temperature and time conditions found. | 84 |
| Table 7.5 Values to calculate dehydration conversion in experiments of 10 minutes. | 88 |
| Table 7.6: Values to calculate dehydration conversion. | 89 |
| Table 7.7: Values to calculate rehydration conversion. | 89 |
| Table 7.8: Particle size influence on conversion. | 90 |
| Table 7.9: Values to calculate dehydration conversion below atmospheric pressure. | 91 |
| Table 7.10: Values to calculate rehydration conversion. | 91 |
| Table 7.11: Particle size influence in evaporation device. | 92 |

List of Acronyms

| | |
|------|---|
| TES | Thermal Energy Storage |
| SHS | Sensible Heat Storage |
| LHS | Latent Heat Storage |
| TCES | Thermochemical Energy Storage |
| PCM | Phase Change Material |
| GHS | Globally Harmonized System |
| CLP | Classification Labelling and Packaging |
| SDS | Safety Data Sheet |
| BA | Boric Acid |
| BO | Boron Oxide |
| TGA | Thermogravimetric Analyser/ analysis |
| TG | Thermogravimetric |
| DTA | Differential Thermal Analyser |
| STA | Simultaneous Thermal Analyser/analysis |
| DTG | Differential Thermogravimetric Analysis |
| DSC | Differential Scanning Calorimetry |
| TBA | Triclinic Boric Acid |
| HBA | Hexagonal Boric Acid |
| R&D | Research And Development |
| XRD | X-ray Diffraction |
| NMR | Nuclear Magnetic Resonance |
| C-R | Coats-Redfern Method |

List of Symbols

| | |
|----------------------|--|
| H_3BO_3 | Boric acid |
| B_2O_3 | Boron oxide |
| H_2O | Water |
| $HBO_2 - III, II; I$ | Metaboric acid modifications |
| Q | Heat stored |
| m_i | Mass of a compound i |
| $c_{p,i}$ | Specific heat of a material i |
| ΔH_{latent} | Heat of phase change |
| ΔH_R | Enthalpy of reaction |
| n_A | number of moles of a compound A |
| $\Delta H_{f,i}$ | Enthalpy of formation of a compound i |
| v_i | Stoichiometric factor of a compound i |
| $H_{f,i}^\circ$ | Standard enthalpy of formation of a compound i |
| T | Temperature ($^\circ\text{C}$) |
| T° | Standard temperature (25°C) |
| ΔH_i^f | Enthalpy of fusion of a compound i |
| ΔH_i^{vap} | Enthalpy of vaporisation of a compound i |
| $T_{equilibrium}$ | Equilibrium Temperature |
| T_f | Fusion point |

| | |
|-----------------|--|
| T_b | Boiling point |
| R | Universal gas constant |
| MM_i | Molar mass of a compound i |
| A | Coefficient value for specific heat calculation in $\frac{J}{mol \cdot K}$ |
| B | Coefficient value for specific heat calculation in $\frac{J}{mol \cdot K^2}$ |
| C | Coefficient value for specific heat calculation in $\frac{J \cdot K}{mol}$ |
| D | Coefficient value for specific heat calculation in $\frac{J}{mol \cdot K^3}$ |
| ΔH_{vb} | Enthalpy of vaporisation at the normal boiling point |
| x | Conversion of the dehydration reaction |
| Δm | Mass difference |
| ω_{H_2O} | Water content |
| E_ρ | Energy density |
| ρ_i | Density of a compound i |
| k | Constant rate |
| n | Reaction order |
| k_0 | Frequency factor |
| q | Heating rate |
| E_a | Activation energy |
| α | Conversion of the rehydration reaction |
| cp_{mix} | Heat capacity of the mixture |
| ΔT | Temperature variation |
| $f(T_2(0))$ | Density of the air at the beginning of the experiment (23°C) |

| | |
|------------------------|--|
| $f(T_2(t))$ | Density of the air inside the lower heating room at a time t |
| $V_{reactor}$ | Volume of the reactor |
| $f(T(n))$ | Density at a time n where T_2 and T_5 are equal |
| $f(T_5(n)), f(T_2(n))$ | Density at the point n for the nitrogen in the reactor and air in the lower heating room |
| $f(T_5(t))$ | Density of the nitrogen in the reactor at a time t |
| $f(T_2(t))$ | Density of the air in the lower heating room at a time t |
| W_i | Weight of a sieve tray i after sieving analysis |
| W_{total} | Total weight of all sieves trays after sieving analysis |

Chapter 1

Introduction

This chapter gives a brief overview of the work. Before defining work targets, the scope and motivations are brought up.

1.1 Overview

1.1.1 Energy

Nowadays energy is an integral part of the economic growth, social and environmentally sustainable development, mostly due to the increase of worldwide human population, technological development and industrialisation of the modern society. Figure 1.1 shows this increase in the world energy consumption since 1980 in quadrillion British Thermal Units (1 BTU= 1055,056J) [1] and Figure 1.2 shows the energy consumption by source in 2016 [2]. According to Figure 1.2, fossil fuel, that is a finite resource, is the conventional primary energy used and nowadays the social demand is much higher than the reserves. Once the energy consumption of conventional primary energy is way higher than the supply, the new sources of energy (renewable energy like solar energy, geothermal or wind energy) become more important, as well as the recycling of waste heat in factories to reduce the energy costs. The use of renewable energy is essential today to decrease the energy crisis that the world is facing due to the fossil resources consumption, and to reduce the carbon dioxide emissions, responsible for the greenhouse effect and environmental pollution. Nevertheless, these renewable sources of energy are time-dependent, non-uniform distributed and intermittent which narrow the large-scale utilisation [3]–[6]. In all, it is mandatory a change in the energy system and the best solution to improve the energy efficiency, storing the surplus energy and avoiding, at the same time, environmental problems is to develop a Thermal Energy Storage (TES) system [7].

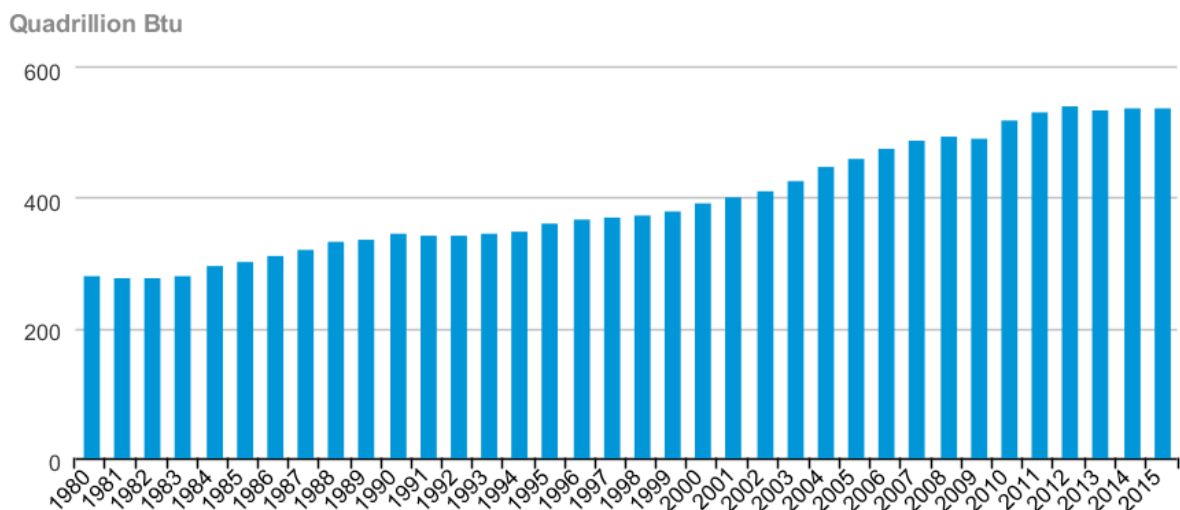


Figure 1.1: World total primary energy consumption from 1980-2015.

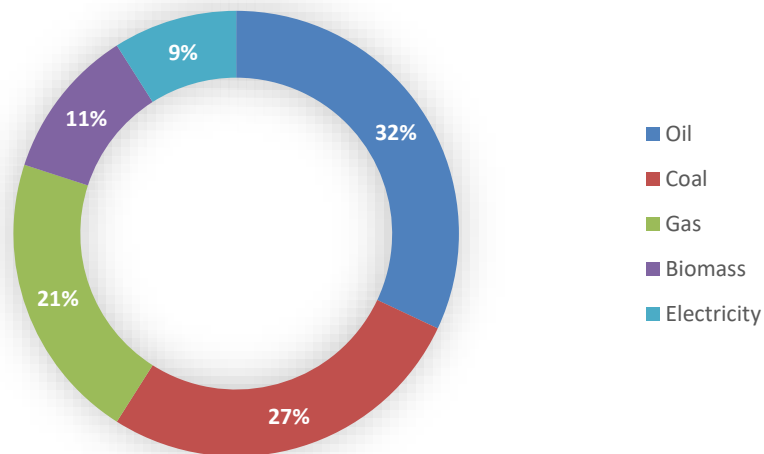


Figure 1.2: World's energy consumption in 2016 by source.

1.1.2 Thermal energy storage

TES is defined as the temporary holding of thermal energy in the form of cold or hot substances for later use [8]. With energy storage, the difference between supply and demand can be reduced because it is possible to store energy for periods where the energy demand is higher than the supply. This stored energy can be used, for example in houses, for building comfort applications or in industry. TES have been proved to be efficient and financially viable, and there are three different ways to store energy, present in Figure 1.3: Sensible Heat Storage (SHS), Latent Heat Storage (LHS) and Thermochemical Energy Storage (TCES). Nevertheless, some ways to store energy have not been yet exploited sufficiently [9].

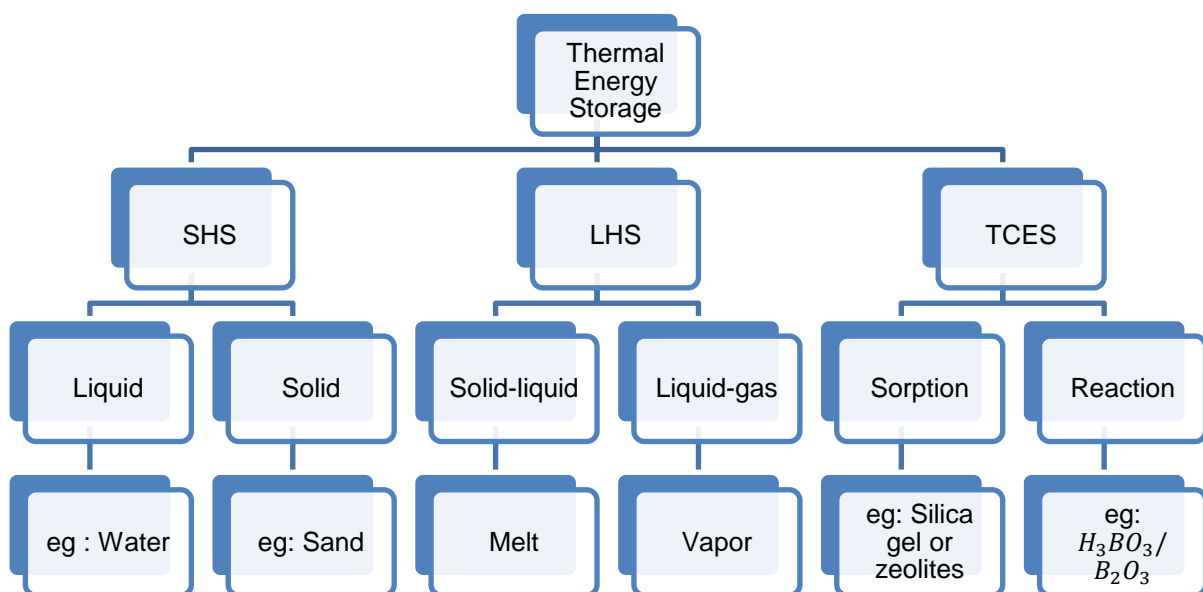


Figure 1.3: Classification of thermal energy storage systems (Adapted from [10]).

Sensible Heat Storage

On SHS, thermal energy can be stored or released by changing the temperature of the storage materials, which can be, for example, water ($T < 100^\circ\text{C}$), molten nitrate salts or rocks ($100\text{-}800^\circ\text{C}$). During the heat storage, the storage medium increases its energy content while during the release, the energy content decreases [11]–[13]. The thermal energy stored by sensible heat can be expressed as

$$Q_{[kJ]} = m_{[kg]} \int_{T_1}^{T_2} c_{p,i} [kJ/kg \cdot K] dT_{[K]} \quad (1.1)$$

Where m is the mass of material, $c_{p,i}$ is the specific heat of a material i and dT the integrated temperature between the temperature of the storage medium T_2 and the surrounding T_1 . It should be noted that the amount of stored heat is proportional to the density, specific heat, volume, and temperature variation of the storage medium [8].

More than 90% of all TES processes used in a wide range of applications are sensible heat storage processes. This technology has been applied for a long time, being the most mature technology, because it is the more accessible and cheapest method to store energy. It has been implemented and evaluated among many large-scale residential applications and industrial applications for example in concentrated solar power and other industrial processes. However, SHS has low thermal capacity making it necessary to install large size storage devices that need insulation due to heat losses [3],[10].

Latent Heat Storage

In this method, the heat is stored while changing phase, i.e. the heat stored is associated with a Phase Change Material (PCM). The heat storage happens, theoretically, at constant temperature and with no differences in material's chemical composition because the heat that is given is only to change the phase of the material and not to increase its temperature. This heat is called heat of phase change or latent heat of a material (ΔH_{latent}) and is used to calculate the heat that can be absorbed by a PCM (equation 1.2).

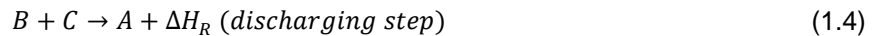
$$Q_{[kJ]} = m_{[kg]} \Delta H_{latent} [kJ/kg] \quad (1.2)$$

PCMs usually can be melt or freeze at a suitable phase change temperature range and are mostly chosen based on cost and stability during long periods. The best PCM known and most used is water, but it can also be used salt solutions or paraffin [14]. PCMs are used in the industry, for example, sodium acetate trihydrate also known as "hand warmer", and are usually packed in tubes, ceilings or wall boards in three different shapes (powder, granulate or board) [7]. This process usually carries also sensible heat storage before and after the phase change process.

Usually, LHS present higher energy density and smaller storage sizes compared to sensible heat storage. However, the properties of PCM will degrade after the reduplicative cycle. In all, the problems with this technology, as well as sensible heat storage, are the low energy density, failure in long-term heat storage and the need of insulation use.

Thermochemical energy storage

There are two types of TCES, chemical sorption (adsorption and absorption) and the chemical reaction, that can be employed to generate heat. When looking at literature information regarding TCES, not always this distinction is made like this [9]. Nevertheless, these two types of TCES are based on the same principle: an appropriate complete and reversible reaction (equation 1.3 and 1.4), where ΔH_R is the enthalpy of reaction.



The difference is that while in chemical sorption energy storage there is no change in the molecular configuration of the compound, in a chemical reaction energy storage, molecular configurations change. Concerning the application field, on the one hand, sorption is mainly used for building applications (to store low- <100°C- or medium grade heat from - 100 to 400°C)[15], such as in space heating and hot water supply using, for example, salt hydrates like zeolites as adsorbents. On the other hand, chemical reaction energy storage is used not only to store heat in regular houses but can also be used to store thermal energy at high temperatures for industrial processes [9],[16].

The energy is stored or released by breaking or reforming the chemical bonds. It involves at least three steps: charging step, storage and discharging (Figure 1.4).

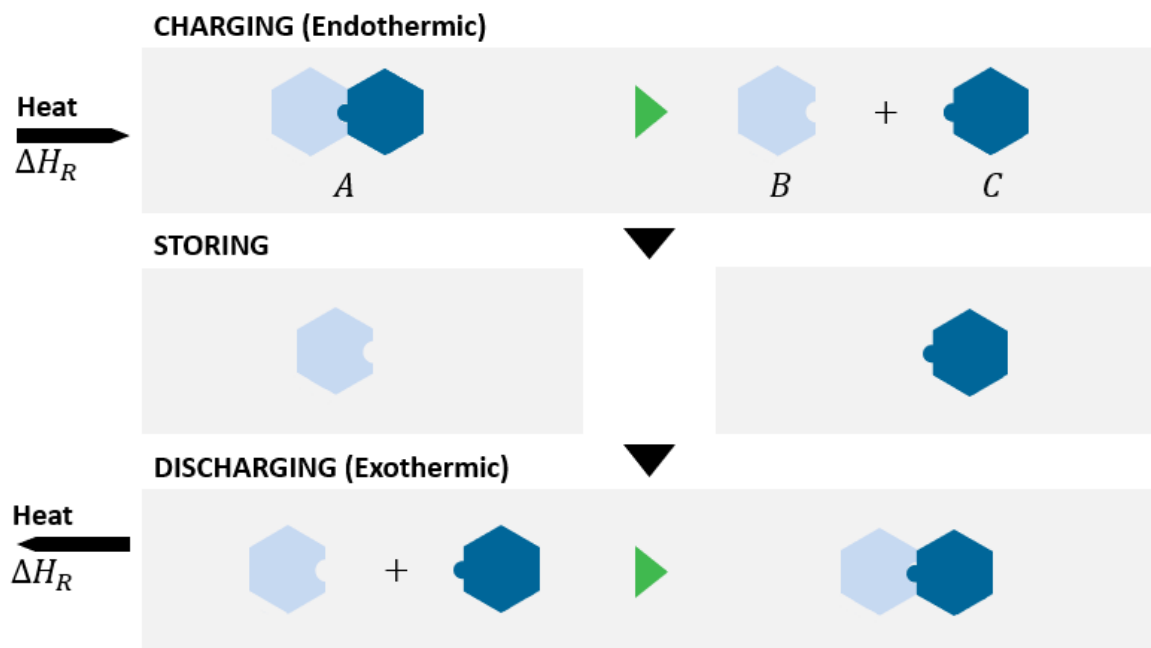


Figure 1.4: Processes involved in a thermochemical energy storage cycle. (Adapted from [7])

In the charging step or dehydration reaction, thermal energy is used to dissociate a chemical reactant **A** into two products, **B** and **C**. The heat is stored/absorbed during the endothermic reaction and the products produced are stored in separate with almost no heat loss at ambient temperature as long as

desired and until the discharging step or rehydration reaction is forced. In this last step, the products B and C are mixed to generate the initial reactant A, while releasing heat in an exothermic reaction [7].

The energy stored in a thermochemical material can be expressed as

$$Q_{[kJ]} = n_{A[mol]} \Delta H_{R[kJ/mol]} \quad (1.5)$$

The primary advantage of TCES is the energy density, approximately 8-10 times higher energy density over SHS and two times higher over LHS [5],[6] allowing large quantities of energy to be stored in small amounts of storage substances. The other advantage is its long-term storage duration without heat losses or need of insulation [3],[17].

Table 1.1 presents the comparison of the three thermal energy storage systems, which show that the thermochemical energy storage is the best technology to store energy.

Table 1.1: Comparison of thermal energy storage systems [4], [7], [18], [19].

| | SHS system | LHS system | TCES System |
|----------------------------|--|--|--|
| Energy density | Small $\sim 180 \text{ MJ}/\text{m}^3$ of material E.g., water $\Delta T=50^\circ\text{C}$ $206 \text{ MJ}/\text{m}^3$ | Medium $\sim 360 \text{ MJ}/\text{m}^3$ of material E.g., $\text{MgCl}_2, \text{KCl}, \text{NaCl}$ $997,2 \text{ MJ}/\text{m}^3$ | High $\sim 1800 \text{ MJ}/\text{m}^3$ of material |
| Insulation | Yes | Yes | No |
| Storage temperature | Charging step temperature | Charging step temperature | Ambient temperature |
| Storage period | Limited due to thermal losses | Limited due to thermal losses and cycling stability | Unlimited |
| Transportability | Normally not | Short distances | Distance theoretically unlimited |
| Heat losses | Depend on the degree of insulation. Long-term storage is only possible with large scale storage | Depend on the degree of insulation. Long-term storage is only possible with large scale storage | No heat losses |

| | | | |
|-------------------|------------------|---|------------------------------|
| Maturity | Industrial Scale | Pilot Scale | Laboratory Scale |
| Technology | Quite simple | Medium/ available for some temperatures | Complex |
| Price | Low | Medium | Extremely high capital costs |

1.2 Motivation and Contents

As previously referred, it is especially important nowadays try to change the fossil fuel consumption for renewable sources of energy. Since renewable sources of energy are mostly seasonal, it is necessary to store the energy for later use. Without this concept, renewable energy could only be used at the moment and according to world's demand. For example, when the supply is bigger than the demand in a solar plant during summer ($> 300^{\circ}\text{C}$), if this concept of energy storage did not exist, the solar heat plant will shut down, and the surplus heat would not be used. Moreover, it is more economical to store thermal energy than electricity [20]. The energy storage concept can also be used to capture the waste energy of existing plants or even for technological applications. In these cases, the heat that is not converted into electricity or reintegrated into the process due to their low-temperature range can be stored for later use in the plant, improving their efficiency and reducing the energy costs [19], [21]. Besides that, this concept can also be used in houses, for hot water production, space heating or greenhouse heating, allowing that this stored energy can be used during the months where there is not much sunlight.

Within all possibilities for energy storage stated in 1.1.2, which are being used to solve these problems mentioned, TCES seems to be the best option to do it, especially in long-term heat storage cases. Since TCES seems so promising but there is still not much research on the subject comparing to other TES systems, and the research that exists is not yet been tested on an industrial scale, it is imperative to continue to improve this research [9], [22].

This master thesis will continue the work done in this field, especially the work done by Thomas Karel [19] but focused on the dehydration step of the reaction. This thesis consists of 6 chapters, including the present one, and a group of appendixes. Chapter 2 starts by introducing some basic concepts about TCES and its current State-of-the-Art. Chapter 3 presents the aim of this master thesis, the work methodology used and the description of the dehydration test rigs. Chapter 4 explains and discusses the results of what has been done in each test rig. Chapter 5 presents some methods of chemical analysis tested to analyse the content of the final dehydration product and, finally, Chapter 6 summarises conclusions and point out aspects to be developed in future works.

Chapter 2

Background and concepts about TCES

This chapter presents some basic concepts about TCES and the current State-of-the-Art.

2.1 TCES

An important concept of energy storage is the heat storage capacity, that is, the amount of energy that material or system can supply in particular conditions and through a specific procedure. This parameter can be defined based on volume (kWh/m^3 or MJ/m^3) or on mass (kWh/kg or MJ/kg) and it is called energy storage density, according to references [2],[23] or energy density and specific energy, respectively, according to [24].

In this master thesis, heat storage capacity will be presented based on volume with the name “energy density”.

2.1.1 General introduction

Different criteria are required to develop an efficient, reliable and profitable TCES system [3],[9],[25]:

1. Reversible reaction without secondary reactions and with cycling stability;
2. High energy density;
3. Extended storage time, practically without heat losses;
4. High final conversion;
5. The reaction products should be easily separated and stably stored;
6. The reactants and products of the reaction must be non-toxic, non-corrosive, non-flammable and non-explosive;
7. Small volume variation during the reaction;
8. High availability of material at low cost.

Briefly, the essential thing in a TCES system is the reversibility of the reaction, as mentioned earlier. This property allows the storage of heat in the endothermic step of the reaction and the release of the same heat in the exothermic step.

Figure 2.1 represents a simplified schematic of a TCES system.

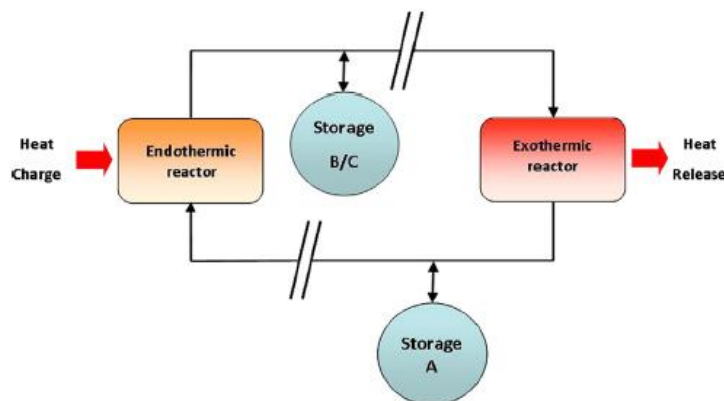


Figure 2.1: Simplified scheme of TCES based on chemical reactions[4].

Researchers have been studying some reversible reactions for TCES purpose. These system pairs can be observed in Table 2.1 as well as the enthalpy of the reaction and the energy density associated with the dehydration reaction.

Table 2.1: Comparison between TCES systems.

| Material | $T_{equilibrium}$ [°C] | ΔH_R [kJ/mol] | Energy Density [MJ/m ³] | Source |
|------------------|---|--|---|---------------|
| H_3BO_3/B_2O_3 | 157,5 | 192,2 | 2238 | [19] |
| $Ca(OH)_2 / CaO$ | 505 | 112 | 1310 | [26] |
| MnO_2/Mn_2O_3 | 530 | 42 | 1210 | |
| $CaCO_3/CaO$ | 896 | 167 | 407 | |

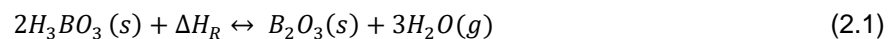
It is possible to see that the H_3BO_3/B_2O_3 system presents higher values of energy density, using low temperature. For that reason and for complying with all the conditions cited in 2.1.1, previous tests showed that the system boric acid / boron oxide system has a big potential as storage medium within the range of low temperature energy storage (0 to 120°C), and a great chance for future technological usages [19], producing temperatures in the range of 50-100°C [27].

2.2 System boric acid/boron oxide

The system that is proposed to study in this master thesis is the Boric Acid (BA)-Boron Oxide (BO) system, more precisely the dehydration step of this reversible reaction.

2.2.1 Thermodynamic concepts

The boric acid/boron oxide reaction, a gas-solid reaction, is shown in equation 2.1.



The direct reaction is called charging step, where the dehydration of BA (H_3BO_3) occurs forming BO (B_2O_3) and it is an endothermic reaction. The reverse reaction is called discharging step where the rehydration of boron oxide to form boric acid again occurs and it is an exothermic reaction. ΔH_R is the enthalpy of the reaction, also known as the energy that is stored in the charging step and it can be calculated through enthalpies of formation ($\Delta H_{f,i}$) of reactants and products multiplied by the

stoichiometric factor (v_i) of the respective compound (equation 2.2).

$$\Delta H_R [kJ/mol] = \sum v_i \Delta H_{f,i} [kJ/mol] \quad (2.2)$$

For the present reaction, ΔH_R is calculated according to equation 2.3.

$$\Delta H_R [kJ/mol] = \Delta H_{f,B_2O_3} [kJ/mol] + 3\Delta H_{f,H_2O} [kJ/mol] - 2\Delta H_{f,H_3BO_3} [kJ/mol] \quad (2.3)$$

The enthalpy of the reaction changes with temperature and pressure. To calculate the enthalpy of reaction at isobaric conditions but at a different temperature than the standard conditions (25°C and 1 atm), it is possible to use equation 2.4 to calculate the enthalpy of formations of the compounds at a specific temperature ($\Delta H_{f,i}(T)$).

$$\Delta H_{f,i}(T) [kJ/mol] = H_{f,i}^o [kJ/mol] + \int_{T^o}^T c_{p,i} [kJ/mol \cdot K] dT [K] \quad (2.4)$$

Where:

- $H_{f,i}^o$ - standard enthalpy of formation of a compound i ;
- $c_{p,i}$ - heat capacity of a compound i ;
- T^o - standard temperature (25°C);
- T - final temperature.

This equation is valid only for materials that do not change its phase. In this reaction, boric acid changes typically its phase at 170,9°C and 300°C (see Table 2.5). So, to calculate $\Delta H_{f,i}(T)$, the heat to change the phase of the material needs to be added in equation 2.4, that is, the enthalpy of fusion and the enthalpy of vaporization, resulting in equation 2.5.

$$\Delta H_{f,i}(T) [kJ/mol] = H_{f,i}^o + \int_{T^o}^{T_f} c_{p,i} dT + \Delta H_i^f + \int_{T_f}^{T_b} c_{p,i} dT + \Delta H_i^{vap} + \int_{T_b}^T c_{p,i} dT \quad (2.5)$$

Where:

- ΔH_i^f - enthalpy of fusion of a compound i ;
- ΔH_i^{vap} - enthalpy of vaporization of a compound i ;
- T_f - fusion point;
- T_b - boiling point.

The enthalpy of fusion can be found in *HSC Chemistry* [28]. However, no data were found for enthalpy of vaporisation. Therefore, the value of the enthalpy of vaporisation for normal boiling point was estimated using the *Vetere* method [29].

$$\Delta H_{vb} [\text{kJ/mol}] = R_{[\text{kJ/mol}\cdot\text{K}]} T_b [\text{K}] \left[A + B \ln T_b + \frac{C T_b^{1,72}}{MM_i [\text{kg/kmol}]} \right] \quad (2.6)$$

Where:

- ΔH_{vb} - enthalpy of vaporization at the normal boiling point ($T=T_b$ and $P=1$ atm);
- R - perfect gas constant;
- A, B, C - constants. $A=4,542$; $B=0,840$; $C=0,00352$;
- MM_i - molar mass of boric acid.

Regarding specific heat calculations ($c_{p,i}$), which are used for equation 2.4 and 2.5, equation 2.7 is used.

$$c_{p,i} [\text{J/mol}\cdot\text{K}] = A_{[\text{J/mol}\cdot\text{K}]} + B_{[\text{J/mol}\cdot\text{K}^2]} 10^{-3} T_{[\text{K}]} + C_{[\text{J}\cdot\text{K/mol}]} 10^5 T^{-2}_{[\text{K}]} + D_{[\text{J/mol}\cdot\text{K}^3]} 10^{-6} T^2_{[\text{K}]} \quad (2.7)$$

A, B, C and D are constant values that change the compound and its temperature range and can be found in *HSC Chemistry database* [28].

In Table 2.2 there are the data used to calculate the enthalpy of formation of the various compounds.

Table 2.2: Data used in reaction enthalpy calculation, at different temperatures [28],[31].

| Compound | $\Delta H_{f,i}^\circ$ [kJ/mol] | A [$\frac{\text{J}}{\text{mol}\cdot\text{K}}$] | B [$\frac{\text{J}}{\text{mol}\cdot\text{K}^2}$] | C [$\frac{\text{J}\cdot\text{K}}{\text{mol}}$] | D [$\frac{\text{J}}{\text{mol}\cdot\text{K}^3}$] | T_{min} [K] | T_{max} [K] |
|---------------|------------------------------------|---|---|---|---|------------------|------------------|
| $H_3BO_3 (s)$ | -1093,99 | 3,775 | 276,168 | 0,233 | -3,551 | 298,15 | 444,15 |
| $H_3BO_3 (l)$ | 22,301 | 179,996 | 0 | 0 | 0 | 444,15 | 800 |
| $H_3BO_3 (g)$ | 62,1226 | 38,835 | 165,163 | -9,423 | -83,874 | 298,15 | 600 |
| | | 99,06 | 37,25 | -49,5 | -7,051 | 600 | 2100 |
| $B_2O_3 (s)$ | -1271,90 | 64,159 | 64,597 | -18,365 | 0,033 | 298,15 | 723 |
| $H_2O (g)$ | -241,826 | 28,408 | 12,477 | 1,284 | 0,360 | 298,15 | 1100 |

The reaction enthalpy at standard conditions is 190,6 kJ/mol, and the reaction enthalpy at various temperatures can be found in the A.1.

Once the enthalpy of reaction is needed for calculations below atmospheric pressure (~175 mbar), the enthalpy of reaction value at atmospheric pressure needs to be correct. The enthalpy of the solids is practically not affected by the pressure, but the enthalpy of the gases is. Thus, as only the water at the

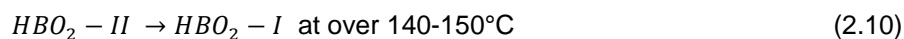
end of the reaction is in the gas phase, the enthalpy variation of the water is calculated to 175 mbar, for each temperature needed. These values were then used to correct the enthalpy of the reaction. The values can be seen in A.1.

2.2.2 Dehydration

As mentioned before, this master thesis will focus only on the energy storage, that is the dehydration of boric acid. To efficiently use the boric acid/boron oxide reaction to store energy there are two essential things to know first, concerning the steps of the reaction and the melting temperatures of the compounds involved in the reaction.

Steps of dehydration

Boric acid converts via metaboric acid to produce boron oxide, due to the loss of free water (moisture) as well as combined water (-OH bonds), according to four step reactions at different temperatures (equation 2.8 to 2.11). These temperatures are inconsistent throughout the literature and only [32] refers the temperature of 80°C as the beginning of dehydration while other literature [33] refers around 100°C as the beginning of the dehydration and [34],[35] mention around 130°C.



The metaboric acid has three different crystal modifications with different properties that occur before the production of boron oxide [35]–[37]:

- Orthorhombic metaboric acid or HBO₂-III;
- Monoclinic metaboric acid or HBO₂-II;
- Cubic metaboric acid or HBO₂-I.

HBO₂-III has molecular form, consisting of discrete trimers and very similar to boric acid structure, while the others have polymeric structure. The structures of HBO₂-II and HBO₂-I look like its precursor except that the rings are connected, and 1/3 of the boron centres are tetrahedral [38].

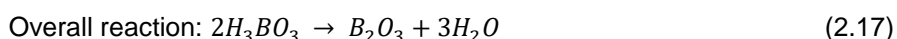
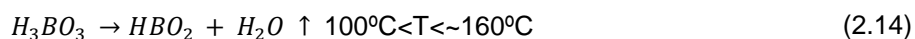
When pure boric acid is dehydrated in open vessels at about 80°C, the dehydration product first is a crumbly crystal of HBO₂-III blended with unconverted H₃BO₃. When the temperature rises, H₃BO₃ slowly disappears and HBO₂-III recrystallises to HBO₂-II. At this stage, the dehydration stops sharply at the composition HBO₂-I unless the time is excessive, or the temperature rises above 150°C. Under these conditions, the dehydration continues slowly, forming a highly viscous liquid (pasty melting state) with a composition between HBO₂-I and B₂O₃ [27],[34],[35]. It is important to refer that the temperatures described in equations 2.8 to 2.11 were for pure compounds. The raw material purity affects the reaction

temperature range so the reaction from 2.9 to 2.11 can start before the completion of reaction 2.8.

Since the different crystalline structures of the metaboric acid cannot be observed in thermogravimetric analysis (TGA), only on DTA (differential thermal analysis) or DSC (differential scanning calorimetry) the metaboric acid structures in the above equations can be summarised as only one [32].



However not all the researchers agree with this reaction in two steps, and in 2014 it was discovered through TGA that the reaction has three steps, each one corresponds to the breaking of one of the three -OH bonds. In the new step, metaboric acid transforms into a disodium salt of boric acid or tetraboric acid [33].



Briefly, when the temperature is under $\sim 150-160^\circ C$ boric acid is always presented as metaboric acid, but above this temperature, boric acid loses all its water and starts to transform into boron oxide.

Melting temperature

The main difference between the three metaboric acid crystal modifications (HBO_2 -III, -II and -I) is due to their different melting temperatures. The melting temperatures of the compounds can be seen in Table 2.3, and the system water/boron oxide and the melting temperatures of the mixture can be observed with more detailed in Figure 2.2. To be noted that the melting temperatures in Table 2.3 are for crystalline compounds and usually when the dehydration occurs, the generated boron oxide is amorphous which does not have a specific melting temperature. It usually starts to soften at $325^\circ C$ and becomes fluid at $500^\circ C$, whereby the values in Table 2.3 are just for reference [36].

Table 2.3: Melting temperatures of crystalline boric acid, metaboric acid and boron oxide [34].

| Compound | Melting Temperature [$^\circ C$] |
|---------------|------------------------------------|
| H_3BO_3 | 170,9 |
| $HBO_2 - III$ | 176 |
| $HBO_2 - II$ | 201 |

| | |
|-------------|-----|
| $HBO_2 - I$ | 236 |
| B_2O_3 | 450 |

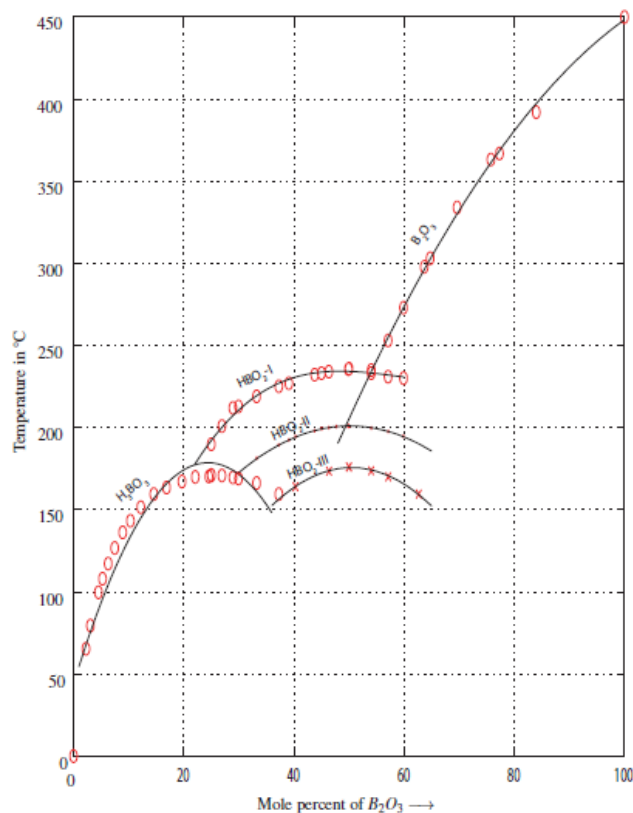


Figure 2.2: B_2O_3 -water system [34].

Analysing Figure 2.2, HBO_2 -III crystallises almost at the same time as H_3BO_3 , while HBO_2 -II and HBO_2 -I grow much more slowly. So, it is possible to verify that due to the melting temperature of the H_3BO_3 and HBO_2 -III mixture at $158.5 \pm 0.5^{\circ}C$, the first stage of the dehydration should be carried out below this temperature. Though, with this initial temperature, the dehydration time will be too long.

2.2.3 Boric acid properties

Boric acid, also called hydrogen borate or orthoboric acid is a colourless crystal which crystallises in plates and prisms or a white powder that can be dissolved mainly in water with little tendency to form highly supersaturated or unsaturated solutions. Due to its negative enthalpy of solution ($-124,7 \text{ kJ/mol}$), the solubility of boric acid in water increases with temperature. In Figure 2.3 it is possible to see the solubility pattern [30].

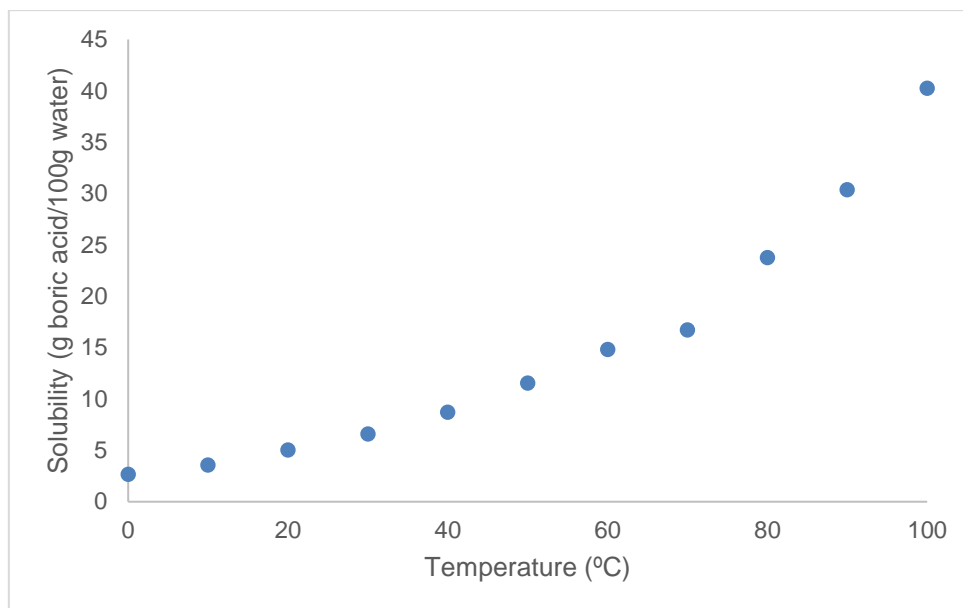


Figure 2.3: Solubility of boric acid in water.

BA can also be dissolved in other compounds that can be found in Table 2.4 [39].

Table 2.4: Solubility of boric acid in other compounds.

| Compound | Solubility at 25°C |
|-----------------|--------------------|
| Glycerol | 17,5 % |
| Ethylene Glycol | 18,5% |
| Methanol | 173,9 g/L |
| Ethanol | 94,4 g/L |
| Acetone | 0,6% |
| Ethyl acetate | 1,5% |

Besides that, BA can also be found in nature as sassolite (the mineral form of boric acid), more precisely in volcanic fumaroles and hot springs. Sassolite's colour can be from white to grey, pale yellow if it includes sulphur or pale brown if it includes iron oxides [40],[41]. BA is not reactive under normal ambient conditions and with controlled storage and handling temperatures and pressures.

When temperature increases above 80-100°C, BA is decomposed in an endothermic reaction, and it forms metaboric acid, water and boron oxide (that is very irritant). This solution attacks metals and steel and brings impurities to the final product and may produce hydrogen that can generate fire and explosion hazard [42],[43].

BA can be applied as an insecticide since affects the insect's metabolism, as an antiseptic and as an

antibacterial substance for mouthwashes, eye washing and others. It can also be used in adsorbents/absorbents industry, to produce agricultural chemicals, other boron compounds, fibreglass and for paints and coatings for example [31],[42],[44].

According to Regulation (EC), No. 1272/2008 (CLP) and GHS (Globally Harmonized System) BA is a hazardous product that may damage fertility and unborn child (Hazard statement-H360FD), and it has some precaution statements associated like mandatory use of personal protective equipment while handling this product (P280, P308+P313). This hazard and precaution statements can be seen with more details in the respective Safety Data Sheet (SDS).

Table 2.5 shows the most significant properties of boric acid [31],[45].

Table 2.5: Properties of H_3BO_3 .

| Property | Value |
|---|---------|
| <i>Molar mass (g/mol)</i> | 61,83 |
| <i>Density (g/cm³)</i> | 1,44 |
| <i>Melting point (°C)</i> | 170,9 |
| <i>Boiling point (°C)</i> | 300 |
| $\Delta H_f^\circ, \text{solid (kJ/mol)}$ | -1094,8 |
| $\Delta H_f^\circ, \text{gas (kJ/mol)}$ | -969,06 |

In the present work boron oxide >99,8% from *Carl Roth* (Figure 2.4) is used to perform dehydration.[46] A sieving test was made, and it was concluded that the particle sizes of boric acid are between 50 mm and 630 mm. More information can be seen in A.6.

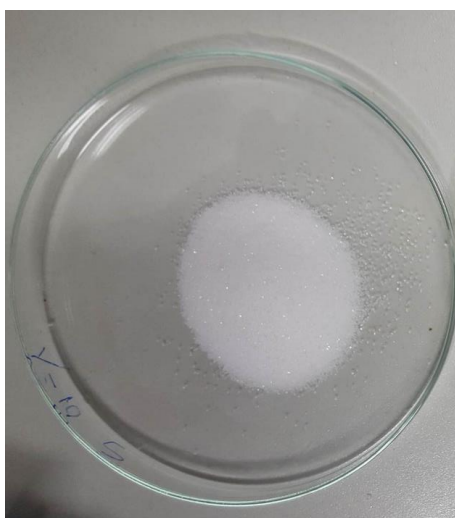


Figure 2.4: Boric acid >99,8% from *Carl Roth*.

2.2.4 Boron oxide properties

Boron oxide, also called boron trioxide, diboron trioxide, anhydrous boric acid or boric oxide is the common oxide of boron. Boron oxide is a colourless, semi-transparent vitrified (glassy) solid or a hard white, odourless crystal with moderate solubility in water (Figure 2.2 and Figure 2.5) [47] and partial solubility in alcohols (methanol) and glycerol [48].

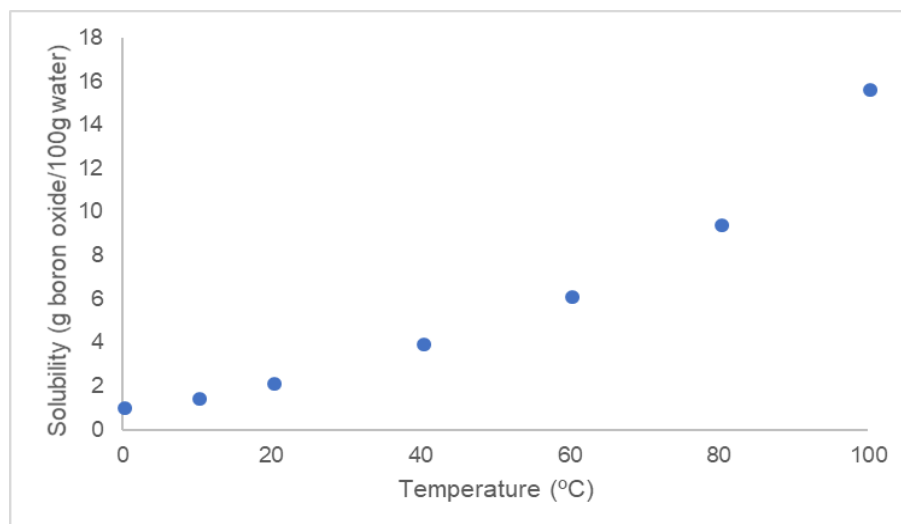


Figure 2.5: Solubility of Boron oxide [30].

Thus, it can appear in glassy form (α - B_2O_3), that is the most common, or in crystalline form. In crystalline form, there are two possible crystal modifications: α - B_2O_3 that occurs in a low-pressure phase (the threshold conditions for crystallization of the amorphous solid are 10 kbar and ~ 200 °C) or β - B_2O_3 that occurs in a high-pressure phase [49],[50]. BO reacts with water to boric acid in an exothermic reaction, and it is stable under normal ambient temperatures. Therefore, due to its hygroscopic nature, exposure to water or moisture should be avoided. BO in the presence of moist air reacts with metal hydrates or alkali metals generating hydrogen that could create an explosive hazard. So, it is particularly important to avoid contact with these strong reducing agents. It also reacts as a weak Lewis acid and may cause metal corrosion (in the presence of oxygen) [51].

It is usually used in speciality glass production (fibreglass), as an insecticide, as the starting material for other boron compounds synthesis, like metallic borates or boron halides or as a solvent for metallic oxides at high temperatures. It is also used to produce ceramic coatings, porcelain enamels and glazes [31],[52].

In Table 2.6 there are the most important properties of B_2O_3 [31].

Table 2.6: Properties of B_2O_3 .

| Property | Value |
|---------------------------|-------|
| <i>Molar mass (g/mol)</i> | 69,62 |

| | |
|--|---------|
| Density (g/cm³) | 2,55 |
| Melting point (°C) | 450 |
| Boiling point (°C) | 1860 |
| ΔH_f°, solid (kJ/mol) | -1274,2 |
| ΔH_f°, gas (kJ/mol) | -844,3 |

According to Regulation (EC), No. 1272/2008 (CLP) and GHS boron oxide is a hazardous product that may damage fertility and unborn child (Hazard statement-H360FD). For this reason, it is necessary to obtain special instructions before use (precaution statement P201) and use personal protective equipment while handling it (P281) [53].

2.3 State-of-the-art

2.3.1 Introduction

The boron oxide production from boric acid, that is, the dehydration of boric acid, has already been researched and there are a few experiments and patents on the topic. However, there is little information about this topic concerning TCES usage. Boron oxide can be produced in the muffle furnace, rotary kiln, fluidised bed, microwave oven and thermobalance using different boron sources like ammonium perborate or several boron minerals and below or at atmospheric pressure. These experiments were based on slow and flash dehydration. It is found that with a slow heating rate the final conversion to boron oxide was reached in an exceedingly long period (days). If the temperatures described in the dehydration steps (equation 2.8 to 2.11) and a slow heating rate (for example 2 K/min) are used, the dehydration time will be a few days. Nevertheless, it should be noted that to successfully use boric acid as a storage system and reduce the financial cost, the dehydration step must occur in the shortest possible time, that is, in a few hours rather than in several days.

Due to the different melting temperatures of the compounds and mixtures (see Table 2.3 and Figure 2.2), if the temperature is increased at about 150-160 °C, the product during drying will undergo a pasty melting. The pasty melting state when cooled will form a vitrified solid with a non-uniform appearance that will have to be ground before using [43],[54]. However, if temperatures below 150-160 °C are used, the pasty melting will not be formed but the dehydration time will be too long.

To solve this problem, some researchers have been developing boric acid dehydration method, through thermal (applying a temperature profile) and kinetic studies.

MOLLARD (1968), suggested using a fluidised bed reactor where the granulated boric acid (mean particle diameter of 0,4 mm) was placed above a diffusion device. This device had a stream of hot air that assures a 150-200% bed expansion to avoid the caking problem, even though the product undergoes a pasty melting state (it is called caking to the glassy solid that occurs after cooling) obtaining a practically anhydrous oxide. The air temperature at the beginning should be 150-160 °C and at the end of operation between 200-250 °C [43].

In this patent there are some suggestions for the temperature profile:

Example 1:

- Stage 1: $T_{air}=162$ °C for 15 min
- Stage 2: $T_{air}=200$ °C for 78 min
- Stage 3: $T_{air}=245$ °C for 40 min
- (Density=0,45 g/cm³ and 98% boron oxide, airspeed 0,08 m/s)

Example 2:

- Stage 1: $T_{air}=160$ °C for 1h30min
- Stage 2: $T_{air}=205$ °C ($T_{solid}=160-175$ °C) → after 1h: $T_{solid}=200$ °C
- (Density=0,44 g/cm³; 97.5% boron oxide)

Example 3:

- Stage 1: 100 - 120 °C for 60 min.
- Stage 2: 170 - 185 °C for 60 min.
- Stage 3: 215 - 225 °C for 60 min.

VASCONI et al. (1987) suggested working under atmospheric pressure in a rotating vessel or a reactor with a stirrer, first at 150 °C to eliminate water until the boric acid is almost converted to metaboric acid. Next, the metaboric acid needed to be gradually heated at a temperature value not exceeding 400 °C to eliminate water until metaboric acid has been completely converted into boron oxide. However, the dehydration time was about 6-20 hours which is a lot [54].

KOCAKUSAK et al. (1995) proposed two ways to completely dehydrate boric acid (100% conversion) in a fluidised bed reactor. The first one was a stagewise dehydration that took 6h to be completed, using the following profile [35]:

- Stage 1: 80 - 130 °C for 210 min.
- Stage 2: 130 - 180 °C for at least 60 min.
- Stage 3: 230 - 250 °C for 60 min.
- (bulk density 0,69 g/cm³, mean particle size 0,41 mm and 99,6 % B_2O_3).

The second method was a continuous dehydration of boric acid with humidity control of the exhaust gas to shorten the process time. In this method, the dehydration occurred continuously for about 3 hours.

- Stage 1: Heat up to 100°C with a rate of 2°C/min.
- Stage 2: Holding 100°C for 90 min.

- Stage 3: Heat up to 150°C with a rate of 2°C/min.
- Stage 4: Reducing the heating rate to 1°C/min to maintain a constant dehydration rate for 30 min.
- Stage 5: Heat up to 300°C with a rate of 1.5 - 2°C/min.
- Stage 6: Holding 300°C until complete dehydration.
- (bulk density 0,69 g/cm³, 99,6 % B₂O₃).

SEVIM et al. (2004) studied the kinetic parameters of the thermal decomposition of boric acid using Thermogravimetric (TG) data. It was determined that the decomposition of boric acid occur in two steps (equation 2.12 and 2.13) and both are suitable in a first-order kinetic model. More reliable results were obtained with Coats-Redfern (C-R) method rather than with Suzuki method because of the successful applications of it to both steps. The activation energies and frequency factors calculated according to the Coats-Redfern method (first-order model) were found as 79,85 kJ/mol and 3,82×10⁴ min⁻¹ for the first reaction and 4,79 kJ/mol and 4,045×10⁻⁵ min⁻¹ for the second reaction, respectively [36].

BALCI et al. (2012) did two experiments, one at isothermal conditions in a muffle furnace and the other at nonisothermal conditions in a Thermogravimetric analyser (TGA). In the first one, they mentioned that boron oxide with a content of 99,93 wt% was formed out of boric acid within three days at low temperature (between 80°C and 130°C) or in 30 minutes in a high-temperature range (more than 130°C). This experiment was done in the temperature range of 80 and 350°C. The second experiment was done from room temperature until 450°C with a heating rate of 5°C/min using air flow rate of 75 cm³/min. In the TGA experiments, the reaction was not completed at any temperature due to the low heating rate (5 °C/min). Therefore, the TGA experiments resulted in lower conversion values than the isothermal ones at low-temperature range [32].

Although the TGA and Differential Thermogravimetric Analysis (DTG) curves indicated three steps of reaction, they assumed that there were only two steps like in [36]: the first step for temperatures below 130°C and second step where the temperature was higher 130°C.

HARABOR et al. (2014) studied the triclinic boric acid (TBA) and hexagonal boric acid (HBA). They have observed three thermally induced processes, instead of two observed by Sevim or Balci [32],[36], which are evident in the DTG, DTA and DSC curves [44]. This difference between works may be due to the poor quality of DTA and TG measurements of Sevim work. It should have been evident in this work that the system still loses mass from 180 up to 550°C [40]. The endothermic peaks for the decomposition steps of TBA have a maximum at 117,56°C, 131,32°C and 160,53°C while for HBA the second stage is camouflaged by the second endothermic step with a maximum of 130,75°C. The third stage has its maximum effect at 160,84°C.

AGHILI et al. (2017) confirmed that the dehydration of boric acid is a triple step process. The first step (between 100°C and 160°C) had an activation energy of 41-61 kJ/mol using isoconversion methods or 55 kJ/mol using the C-R model fitting method and it was concluded that the reaction in step-I was controlled by nucleation and growth model. However, step-II (160°C to 195°C) and step-III (195°C to 400°C) were overlapped so it was not possible to carry out separately kinetic analysis [33].

Regardless of this studies about boron oxide production, the first study concerning dehydration of boric acid for a thermochemical energy storage purpose was developed by Thomas Karel at TU Wien [19]. KAREL (2016) conducted experiments for the dehydration and rehydration reactions with solid boric acid, solid boron oxide and water vapour, grounding his work on MOLLARD (1969) patent and using the following temperature profile.

- Stage 1: 100 - 120 °C for 60 min.
- Stage 2: 170 - 185 °C for 60 min.
- Stage 3: 215 - 225 °C for 60 min.

Nevertheless, the dehydration time was about 5 hours (instead of the theoretical 3 hours), and the conversion of the reaction was about 85%, using particle size between 200 and 630 µm to avoid the mixture from sintering.

2.3.2 Problematics

Analysing the literature cited above (2.3.1) about boron oxide production from boric acid and for TCES purposes, it is possible to summarise the main problems of the dehydration of boric acid.

The first problem is the start and final temperature of the dehydration reaction because this information is not concordant in the literature found and it is particularly important to know these for future work. Also, it is also necessary to clarify how many intermediate steps of the reaction exist.

The second problem is the melting temperatures of the compounds and mixture and the dehydration time (see Figure 2.2): If the temperature is raised above 150-160°C, the dehydration time will be reduced, but the mixture will create a pasty melting state that leads to a vitrified/ glassy solid when cooled.

Furthermore, the pasty melting state is very corrosive and cannot be handled in steel vessels or steel refractories due to the impurities that it brings to the final product and possible hydrogen formation that can generate fire and explosion hazard.

Regarding the particle size, there is a considerable particle range used in these R&Ds, but no one did experiments with different particles sizes, comparing the results to see which range of particles was more suitable.

Finally, it is essential to choose the right chemical method to analyse the final dehydration product because without the right method it is not possible to know if the final product of the reaction is only boron oxide, as expected.

2.3.3 Reactors type

In solid-gas reactions, there are a few options regarding the reactors selection like a fluidised bed, rotary kiln or fixed, a packed bed or a batch reactor with a stirrer to decrease the agglomeration [9],[16],[54].

In previous research about boron oxide production and its use for TCES applications mentioned in 2.3.1,

a fluidised bed reactor was used [19],[35],[43]. Nevertheless, in another's TCES R&D using different reaction system like calcium hydroxide-calcium oxide system, a rotary kiln was used [16],[55],[56].

On the one hand, in a fluidised bed reactor, there is rapid mixing of particles which increase the heat and mass transfer rates. This type of reactor is extremely good for continuous operations. However, with higher temperatures, the fine particles begin to agglomerate and sinter [57]. On the other hand, in a rotary kiln, the product particles are well-mixed so the product can achieve uniform temperatures, and it is possible to achieve higher temperatures and conversion than in a fluidised bed [55]. Though, it is difficult to control the melting state of the products.

In all, even though both reactors have advantages and disadvantages, it is possible to use one of them in a laboratory, pilot or larger scale. It is also necessary to remember that, as already mentioned in 2.3.2, the pasty melting resulting from the dehydration of boric acid is very corrosive to metals and steel and therefore it is necessary to avoid direct contact with the reactor.

To summarise, Table 2.7 presents the comparison between fluidised bed and rotary kiln reactors.

Table 2.7: Comparison between the fluidised bed and rotary kiln reactor [57].

| | Solid catalysed gas phase reaction | Gas/solid reaction | Temperature distribution in the bed | Particles | Pressure drop | Heat exchange and heat transport | Conversion |
|----------------------|--|--|---|--|--|--|--|
| Fluidised bed | For small granular or powdery non-friable catalyst. Rapid deactivation of solids. Excellent temperature control allows large-scale operations. | Can use a wide range of solids with much fines. Large-scale operations at uniform temperature are possible. Excellent for continuous operation yielding a uniform product. | Temperature is almost constant throughout. This is controlled by heat exchange or proper continuous feed and removal of solids. | Wide size distribution and much fines possible. Erosion of vessel and pipelines, attrition of particles and their entrainment may be severe. | For deep beds pressure drop is high, resulting in significant power consumption. | Efficient heat exchange and large heat transport by circulating solids, so that heat problem is seldom limiting in scale up. | For continuous operations, mixing of solids and gas bypassing result in poorer performance than other reactor types. For high conversion, staging or other unique design is necessary. |
| Rotary Kiln | Not used | Widely used. Suitable for solids which may sinter or agglomerate. | Temperature gradients in the direction of solids flow may be severe and difficult to control. | Any size, from fines to large lumps. | Very low | Poor exchange, therefore very long cylinders often needed. | Close to counter current plug flows, hence conversions can be higher. |

Chapter 3

Experimental set-up

This chapter presents the aim of this master thesis, the work methodology used and the description of the dehydration test rigs.

3.1 Aim

As mentioned before, the reversible reaction of boric acid/boron oxide for TCES purposes was only investigated for the first time at TU Wien by Thomas Karel [19] and Markus Deutsch [13],[21]. This master thesis aims to continue studying the reverse system H_3BO_3/B_2O_3 regarding its potential as a thermochemical energy storage, continuing Karel's work but focused mainly on the dehydration step of the reaction.

The aim of this thesis can be divided into two groups:

- First, the variation of mass during the experiment with temperature will be studied to see if it is concordant with the ones found in literature and a kinetic analysis will be performed. With this information, it will be possible to start the experiments with the aim of finding the best possible conversion (always above 90%) using the lowest temperature and dehydration time allowed, to reduce financial costs. For this to happen, it is necessary to establish a compromise between time, temperature and conversion. At last, it is essential to understand how the pressure can influence the temperature, dehydration time, final appearance of the product and, consequently, the conversion of the reaction.
- After the dehydration experiments, the other goal of this master thesis is to find an adequate qualitative chemical analysis method to analyse the final product of dehydration and understand if it is only boron oxide or if there is boric acid or metaboric acid in the final sample.

In all, to use this system in TCES, temperature profile, dehydration time, pressure, particle size range and final appearance of the dehydration product will be studied to understand how these parameters can influence the conversion and the energy density of the reaction.

3.2 Test Rigs

3.2.1 Methodology

Figure 3.1 shows the methods used in this work starting from a boric acid sample and passing through the purpose of each test equipment used.

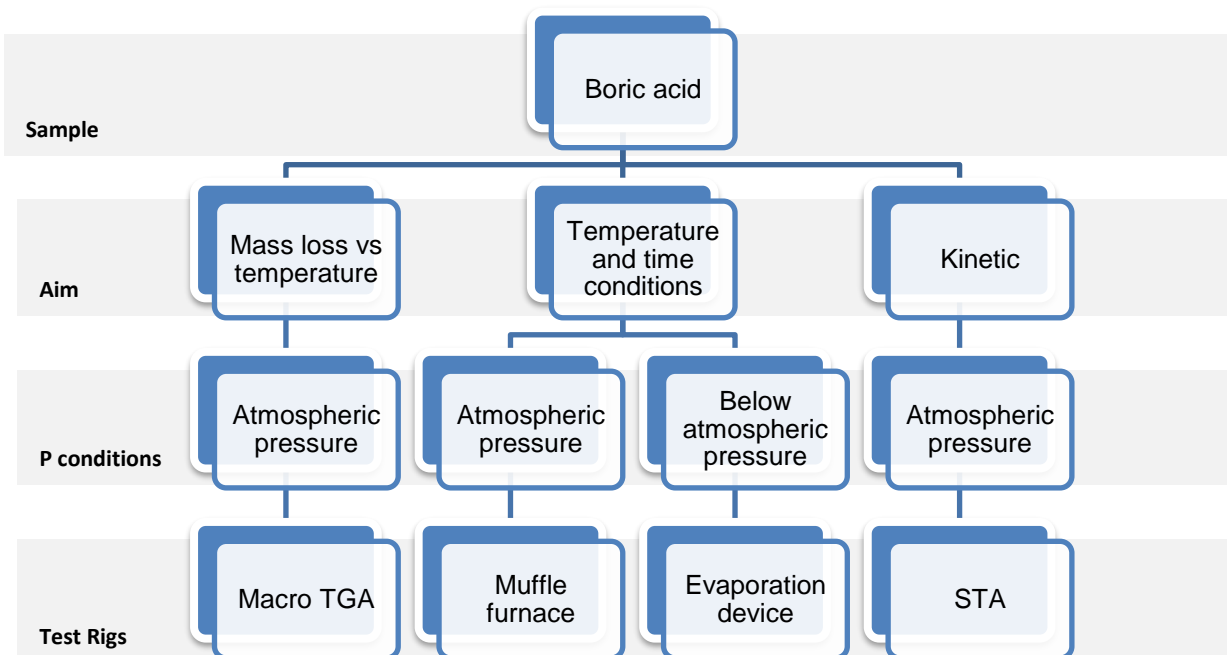


Figure 3.1: Methodology.

The first aim, starting from pure boric acid samples, was to determine the mass loss over temperature inside of the reactor, performing a thermogravimetric analysis in a macroscopic TGA, to set the temperature range for the next test rigs. With this, it was possible to determine the optimum temperature/time conditions for the dehydration reaction in two different test rigs: in a muffle furnace at atmospheric pressure and an evaporation device below atmospheric pressure. After the optimum temperature/time conditions were found, the experiments were repeated using generated boric acid, instead of pure boric acid, and the results were compared. From the test rigs results, it will be possible to use the optimum temperature and time conditions selected, for future work, in a lab-scale reactor, to perform the dehydration reaction.

At the same time, it was also possible to perform a kinetic analysis using a simultaneous thermal analyser to know more about the reaction, especially the number of steps of the reaction and the kinetic.

3.2.2 Macroscopic TGA

A thermogravimetric analyser, TGA, continuously measures the mass (-loss) while the sample is exposed to a constant heating rate (isokinetic) or constant temperature (isothermal). That way, mass, temperature, time and the moisture content (in the case of this TGA) in a TGA are considered base measurements. The macro TGA apparatus used, built by Claus Schlägner during his master thesis at TU Wien [58], can be seen in Figure 3.2 and in Figure 3.3 it is possible to see, with more detail, the reactor inside of the insulation. This apparatus is different from the standard TGA once one can use a higher amount of reactant (grams instead of milligrams).

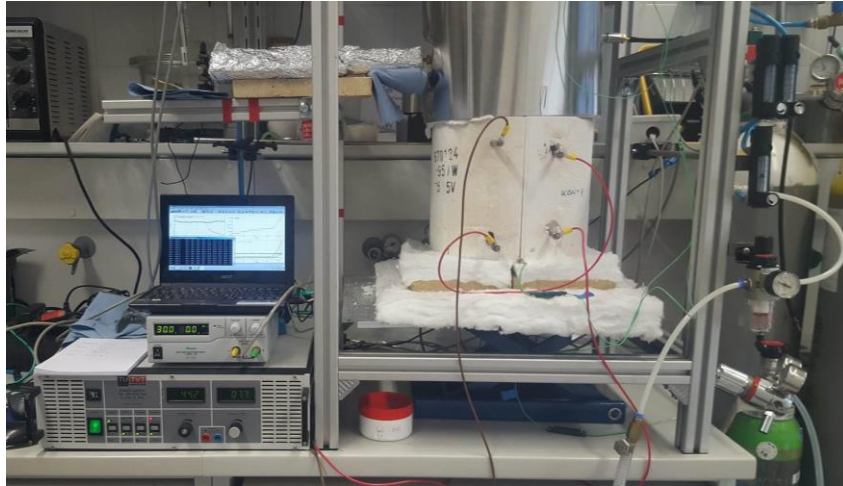


Figure 3.2: TGA apparatus.



Figure 3.3: Reactor used in the TGA apparatus.

This thermogravimetric (TG) system includes a reactor connected to a scale to measure the mass of the reactor over time. The reactor has an inlet and outlet gas/vacuum/ambient air used to create a controlled atmosphere reaction. After applying, the outlet gas is released into the atmosphere. Also, five thermocouples were used to measure the temperature:

- T_1 measures the temperature in the upper heating room;
- T_2 the temperature of the lower heating room;
- T_3 the room temperature at the bottom of the apparatus;
- T_4 the room temperature on top of the apparatus;

- T_5 the temperature inside of the reactor.

The humidity as well as the temperature at the inlet and outlet of the reactor, measured with two “humidity and temperature transmitters” from *Elektronik*, are also checked. As it is possible to see in Figure 3.2 and Figure 3.3, the reactor was isolated with glass wool and refractory brick to avoid heat losses. It should be noted that it was not possible to choose the final temperature that was going to be achieved at the end of the experiment neither the heating rate of the reaction. The temperature was selected, controlling the electric current used to heat up the reactor. So, once in this device the heating rate cannot be controlled, the temperature was maintained constant, and the purge gas flow was changed.

To conclude, there is a procedure for turning the apparatus on: when the reactant is inside the reactor, it is necessary to wait approximately 400 seconds until turn on the gas supply. This procedure is made to prevent recording mass changes from the manipulation of the reactor when the reactor is being set up for the beginning of the experiment. After another 400 seconds, it is possible to turn on the heating current. When the trial is concluded, first the heating is turned off, and after that, the gas flow is reduced to a value near to zero, but not zero, until the apparatus is at room temperature. Thus, the first 800 seconds (~13,3 min) of recordings are not presented in the graphics.

At the beginning of the experiments, the mass appears to increase, which is not reasonable since the decomposition of the sample always decreases the mass of the testing sample. This is called Buoyancy effect.

Buoyancy Effect of TGA experiment [58]–[60]

Every substance found in a gas atmosphere is exposed to a buoyancy force. The buoyancy force is the upward force exerted on an object when it is, in this case, surrounded by gas, and its value is equal to the weight of the gas displaced by the object (Figure 3.4). This effect results in “apparent” mass changes, that is, the mass exceeded the original mass. The degree of buoyancy, and thus the degree of mass change, are mainly related to the volume of the substance and the density of the predominant gas.

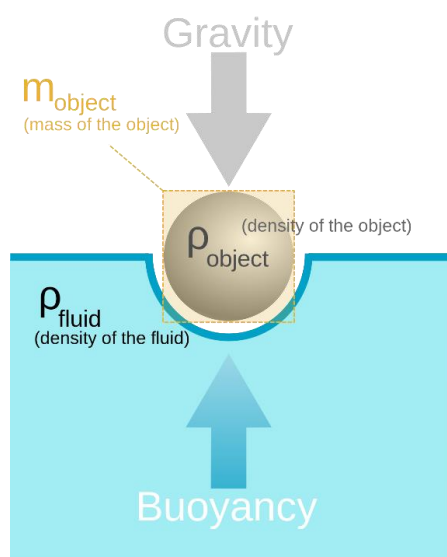


Figure 3.4: Buoyancy effect.

During the experimental work, the reactor is heated by radiation of the heating shell up to the temperature of the wall and the gas in the system is heated by natural convection. In the initial stage, the gas temperature of the heating room is higher than the temperature inside the reactor. The buoyancy of the gas itself decreases, which leads to a faster decrease in the density of the air in the heating room than inside the reactor. Therefore, the reactor appears to gain weight. As soon as the temperature inside of the reactor exceeds the outside temperature, the density of the nitrogen inside the reactor decreases but at the outside, it remains constant, and then the mass of the reactor appears to decrease. Consequently, the most substantial effect is seen at lower temperatures, usually at the start of the experiments, with only smaller increases being observed at higher temperatures because at this point radiation becomes the primary mechanism for heat transfer.

Two corrections were used to solve the problem of buoyancy effect:

- $T_5 < T_2$ when the temperature of the reactor is lower than the temperature of the lower heating room;

$$\Delta m_{1[g]} = (f(T_2(0)) - f(T_2(t))) \cdot (V_{reactor} - V_{sample}) \quad (3.1)$$

- $T_5 > T_2$ when the temperature of the reactor is higher than the temperature of the lower heating room.

$$\Delta m_{2[g]} = f(T_2(0)) - f(T(n)) - (f(T_5(n)) - f(T_2(n))) - (f(T_5(t)) - f(T_2(t))) \cdot (V_{reactor} - V_{sample}) \quad (3.2)$$

Where:

- $f(T_2(0))$ - Density of the air at the beginning of the experiment (23°C);
- $f(T_2(t))$ - Density of the air inside the lower heating room at a time t;
- $V_{reactor}$ - Volume of the reactor, 1L;
- $f(T(n))$ - Density at a time n where T_2 and T_5 are equal;
- $f(T_5(n)), f(T_2(n))$ - Density at the point n for the nitrogen in the reactor and for air in the lower heating room;
- $f(T_5(t))$ - Density of the nitrogen in the reactor at a time t;
- $f(T_2(t))$ - Density of the air in the lower heating room at a time t.

To these equations, the density of air and nitrogen versus temperature (°C) were calculated ($R^2=1$). [61]

$$f(T_2(t)) = 1,336 \times 10^{-11}T^4 - 1,991 \times 10^{-8}T^3 + 1,225 \times 10^{-5}T^2 - 4,462 \times 10^{-3}T + 1,275 \quad (3.3)$$

$$f(T_5(t)) = 3,241 \times 10^{-11}T^4 - 3,183 \times 10^{-8}T^3 + 1,431 \times 10^{-5}T^2 - 4,455 \times 10^{-3}T + 1,234 \quad (3.4)$$

3.2.3 Simultaneous thermal analyser

It is essential to use the minimum mass of the reactant possible and control the heating rate to perform a kinetic study once an increasing mass leads to an increasing diffusion resistance in bulk, which influences the reaction kinetics, as well as the slow removal of the gaseous phase from the sample bulk. So, the smaller sample mass generates a smaller amount of gas and heat during the reaction, and thus, reduces the partial pressure and temperature gradients [62]. For these reasons, the kinetic study was performed in a simultaneous thermal analyser (STA) instead of the macro TGA.

Simultaneous TGA-DTG/DSC measures both weight changes (TGA-DTG) and heat flow (DSC) in a material as a function of temperature or time in a controlled atmosphere.

From the combination of TGA, DTG and DSC one obtains a broad range of information. In TGA and DTG, it is possible to know the mass change as a function of temperature and time. Although the first derivative of TGA (DTG) gives the same information as the TGA, it is possible to note the small features and boulders on the curve more efficiently because they appear as peaks. Besides this, in TGA-DTG it is only possible to see the events that do involve mass change, like the dehydration of boric acid.

In DSC the difference in the amount of heat required to increase the temperature of a sample and reference is measured as a function of temperature. Both the sample and reference are kept at nearly the same temperature throughout the experiment, and the heat flux will be measured. With this, it is possible to detect the endothermic and exothermic transitions of the reaction as a function of temperature as well as the enthalpy of solids, phase changes or crystalline transitions. However, in DSC in addition to being possible to show the events which involve mass change, it is also possible to see those that do not involve mass change like the crystallisation or melting of metaboric acid and boric acid. For these reasons, the combination of all the techniques should be used to obtain better results in the kinetic analysis [63].

As it happens in the macro TGA, there is also Buoyancy Effect in STA. However, this is corrected automatically by the program once a correction run was performed with the same conditions used in the experiments, but with the empty crucible.

In this thesis NETZSCH, STA 449 C was used, and the pictures of the STA and the scale of STA with the reference and the sample crucible can be seen in Figure 3.5. In this analyser, the reactor is heated by conduction of the heating shell up to the temperature of the wall, and natural convection heats the nitrogen inside the reactor.

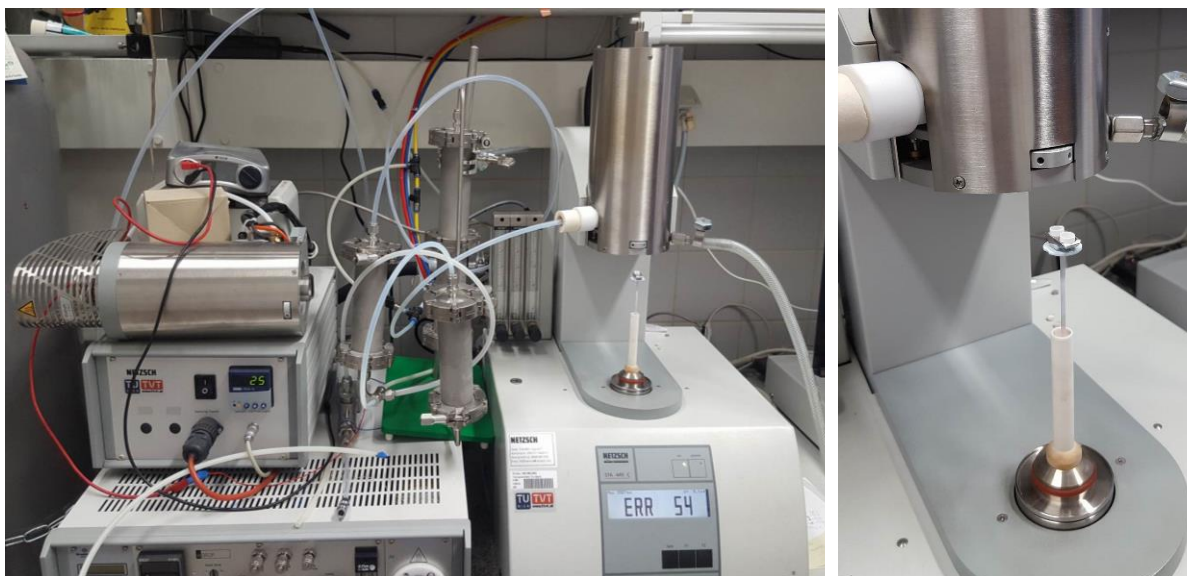


Figure 3.5: Simultaneous thermal analyser used (left) and a detail of its scale (right).

3.2.4 Muffle furnace

A muffle furnace is usually a refractory brick insulation heating chamber with a folding door and a chimney, to remove exhaust gas from the furnace, which works at atmospheric pressure. Muffle furnaces are regularly heated to desired temperatures by conduction, convection, or radiation from electrical resistance heating elements located in the walls and bottom of the furnace. Since the heating chamber is insulated, the heat cannot escape, maintaining the temperature constant inside the chamber. It is used for high-temperature applications such as melting glass, creating enamel coatings, technical ceramics or soldering and brazing [64],[65].

In this master thesis, *Nabertherm* muffle furnace is used to dehydrate boric acid and eliminate the moisture and the water in its composition, producing boron oxide. This machine has a controller to control the temperature in two steps and can achieve temperatures between 30°C and 3000°C. It is important to note that the temperatures referred are for the air inside the muffle furnace and not for the sample. The temperature of the sample will be a little bit lower.

Figure 3.6 shows the temperature program controller and the muffle furnace used during this master thesis.



Figure 3.6: Temperature program controller (left) and muffle furnace (right).

3.2.5 Evaporation device

To study the pressure influence on temperature, dehydration time, the final appearance of the product and therefore the conversion and energy density, an evaporation device was used.

Usually, this technique is used to purify solids once the solids vaporise and condense on a chilled surface known as a cold finger. The vapours leave impurities behind, making the collection of the pure compound possible. However, in this master thesis, this device is not used with this goal. The goal is to dehydrate boric acid at reduced pressure with the help of a heating plate.

The method is performed on solids with vapour pressures below their melting points, and the main advantages of using this apparatus are the low working temperatures and reduced exposure of the sample to gases and moisture from the air that otherwise might damage the final product. It is expected that the melting and boiling point of the boric acid decrease with the pressure drop. Thus, less temperature is needed to achieve the same objectives as when working at atmospheric pressure.

Figure 3.7 shows the equipment used for “below atmospheric pressure” experiments. This device is composed of:

- A Büchner flask (number 1, see Figure 3.7), also known as vacuum flask. The vacuum flask is a thick-walled Erlenmeyer flask which provides it with the strength to resist the pressure difference while holding a pressure below atmospheric pressure inside, with a short glass tube where the hose is connected (number 2, see Figure 3.7).
- A hose connected the Büchner flask to a pump/vacuum source that, in this case, can reach approximately 160-180 mbar.
- A heating plate, where the Büchner flask is heated on that can reach temperatures up to 350°C.
- A cold finger located on top of the Büchner flask. The cold finger, used in the evaporation device,

is a piece of laboratory equipment that is used to generate a localised cold surface. This device is a cold trap that usually consists of a chamber where a coolant fluid (cold tap water in this case) can enter and leave (number 3 and 4, see Figure 3.7) and allow the desired sublimated compounds, which are in the Büchner flask, to be deposited and recrystallised again. The cold finger is attached to the flask through an elastomer adapter (number 5, see Figure 3.7).

So, boric acid inside of Büchner flask is heated up to the desired temperature. Due to temperature and pressure, it starts to sublime, and when the gas is in contact with the cold finger, it recrystallises. In this process, the water will be removed, and boron oxide will be produced.

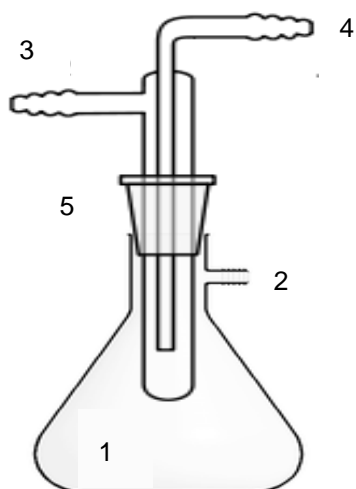


Figure 3.7: Evaporation device.

Chapter 4

Test results and discussion

This chapter explains what it was done on each test rig, showing and discussing the results.

4.1 Experiments and results

At the end of all dehydration experiments, final conversion, x , and boron oxide energy density, E_ρ , were calculated to be able to compare the results with the data found in the literature (see Table 2.1).

The final conversion of the reaction was calculated based on water content difference, except for STA data, that was calculated based on the ratio between the mass loss at an instant t and the mass loss at the end of the experiment.

$$x_{[\%]} = \frac{\Delta m_{[g]}}{\omega_{H_2O_{[g]}}} \times 100 \quad (4.1)$$

Where:

- Δm - Mass difference between the beginning and the end of the experiment, that is, the amount of water of boric acid that is lost during the dehydration;
- ω_{H_2O} - Water content of boric acid, that is, the stoichiometric water value at the beginning of the experiment.

ω_{H_2O} can be calculated based on equation 4.2.

$$\omega_{H_2O_{[g]}} = \frac{m_{H_3BO_3_{[g]}} \cdot v_{H_2O}}{M_{H_3BO_3_{[g/mol]}} \cdot v_{H_3BO_3}} \cdot M_{H_2O_{[g/mol]}} \quad (4.2)$$

- $m_{H_3BO_3}$ - Boric acid mass measured at the beginning of the experiment;
- v_i - Water and boric acid stoichiometric factor;
- M_i - Water and boric acid molar mass.

After calculating the conversion, it is possible to calculate the energy density for the dehydration step, E_ρ , according to equation 4.3.

$$E_\rho_{[kJ/m^3]} = \frac{\Delta H_R^m_{[kJ/kmol]} \cdot \rho_i_{[kg/m^3]}}{MM_i_{[kg/kmol]} \cdot v_i} \cdot x \quad (4.3)$$

- ΔH_R^m - Theoretical reaction enthalpy at the mean temperature of the reaction;
- ρ_i - Density of boric acid;
- MM_i - Boric acid molar mass;
- v_i - Boric acid stoichiometric factor;
- x - Conversion of the dehydration reaction.

In TGA/ STA, equation 4.4 is also used to calculate the mass loss. In the end, it is possible to compare this value with the theoretical one (-43,70%).

$$mass\ loss_{[\%]} = \left(\frac{m_t [g]}{m_i [g]} \right) \times 100 \quad (4.4)$$

- m_t - Mass at a specific time;
- m_i - Initial mass.

Propagation of uncertainty

There are two types of errors: systematic or random. Systematic errors are determinable and correctable and can be instrumental errors (calibration) or due to impurities in the compounds whereas the random errors cannot be eliminated but minimised (for example always making measurements with the same operator and with the same apparatus). In A.2 it is possible to see the error calculation.

4.1.1 Macroscopic TGA

Approximately 30,00 g of boric acid was put inside of the reactor with a protective sleeve to protect the reactor from the glassy state of the product that is predicted to occur, and that is corrosive for the material of the reactor. This way was easier to clean, and the pipe blocks were prevented. As referred in the chapter 3.2.2 it was necessary to wait before turning on, first the gas supply, in this case, nitrogen, and then the heating. Regarding the gas, nitrogen was used instead of air since the humidity of the air could influence the results. This purge gas flow is essential because it helps to remove the arising gaseous product so that the reaction is not affected by an increase of partial pressure.

The temperature in 5 spots of the TGA apparatus, moisture content as well as the temperatures associated with them, and the mass difference was measured during these experiments, over time. As mentioned above (3.2.2), the temperature is selected, controlling the electric current used to heat up the reactor.

A few tests with different values of purge gas flow and heating current were made but only the two most important are presented:

1. 4 L/min N₂, 12 A;
2. 6 L/min N₂, 12 A.

It is important to note that all the experiments were stopped when the mass appeared constant and when the relative humidity at the outlet started to decrease and approached zero. Only at that time, it was possible to know that there was no more water inside the product/reactor to leave and the dehydration reaction was finished.

In the first experiment, 4 L/min of nitrogen and the maximum heating current possible, around 12-12,5 A, were used. Figure 4.1 depicts the mass and temperature variation over time, achieving a maximum temperature of 455°C in T_5 .

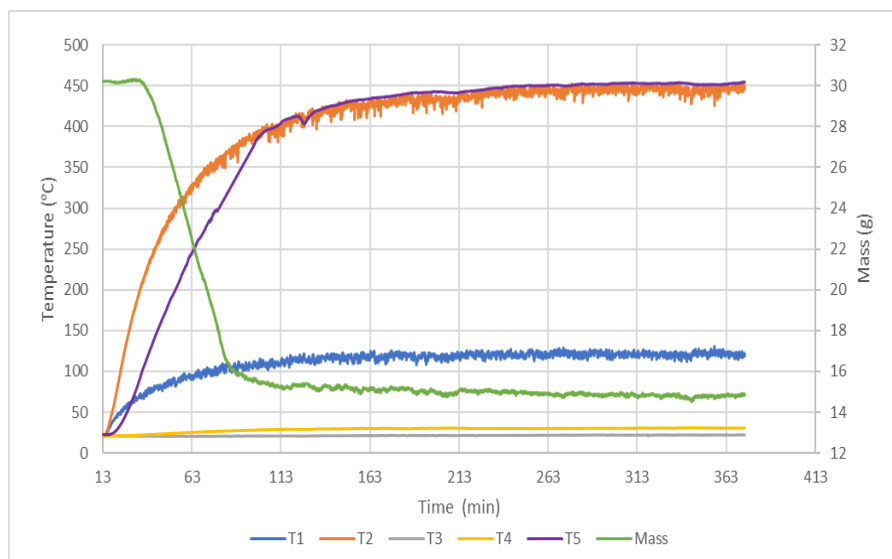


Figure 4.1: Mass and temperature variation over time in experiment 1.

The experiment shows that, at a certain point, the temperature inside the reactor (T_5) was higher than the temperature of the lower heating room (T_2). This happens because of the non-ideal isolation. Natural convection in the heating room leads to a permanent exchange with the environment. The gas of the lower heating room reaches the equilibrium temperature which is lower than the temperature of the reactor wall, that is heated up through radiation of the heating shell. The gas inside the reactor is heated up the wall temperature. Accordingly, there are higher temperatures inside the reactor (T_5) than outside (T_2). It is also possible to verify that T_1 (upper heating room) is lower than T_2 (lower heating room). This happens because of the poor insulation used on top of the apparatus comparing to the bottom. T_3 and T_4 were just to control the room temperature and are practically the same, as expected.

Figure 4.2 depicts the mass loss over temperature inside the reactor.

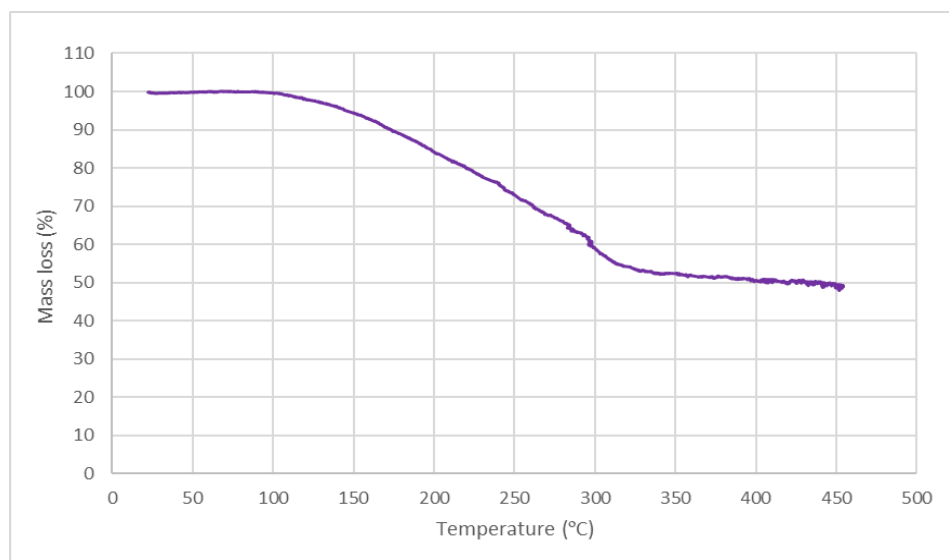


Figure 4.2: Mass loss over temperature for experiment 1.

According to Figure 4.2, the reaction starts around 90-100°C which is concordant with the literature data

(see 2.3.1). From 100°C to 400°C there is the period when the reaction was occurring, and at 400-450°C it seems to begin to stop. In this trial the relative humidity at the outlet (see Figure 7.3) starts to increase at 81°C and has a very steep increase, reaching 100% when the temperature was 150°C, remaining constant until 430°C. At ~455°C the relative humidity at the outlet is almost zero which means that the reaction stops. However, it was observed that the moisture began to condensate at the outlet because the reaction happened too fast. Consequently, it was decided to carry out another experiment with the same conditions but increasing the nitrogen flow rate to prevent condensation of the moisture and to see if 4 L/min was enough to remove all the water or if more flow rate was needed.

In the second experiment, as mentioned above, instead of 4 L/min of nitrogen 6 L/min was used to see if it is possible to remove all the water inside the reactor/product. Figure 4.3 shows the mass and temperature variation over time and Figure 4.4 represents the mass loss versus temperature inside of the reactor.

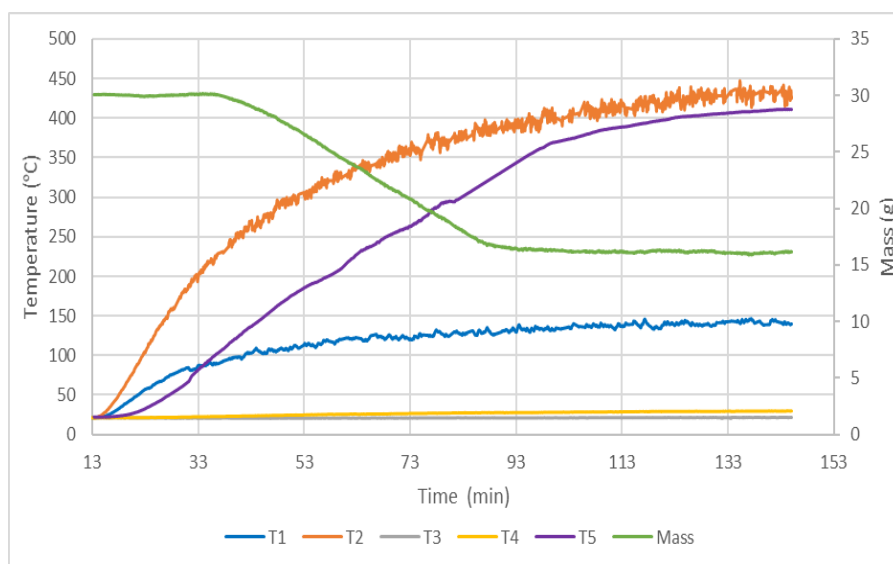


Figure 4.3: Mass and temperature variation over time in experiment 2.

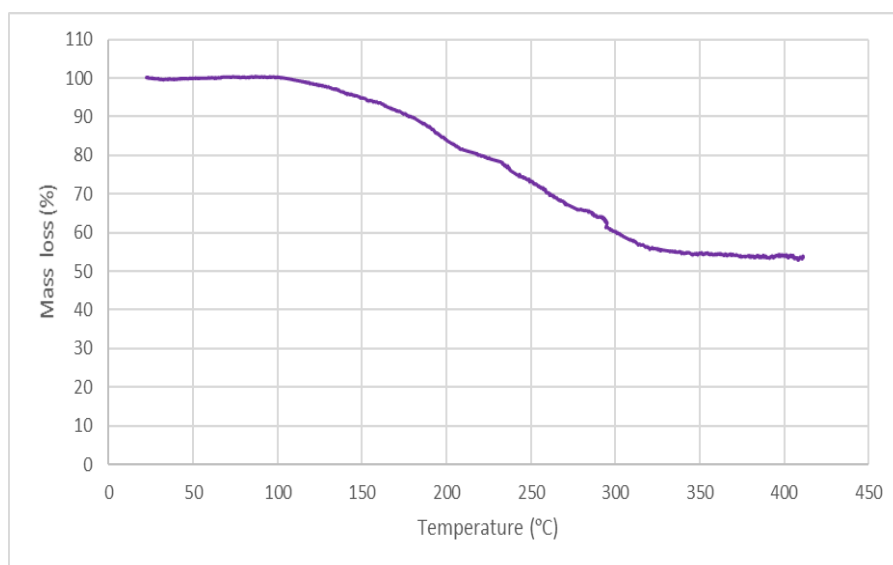


Figure 4.4: Mass loss over temperature inside the reactor for experiment 2.

As one can see, this experiment validates the previous one since it can be proven that the beginning of the reaction occurs around 90-100°C and stops around 400°C, when the mass looks constant. According to the graphic of the relative humidity (Figure 7.5), it is possible to observe that it starts to increase at 90°C reaching the maximum steam removed from 150°C to 342°C which agree with Figure 4.4 and Figure 4.2. Looking at the mass loss, one can see that is not equal in both experiments. In fact, the theoretical mass loss is -43,70% but in Figure 4.2 and Figure 4.4 is $-50,84 \pm 0,08\%$ and $-46,27 \pm 0,07\%$, respectively. This means that, in addition to the error associated with the electronic scale and the propagation of uncertainty, some part of the reagent (possibly boric acid or metaboric acid that did not react) may have evaporated. Besides this, since the reactor is hanging on the scale, it is overly sensitive to vibrations/taps which may also influence the mass value over time. Moreover, mass loss is higher in the first experiment than in the second one, probably because of the rapid reaction rate of the reaction that increases the removal of water from the sample. Besides this, even controlling the heating current the reactor does not always heat up to the same temperature. In experiment 2 it seems that the reaction has ended at 400°C but compared with the first experiment that goes up to 450°C, it is possible to see that there is still mass loss. Once the heating current was not exactly the same in the two experiments, because it is challenging to maintain it regularly, another experiment was done at 4 L/min, and 12 A. This experiment was made to compare the results and it was possible to see that the maximum temperature achieved inside of the reactor decreases from 455 °C to 437 °C which means that the mass loss decreases from -50,84% to -50,26% (difference of 0,58%). Since this mass difference is not so relevant compared to the other reasons for the mass loss being above the theoretical value, this mass difference will be neglected to compare the two experiments.

In all the tests, the final product was like a hard glassy solid at room temperature as described in the state-of-the-art. (see Figure 4.5).



Figure 4.5: Appearance of the final product.

All in all, one can conclude that the reaction starts between 90-100°C like BALCI et al. and HARABOR et al. referred and stops around 400°C. Although it is not possible to confirm the temperatures at which the intermediate reactions starts to occur or how many intermediate steps are because the mass loss

over temperature does not have any changes in the slope of the graphic, this does not mean that these reactions do not occur. Since these changes, related to the intermediate reactions, are due to the crystal modifications of metaboric acid or due to the formation of tetraboric acid ($H_2B_4O_7$), a DSC analysis, using less amount of boric acid is needed to observe them and conclude how much steps there are and its respective temperatures.

So, using this temperature range, it is possible to begin the experiments in the muffle furnace and in the evaporation device and discover which are the optimum temperature and time conditions to perform the reaction for TCES purposes.

4.1.2 Simultaneous thermal analyser

A mass of $0,0020 \pm 0,0002$ g of boric acid with a particle range between 125-80 μ g was used to perform three experiments with different heating rates: 2 K/min, 4 K/min and 8 K/min. Before the real tests, a correction run for the buoyancy effect (see 3.2.2) was made (using the same conditions as the real trials but with the empty crucible). Table 4.1 presents all the information needed to perform these experiments. All the experiments started at room temperature for 10 minutes, and then the temperature of the reactor was increasing until 400°C (though the temperature of the sample deviates $\sim 60^\circ$ C from the reactor temperature), with a heating rate of 2,4 and 8 K/min. When the temperature reached 400°C, it remained constant for 30 minutes and decreased again until room temperature, using a fast heating rate because this last part is not essential for the results.

Table 4.1: Data used in STA.

| | |
|---|--------|
| T_{max} [°C] | 400 |
| $T_{average,sample}$ [°C] | 346,27 |
| <i>Nitrogen flow</i> $\left[\frac{mL}{min} \right]$ | 100 |
| <i>Protective nitrogen flow</i> $\left[\frac{mL}{min} \right]$ | 10 |
| <i>Theoretical mass loss</i> [%] | -43,70 |

With these experiences, it is possible to obtain the mass loss over time and temperature, the DTG and DSC curve. So, to understand what happened during the reaction it is important to analyse the three curves together. In this case, the DSC signal has some interference, and the signal is not sensitive enough to the correction made at the beginning since the sample mass used was very low. In Figure 4.6 and Figure 4.7 it is possible to see the TGA-DTG and DSC curves for the heating rate of 2 K/min.

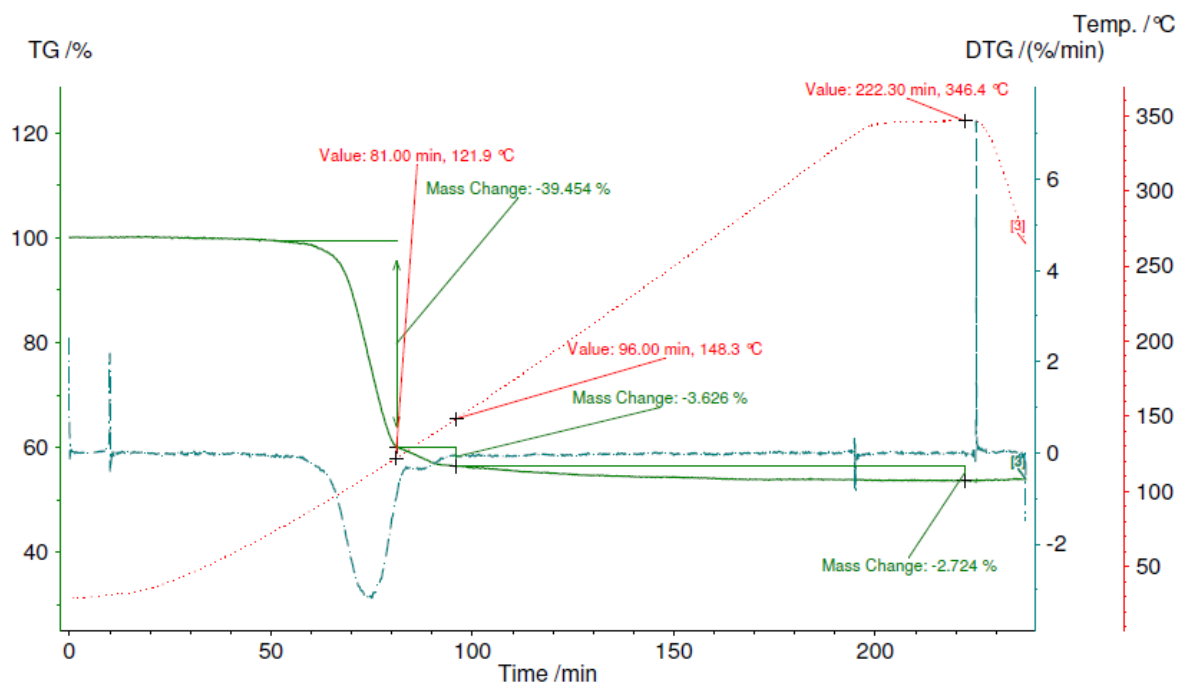


Figure 4.6: TGA and DTG for a heating rate of 2 K/min.

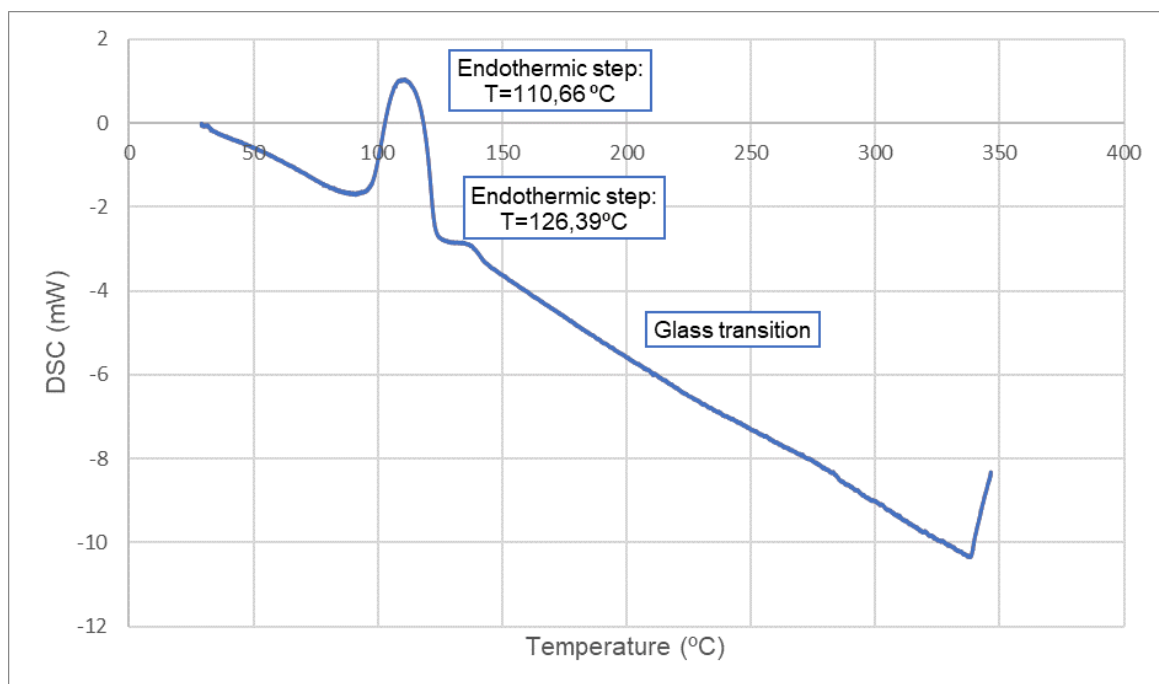


Figure 4.7: DSC signal for a heating rate of 2 K/min.

Looking at Figure 4.6 it is possible to see two endothermic steps of the reaction with a total mass loss of -45,81% (more 2,10% than expected). The first step occurs between 90 and 121,9°C and the second step between 121,9°C and 148,3°C. Although there is not another peak in the DTG curve, it is possible to see in Figure 4.6 that between 148,3°C and 346,4°C, there is a mass loss of 2,72% due to residual water evaporation or evaporation of the reactant. So, officially instead of three reaction steps mentioned

above (equation 2.14 to 2.16), only two reaction steps (equation 2.12 and 2.13) can be distinguished and, according to this, officially the mass loss is -43,09% (less 0,61% than expected) instead of -45,81%. This could mean that these experiments suffered the same problem as in [36], that is, only two steps of the reaction are identified although at the end of the reaction there is still a mass loss that is not associated with any peak in DTG or DSC signal. The mass loss without any corresponding peak in the DTG or DSC signal corresponds to the excess of mass loss verified when comparing to the theoretical value. This situation maybe happened due to the reasons above, (see 2.3.1) - poor quality of DTA and TG measurements although this is unlikely - or to the fact that a minimal amount of boric acid was used (~2 mg).

The DSC signal confirms the two steps presented in the TGA-DTG signal and shows a glass transition that appears as a step in the baseline of the recorded DSC signal. The glass transitions may occur as the temperature of an amorphous solid is increased and is due to the sample suffering a change in heat capacity without any formal phase change occurs. As the temperature increases, an amorphous solid will become less viscous which agrees with the final appearance of the product at the end of the reaction.

In A.4, it is possible to find the TGA-DTG and DSC signal for the heating rates of 4 K/min and 8 K/min. As expected, the higher the heating rate, the worst the steps are defined probably due to the overlap of steps. Such as in the experiments with a heating rate of 2 K/min, only two steps of the reaction can be distinguished so that the same justifications mentioned above can also be used for higher heating rates (4 K/min and 8 K/min). In addition to these justifications, for higher heating rates of 4 K/min and 8 K/min, the other possible explanation is the fact that the steps may have been overlapped due to the rapid heating [44]. Concluding, with higher heating rates it is possible to see that the peaks of the DSC curve move to higher temperatures, which agrees with what was expected.

Though, the results obtained in the three experiments cannot be compared with literature values because one can only compare data obtained with the same conditions (heating rate and initial mass). Even so, in [32] the DTG signal presents two peaks (one at 156°C and another at 191°C for a heating rate of 5 K/min), as in these experiments, but the peaks are shifted to the right relative to the experience performed at 2 K/min and 4 K/min, which was expected.

From this information, it is possible to do a brief kinetic study. Reading all the work done in this area it was concluded that the best model for isokinetic (or non-isothermal) analysis to be used in this reaction is the Coats-Redfern (C-R) model-fitting method applied between 80°C and 346°C. This is because the method can be successfully applied in both reactions [33],[36],[66].

This method is based on the decomposition reaction of a solid expressed as



Where the reaction rate of A is

$$\frac{dx}{dt} = k(1-x)^n \quad (4.6)$$

Where:

- x - Conversion fraction calculated based on fraction between the mass loss at an instant t and the mass loss at the end of the experiment;
- k - Constant rate;
- n - Reaction order.

If the heating rate (q) is considered, equation 4.6 can be expressed as

$$\frac{dx}{dT} = \frac{k_0}{q} (1-x)^n \exp\left(\frac{-E_a}{RT}\right) \quad (4.7)$$

Where:

- k_0 - Frequency factor;
- $q = \frac{dT}{dt}$ - Heating rate;
- E_a - Activation energy;
- R - Universal gas constant.

Integration of equation 4.7 between $0 \rightarrow x$ and $T_0 \rightarrow T$ equation 4.8 is obtained.

$$\frac{1 - (1-x)^{1-n}}{(1-n)} = \frac{k_0}{q} \int \exp\left(\frac{-E_a}{RT}\right) dT \quad (4.8)$$

The right-hand-side of this equation has no exact integral, but it can be expanded into an asymptotic series, and the higher-order terms are ignored obtaining equation 4.9 for $n \neq 1$.

$$\frac{1 - (1-x)^{1-n}}{(1-n)} = \frac{k_0 R}{q E_a} \left(1 - \frac{2RT}{E_a}\right) \exp\left(\frac{-E_a}{RT}\right) \quad (4.9)$$

$\frac{k_0 R}{q E_a}$ is constant for any define value of n and q . So, assuming $\frac{2RT}{E_a} \ll 1$, equation 4.10 is obtained for $n \neq 1$.

$$\frac{1 - (1-x)^{1-n}}{T^2(1-n)} = \frac{k_0 R}{q E_a} \exp\left(\frac{-E_a}{RT}\right) \quad (4.10)$$

For $n=1$ from equation 4.8, one can obtain equation 4.11.

$$\frac{-\ln(1-x)}{T^2} = \frac{k_0 R}{q E_a} \exp\left(\frac{-E_a}{RT}\right) \quad (4.11)$$

Assuming that

$$f(x) = \frac{1 - (1-x)^{1-n}}{(1-n)} \quad (n \neq 1) \quad (4.12)$$

$$f(x) = -\ln(1-x) \quad (n = 1) \quad (4.13)$$

The general Coats-Redfern can be written as:

$$\ln \frac{f(x)}{T^2} = \ln \left(\frac{k_0 [s^{-1}] R_{[kJ/mol \cdot K]}}{q_{[K/s]} E_{a [kJ/mol \cdot K]}} \right) - \left(\frac{E_a [kJ/mol]}{R_{[kJ/mol \cdot K]} T_{[K]}} \right) \quad (4.14)$$

Plotting $\ln \frac{f(x)}{T^2}$ vs $\frac{1}{T}$ and changing the order of the reaction to select the order that gives the best linear fit, the frequency factor and the activation energy can be determined (Figure 4.8). As mentioned before, two steps of the reaction were distinguished and since in Figure 4.8 it is possible to see 2 different segments, it would be suitable to consider two different regions for kinetic calculations: Region I for $1/T > \sim 0,0025 \text{ K}^{-1}$ where the first reaction occurs and Region II for $1/T < \sim 0,0025 \text{ K}^{-1}$ where the second reaction occurs (see equations 2.12 and 2.13).

According to the Figure 4.6, Figure 7.6, Figure 7.8, it is possible to see the two regions and the limit temperature between them: $T=121,9^\circ\text{C}$ for 2 K/min; $T=134^\circ\text{C}$ for 4 K/min and $T=134,4^\circ\text{C}$ for 8 K/min, respectively.

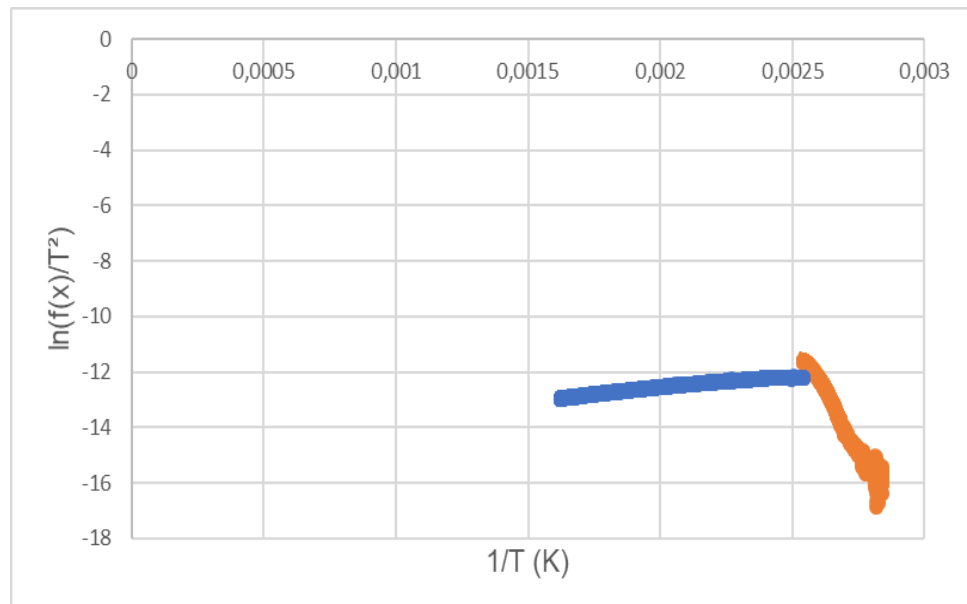


Figure 4.8: Coats-Redfern method used for the dehydration of boric acid at 2 K/min
(Region-I, Orange; Region-II, Blue).

In Table 4.2 it is possible to see R^2 values for different orders of reaction calculated for the two regions using a heating rate of 2 K/min.

Table 4.2: R^2 values for different reaction orders using the C-R method.

| Partial order | Region I | Region II | Partial order | Region I | Region II |
|---------------|----------|-----------|---------------|----------|-----------|
| 0 | 0,9813 | 0,9872 | 1 | 0,9834 | 0,2540 |
| 1/3 | 0,9834 | 0,9617 | 3/2 | 0,9790 | 0,7492 |

| | | | | | |
|------------|--------|--------|------------|--------|--------|
| 1/2 | 0,9839 | 0,9286 | 2 | 0,9710 | 0,7907 |
| 2/3 | 0,9790 | 0,7492 | 5/2 | 0,9600 | 0,8086 |
| 3/4 | 0,9841 | 0,6242 | 3 | 0,9469 | 0,7424 |

For the two regions, Table 4.2 shows that the best r-square values were obtained at partial order 3/4 for the first region and 0 for the second region. It is expected the decrease of partial order once conversion was defined according to the initial weight to be converted to boron oxide [32]. So, a further increase in the reaction temperature, where the second reaction primarily occurs, triggered a decrease in the reaction order. However, partial orders of 0 usually are decompositions where the rate of the reaction does not change with the concentration of the reactant.

For the others heating rates (4 K/min and 8 K/min) the same procedure was repeated, and in Table 4.3 one can observe the activation energy and frequency factor obtained for each heating rate.

Table 4.3: Results of kinetic analysis using the C-R method.

| Heating rate [K/min] | Region | Partial reaction order, n | k_0 [s ⁻¹] | E_a $\left[\frac{kJ}{mol} \right]$ |
|--------------------------------|---------------|--|--------------------------|---------------------------------------|
| 2 | I | 3/4 | $1,89 \times 10^{15}$ | 132,2 |
| | II | 0 | $-1,87 \times 10^{-5}$ | -7,6 |
| 4 | I | 3/2 | $4,13 \times 10^{16}$ | 140,8 |
| | II | 0 | $-2,14 \times 10^{-3}$ | -8,0 |
| 8 | I | 3/4 | $4,04 \times 10^{12}$ | 111,2 |
| | II | 0 | $-7,32 \times 10^{-5}$ | -7,7 |

Since Region-I has high activation energy, it is concluded that the 1^o reaction plays an essential role in the accomplishment of the overall reaction once it is the step of the reaction where boric acid transforms into metaboric acid. Since the activation energy is the minimum energy that the reagents need to initiate the chemical reaction, the higher the activation energy, the slower the reaction because it increases the difficulty for the process to occur. So, with the increase in the heating rate, one can see that is more difficult the process to occur. However, Region-II presents negative activation energy. The fact that the activation energy is negative is not so reasonable, but there are reactions where the rate of the reaction decreases with increasing temperatures. This happens because when one increases the temperature, it can sometimes reduce the probability of molecules colliding as the increased momentum carries the molecules away from the potential "collision zone". So, when one tries to fit the rate constant into a C-R

model, it results in negative activation energy. However, these reactions are usually the ones without barriers, so there is no activation energy at all for the second region. The fact that there is no activation energy for the second region means that the second reaction is only dependent on the first one, which is evidenced by the fact that the reaction rate does not vary a lot at higher temperatures. Concluding, only the activation energy and frequency factor values for the region-I are interesting.

4.1.3 Muffle furnace

In these tests, an average of $2,0000\text{g}\pm 0,0030\text{g}$ of boric acid >99,8% from *Carl Roth* was put inside of ceramic crucibles (previously cleaned at the muffle furnace for about one hour at 500°C to eliminate all moisture present in the ceramic), to perform the dehydration reaction. The temperature inside of the muffle furnace, as well as the dehydration time, were the only things that change during these tests. Based on the information given by the macro TGA (see 3.2.2 and 4.1.1), the temperature range that was going to be used was restricted between $90\text{-}100^{\circ}\text{C}$ and 400°C . However, considering that the boiling point of the pure boric acid is 300°C , it is necessary to be careful when using temperatures higher than this because there may still exist boric acid in the sample that did not convert into boron oxide and evaporate, thus losing a part of the reactant. Since there may be errors associated with the conversion values, the propagation of uncertainties was performed and can be analysed in A.2.

Experiments were conducted from the lowest temperature to the highest temperature tested. During the experiments, theoretical conversion of the dehydration reaction (x) was calculated and based on that the new temperatures that were going to be used during the following tests, were selected. Moreover, regarding the dehydration time, first it was tried to use the same time for all the experiments, 10 minutes, and from the obtained results, increase or decrease the dehydration time to see if there is any significant difference.

Figure 4.9 shows the conversion variation over the temperature of some experiments performed using the same dehydration time of 10 minutes.

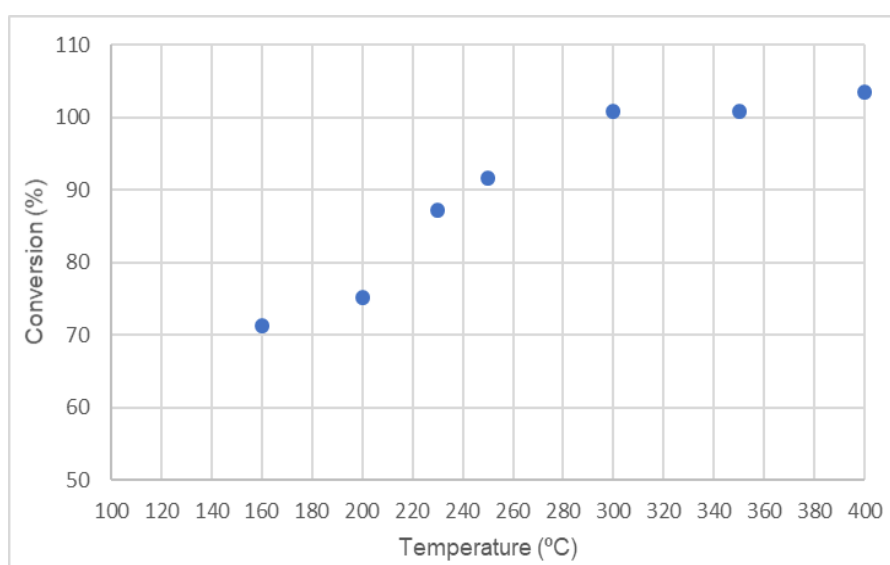


Figure 4.9: Conversion evolution over temperature, using the same dehydration time.

As expected, for the same amount of time, if one increases the temperature of the experience the conversion will increase. When temperatures close to the boiling point were reached, the dehydration conversion is near 100%.

Figure 4.10 shows the conversion variation over two hours using different temperatures. To be noted that each point of the graphic corresponds to one experiment. The rest of the experiment's results can be found attached in A.5.1.

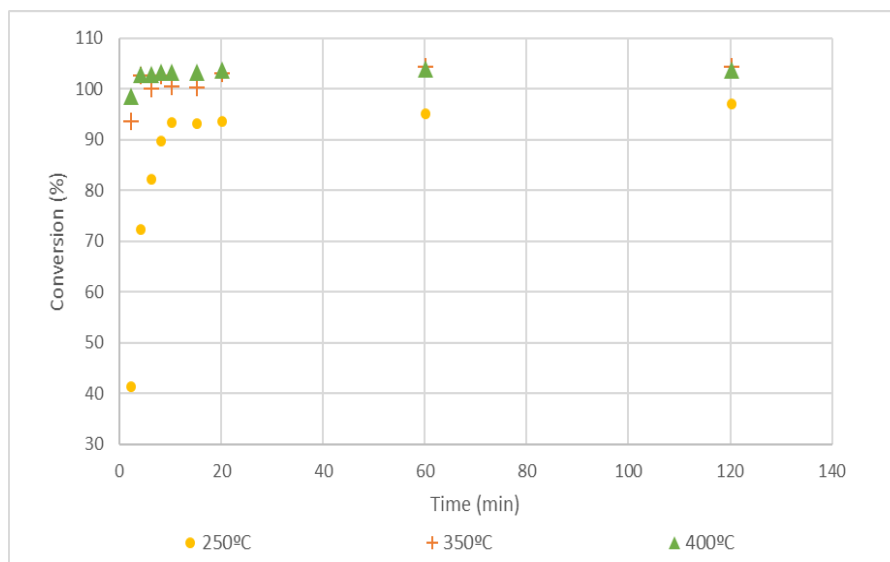


Figure 4.10: Conversion over time at different temperatures and dehydration time.

For the same temperature, conversion is increasing over time. This increase is more accentuated in the first minutes and tends to stabilise over time. For the same amount of time, the same happens to conversion, that is, conversion increases with temperature. Also, when one uses higher temperatures, the conversion is practically the same at any time and always above 100% (maximum 105%). There are some explanations for this to happen: the first is the 300°C of boric acid boiling point which means that when this temperature is reached if any boric acid, which has not yet converted due to the time factor, is still present, it can evaporate. That is if one increases the time of the experiment at temperatures below 300°C to convert all the boric acid in metaboric acid and after that increase the temperature it is probable that the conversion values will be closer to 100% without boric acid losses. The other reason is the use of ceramic crucibles. After the reaction, it has been found that these are damaged (see Figure 4.11) which may mean that the coating of the crucible reacts with the boric acid or metaboric acid, thus decreasing the amount of reagent that will be used for the dehydration. Since these hypotheses decrease the amount of reagent that will be used for dehydration and conversion calculations are based on the ratio between the experimental water mass difference, and the theoretical mass of water at the beginning, if there is a reagent loss the final mass will be lower than expected because the reagent loss will be considered as water loss, translating into higher-than-expected conversions. Furthermore, the conversion results may have some systematic and random errors associated. The propagation of errors associated with the scale where the boric acid was measured was calculated and can be analysed in A.2. It was concluded that this error is too small (until 0,02 %), so the other justifications are more correct to justify the fact that the conversion is above 100%. Hereupon, the errors will not be shown in the tables

and graphics.



Figure 4.11: Ceramic crucible after the dehydration reaction.

Overall, it is essential to make a compromise between conversion, temperature and dehydration time. That way, of all the experiments performed, the experiments using temperatures around 250°C, more specifically at 250°C for 10 minutes, a temperature range between 160 and 250°C (see Figure 4.12) and 350°C for 10 minutes, were the best ones to perform the dehydration, obtaining conversions above 90%.

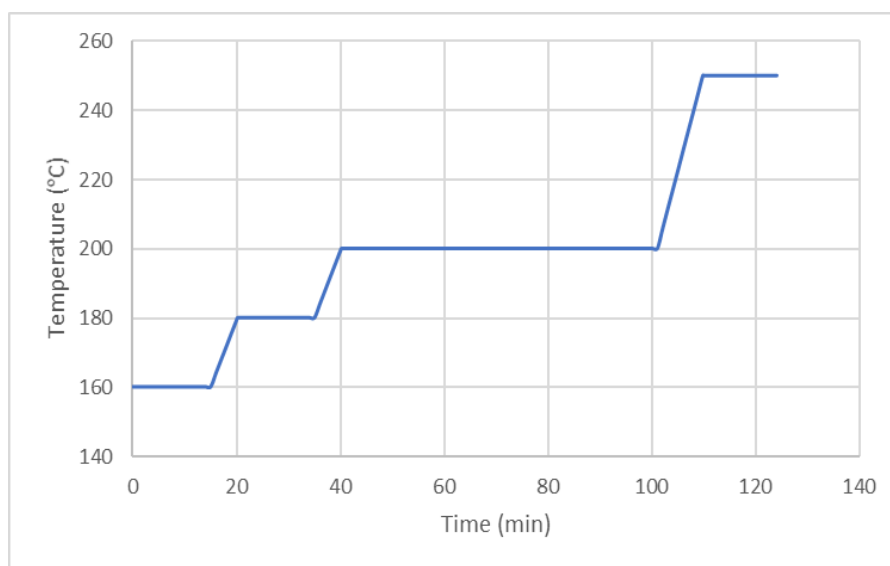


Figure 4.12: Heating rate for the experiment between 160°C and 250°C.

The results of these experiments can be analysed in Table 4.4.

Table 4.4: Dehydration results in the optimum conditions of temperature and dehydration time.

| Temperature [°C]/Time [min] | 160°C, 15 min | 250°C | 350°C |
|-----------------------------|--|---------|---------|
| | + 180°C, 15 min + 200°C 60 min + 250°C 15 min. | 10 min | 10 min. |
| $m_{H_3BO_3\ inicial} (g)$ | 2,0010 | 2,0003 | 2,0010 |
| $m_{final} (g)$ | 1,1700 | 1,1785 | 1,1201 |
| $\Delta m (g)$ | 0,83100 | 0,82180 | 0,88090 |
| W_{H_2O} | 0,8738 | 0,8735 | 0,8738 |
| $x (\%)$ | 95,10 | 94,08 | 100,8 |

Since one of the primary goals is to find the optimum temperature and dehydration time that is going to be used in future TCES applications, ensuring that the conversion is at least 90%, according to all the information above it is better to use temperatures of 250°C with a dehydration time between 10 to 20 minutes. The main reasons are that the conversion is above 90% and it is possible to save at least 1h50min of dehydration time when comparing these results with the experiment that took 2 hours to be completed (Figure 4.10). Also, increasing the conversion by approximately 4% is quite time-consuming, and it is not worth spending a further 1h50min to increase only 4% of conversion. Besides that, the criteria used to choose between the temperature of 250°C and 350°C or 400°C is the boiling point of boric acid and the fact that is possible to reduce costs using lower temperatures and dehydration time but maintaining the conversion higher enough to store energy and perform the rehydration step.

Additionally, these samples were analysed with Raman spectroscopy, to confirm if the final dehydration product is boron oxide, as expected (see 5.1.2).

Appearance of the final dehydration product

Regarding the final appearance of the product, it usually was in a pasty melting state, with little bubbles of possible BO inside when it came out of the muffle but forming a glassy/vitrified solid when it was at room temperature. The results obtained were very similar to the description gave by [43]. However for temperatures above 300°C and with longer dehydration time (about 2 hours) the final product underwent a molten bath state (more liquid than the pasty melting state) when it came out of the muffle and a glassy solid after cooling down. These differences can be seen in Figure 4.13, and Figure 4.14 and the molten bath state is easily justified because at this temperature amorphous boron oxide that has formed, can become soften at 325°C [36].



Figure 4.13: the General look at the product after dehydration below 300°C.



Figure 4.14: Dehydration for 10 min at 350°C.

This glassy solid is easy to crush and grind but very difficult to remove entirely out of the crucible. As referred before, when one tried to clean the ceramic crucibles after using them, it was possible to note that the coating of the ceramic crucibles was damaged during the experiment and some part of the sample stay stuck on the bottom of the crucible. This event takes place once boric acid and boron oxide are used in the glass industry and to produce coatings, and they may react with the ceramic crucibles coating. For this reason, metallic crucibles were tested, and the result was even worse. The sample, after dehydration, was stuck entirely into the walls of the metallic crucible and impossible to remove, even a little part of the sample, to analyse its content.

Generated boric acid

After finding the best temperature and time conditions to perform the dehydration at atmospheric pressure, it was possible to repeat the same experiments but with generated BA from Joana Reis's experiments [67], with λ of 10. The objective was to compare the conversion results using pure and generated boric acid, verify the difference in the conversion values and to know if it is possible to perform the dehydration reaction with the product of the rehydration. Even though it was stated before that the temperature of 250°C for 10 minutes was the best option to perform the dehydration, the tests with generated boric acid were made for the best three conditions of temperature and time found, to have more information.

It is important to say that λ is the water ratio defined as the ratio of the amount of water to the stoichiometric needed amount of water and lambda of 10 was chosen according to Joana's thesis.

Generated boric acid after the rehydration process is dissolved in water. To be able to use it in the dehydration step, it must be dried to remove excess water. Three different conditions used for the drying process can be found in Table 4.5.

Table 4.5: Conditions used to dry generated BA.

| Equipment | Conditions |
|-------------------|--|
| Muffle furnace | 75°C, one day |
| | 65°C, two days |
| Vacuum filtration | 400 mbar until it does not appear to have water. |

The muffle furnace conditions were chosen according to equations 2.8 to 2.11 while in vacuum filtration, 400 mbar of pressure were used until the sample looks dry. Since only the rehydration results were satisfactory with the vacuum filtration, obtaining only boric acid, the following data shown refer to the results obtained exclusively with this drying process. In the end, the generated BA was analysed through Raman spectroscopy, and the results confirm the chosen method (Figure 5.10).

Figure 4.15 shows the appearance of the generated boric acid after the drying process. It is possible to see that the particle shape and dimension are different from the pure BA (see Figure 2.4). Figure 4.16 shows the final appearance of the sample after the dehydration process. As it is possible to see, Figure 4.16 is very similar to the final product (Figure 4.13 and Figure 4.14) produced with pure boric acid which means that the particle dimension and shape of the generated BA does not show any influence in the final appearance of the product.

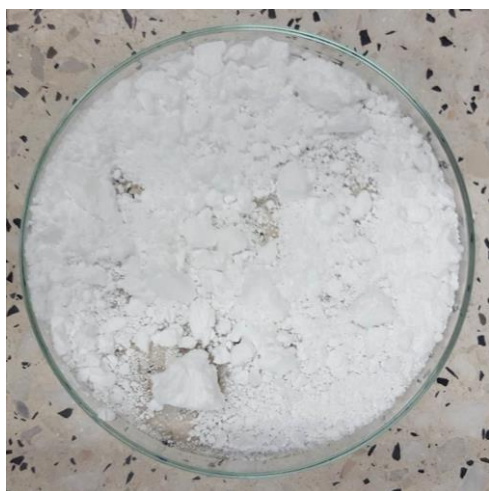


Figure 4.15: Generated BA after drying process.

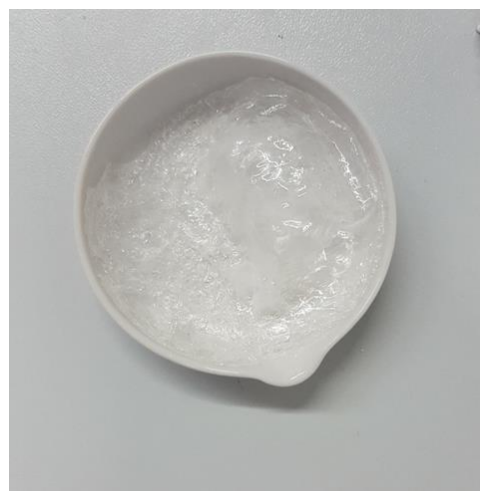


Figure 4.16: BO after dehydration reaction, using generated BA.

In Table 4.6 it is possible to see the dehydration conversion for the optimum temperature and time conditions using Joana's generated boric acid.

Table 4.6: Dehydration conversion for the optimum conditions using generated BA.

| Temperature [°C]/ Time [min] | 160°C, 15 min + 180°C, 15 min + 200°C 60 min + 250°C 15 min. | 250°C 10 min. | 350°C 10 min |
|----------------------------------|---|------------------|-----------------|
| $m_{H_3BO_3\text{ inicial}} (g)$ | 2,0003 | 2,0005 | 2,0000 |
| $m_{final} (g)$ | 1,1723 | 1,2006 | 1,1413 |
| $\Delta m (g)$ | 0,82800 | 0,79990 | 0,85870 |
| W_{H_2O} | 0,8735 | 0,8736 | 0,8734 |
| $x (\%)$ | 94,79 | 91,57 | 98,32 |

As expected the conversion values for generated boric acid are lower than with the pure boric acid, with a deviation of 0,36%, 2,67 % and 2,47% for 160°C to 250°C, 250°C and 350°C, respectively. These deviations may be due to some impurities that arose during the rehydration or the drying process or due to the different particle sizes and shape of the generated boric acid, which although not seems to influence the final appearance of the dehydration product, may show some influence in its composition and conversion.

This way, the influence of particle size on the conversion was analysed for this temperature/time conditions.

Particle size influence in the dehydration reaction

The particle size influence in conversion was studied once there was a difference between the conversion using generated and pure boric acid. The results of these tests, as well as the previous explanation about how it is possible to obtain different particle sizes of boric acid for the experiment, can be seen in the appendix A.5.1 and A.6.

To summarise, it was expected to obtain higher conversions with smaller particle sizes due to the higher contact surface for heat transfer. However, it is not possible to conclude that the particle size can influence the dehydration reaction conversion. On the one hand, the results obtained at 250°C for 10 minutes show that the conversion is a little bit higher when using bigger particles sizes. However, on one the other hand, it is not possible to conclude nothing with the results using a temperature range 160°C+180°C+200°C+250°C once there is no pattern in the conversion values, and they are very similar to each other.

Energy density

Based on the previous data it is now possible to calculate the energy density (equation 4.3) for each temperature and time conditions selected. Table 4.7 depicts the enthalpy of reaction and the energy density data for each temperature/time conditions.

Table 4.7: Energy density values the bests temperature/time conditions.

| | Type of boric acid used | 160°C, 15 min + 180°C, 15 min + 200°C 60 min + 250°C 15 min. | 250°C 10 min. | 350°C 10 min |
|--|-------------------------|---|------------------|-----------------|
| $\Delta H_R^m \left[\frac{kJ}{mol} \right]$ | Pure | 169,02 | 160,64 | 80,14 |
| | Generated | | | |
| $E_\rho \left[\frac{MJ}{m^3_{H_3BO_3}} \right]$ | Pure | 1872 | 1760 | 940,8 |
| | Generated | 1866 | 1713 | 917,6 |

4.1.4 Evaporation device

At the beginning of these experiments, an average of 5,00±0,01g of pure boric acid was put into the Büchner flask. First of all, the experiments were done with a magnetic stirrer, but it did not mix correctly, and all the product went to the walls of the flask. Although an appropriate stirrer would improve the uniform heating of the reactant, in this case, with the existing stirrer, would only get worse, so it was decided to perform the experiments without a stirrer.

After that, a pressure around 175 mbar was reached, and the product was heated up to the desired temperature. One should note that the vacuum pump is not very consistent regarding the pressure achieved and may vary a little between experiments.

Concerning the choice of temperatures and dehydration time, they were chosen based on the muffle furnace experiments. First, the same temperatures and time conditions were used, especially the optimum temperature and time conditions determined for the muffle furnace. Although these conditions work at atmospheric pressure, obtaining conversion values near 100% (see 4.1.3) the same did not happen when working below atmospheric pressure, obtaining conversion values underneath 80%. These results were not expected since the decrease in pressure decreases the melting point and boiling of the boric acid. However, in an evaporation device, if one wants to use lower temperatures, the time to achieve a higher conversion will be longer when compared to muffle furnace due to the different temperature gradients. This condition can, in fact, be suitable for other applications where time factor is not essential but concerning specifically TCES it can be a drawback. For example, working at 250°C for 10 minutes in the muffle results in 92% conversion while in evaporation device only 67% of conversion was achieved, which forces to increase the dehydration time in 20 min to obtain a higher conversion of 96%. So, it was tried to use higher temperatures until 350°C (maximum temperature of the heating plate existing in the laboratory) to see if the conversion increased and in fact, it worked.

In all dehydration experiments, the best results were obtained with “250°C for 30 min”, “300°C for 30 min” and “150°C for 30 min+150°C to 300°C for 4,02 min+300°C for 60 minutes” (27-150°C:3,3 min+150°C for 30 min+150-300°C: 4,02 min+300°C:60 min; a total of 97,3 minutes). Table 4.8 shows the results of the best experiments made and the rest of the experiments done can be found in the

annexe A.5.2 in more detailed.

It is important to mention once again that it is vital to make a compromise between temperature, dehydration time and conversion. So, using the conversion value as the decisive factor, if it is possible for the same amount of time uses a lower temperature, the lower temperature will be preferentially chosen, even if the conversion is 2,7% lower. Therefore, in this case, 250°C for 30 min is considered the optimum temperature/time conditions to use in TCES. Even so, these results were confirmed with the help of a chemical analysis method (see 5.1.2).

Table 4.8: Dehydration results in the optimum conditions of temperature and dehydration time.

| Temperature [°C]/ Time [min] | 250°C for 30 min | 300°C for 30 min | 150°C for 30 min |
|----------------------------------|------------------|------------------|-----------------------|
| | | | + 300°C for 1 hour |
| $m_{H_3BO_3\text{ inicial}} (g)$ | 5,00 | 5,00 | 5,00 |
| $m_{\text{final}} (g)$ | 2,90 | 2,84 | 2,97 |
| $\Delta m (g)$ | 2,10 | 2,16 | 2,03 |
| W_{H_2O} | 2,18 | 2,18 | 2,18 |
| $x (\%)$ | 96,2 | 98,9 | 93,0 |

Appearance of the final dehydration product

The main advantage of working below atmospheric pressure is the final appearance of the product obtained. In this case, it is a hard powder (Figure 4.17), entirely different than the glassy solid obtained through dehydration in the muffle furnace, which can easily be crushed and is extremely easy to solubilise in water during the rehydration test. This difference is probably due to sublimation of boric acid before the reaction occurs.

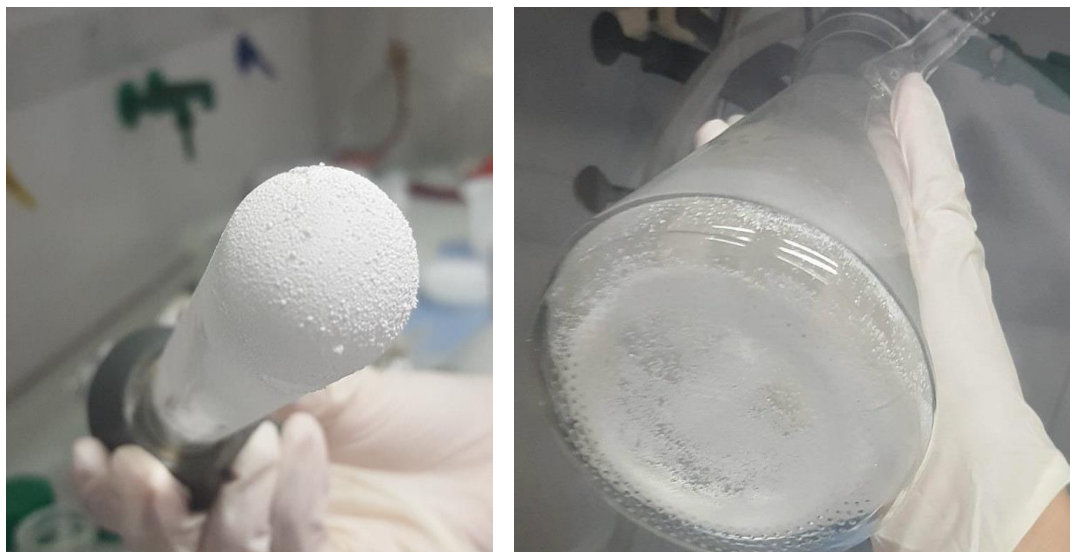


Figure 4.17: Results of the dehydration reaction below atmospheric pressure.

In Figure 4.18 it is possible to see the difference between boric acid and the boron oxide produced using pure boric acid, which is agglomerated, and the particles are more defined and less bright. The drawback of this apparatus is that in all the experiments that were made, the sample sublimed and recrystallised again in the cold finger, which makes it more difficult to remove all the product to measure the mass difference at the beginning and the end of the experiments. For this reason, this apparatus has a lot of associated errors (scale errors and operator errors) that decrease the veracity of the results.



Figure 4.18: Difference between sheer boric acid(left) and generated boron oxide (right).

Generated boric acid

The tests performed with the optimum temperature and dehydration time conditions defined above were repeated using the same procedures as in muffle furnace but with generated boric acid from Joana Reis's experiments. Figure 4.19 shows the final appearance of the product after dehydration below atmospheric pressure. It is possible to see that it looks like the boron oxide produced with pure boric acid (Figure 4.18) which proves once again that the particle size of the boric acid does not influence the

final appearance of the dehydration product.



Figure 4.19: Boron oxide after dehydration with generated boric acid.

In Table 4.9 it is possible to see the dehydration conversion for the best temperature and time conditions, using Joana's generated boric acid.

Table 4.9: Dehydration results in the optimum conditions using generated boric acid.

| Temperature [°C]/ Time [min] | 250°C for 30 min | 300°C for 30 min | 150°C for 30 min |
|---------------------------------|------------------|------------------|-----------------------|
| | | | + 300°C for 1 hour |
| $m_{H_3BO_3\ inicial} (g)$ | 5,00 | 5,00 | 5,00 |
| $m_{final} (g)$ | 3,03 | 2,85 | 2,96 |
| $\Delta m (g)$ | 1,97 | 2,15 | 2,04 |
| W_{H_2O} | 2,18 | 2,18 | 2,18 |
| $x (\%)$ | 90,2 | 98,5 | 93,4 |

Comparing Table 4.8 and Table 4.9, the dehydration conversion values using generated boric acid are lower than the ones obtained with pure boric acid with a deviation of 6,2%, 0,5% and 0,5%, respectively. It is also verified that the deviation is more pronounced when the temperature is lower. Once again, a possible explanation for that can be the particle shape and size of boric acid or the operator error when the sublimation of boric acid occurs (if the sublimation occurs the product will be stuck in the cold finger and must be removed before weight). However, it is exceedingly difficult to remove all the product. The explanation for the fact that for "150°C (30min) + 300°C (60 min)" better results were obtained using generated boric acid instead of pure boric acid is that it may still exist water in generated boric acid, but

it is not shown in Raman spectroscopy.

Concluding, the best advantage of working under atmospheric pressure is the final appearance of the product.

Particle size influence in the dehydration reaction

Particle size influence in the dehydration conversion was once again tested, using the optimum temperature and time conditions cited above the results can be found in A.5.2 (Table 7.11), but once again it is impossible to conclude anything.

Energy density

Based on the previous data it is now possible to calculate the energy density for each temperature and time conditions. Table 4.10 presents the enthalpy of reaction and the energy density data for each temperature/time conditions.

Table 4.10: energy density values the bests temperature/time conditions.

| | Type of boric acid used | 250°C for 30 min | 300°C for 30 min | 150°C for 30 min+300°C for 60 min |
|--|-------------------------|------------------|------------------|-----------------------------------|
| $\Delta H_R^m \left[\frac{kJ}{mol} \right]$ | Pure | 160,69 | 75,157 | 164,66 |
| | Generated | | | |
| $E_\rho \left[\frac{MJ}{m_{H_3BO_3}^3} \right]$ | Pure | 1800 | 865,8 | 1783 |
| | Generated | 1688 | 861,8 | 1792 |

Chapter 5

Analysis methods

This chapter explains the analysis methods used to analyse the final dehydration product.

5.1 Introduction

It is expected that at the end of the dehydration, boron oxide exists in the final product. Finding an appropriate method to analyse the generated boron oxide proved to be a difficult task because, as it was discovered during the experiments, generated boron oxide is always in a glassy form ($g\text{-}B_2O_3$) instead of crystalline. To confirm if boron oxide is in the final product, on one hand, a rapid rehydration test was conducted, where it was possible to calculate the rehydration conversion and see the reversibility of the reaction. On the other hand, some chemical analysis methods were tested to confirm if there are boric acid residues or metaboric acid in the sample, besides boron oxide.

Figure 5.1 presents the methodology used for the analysis methods.

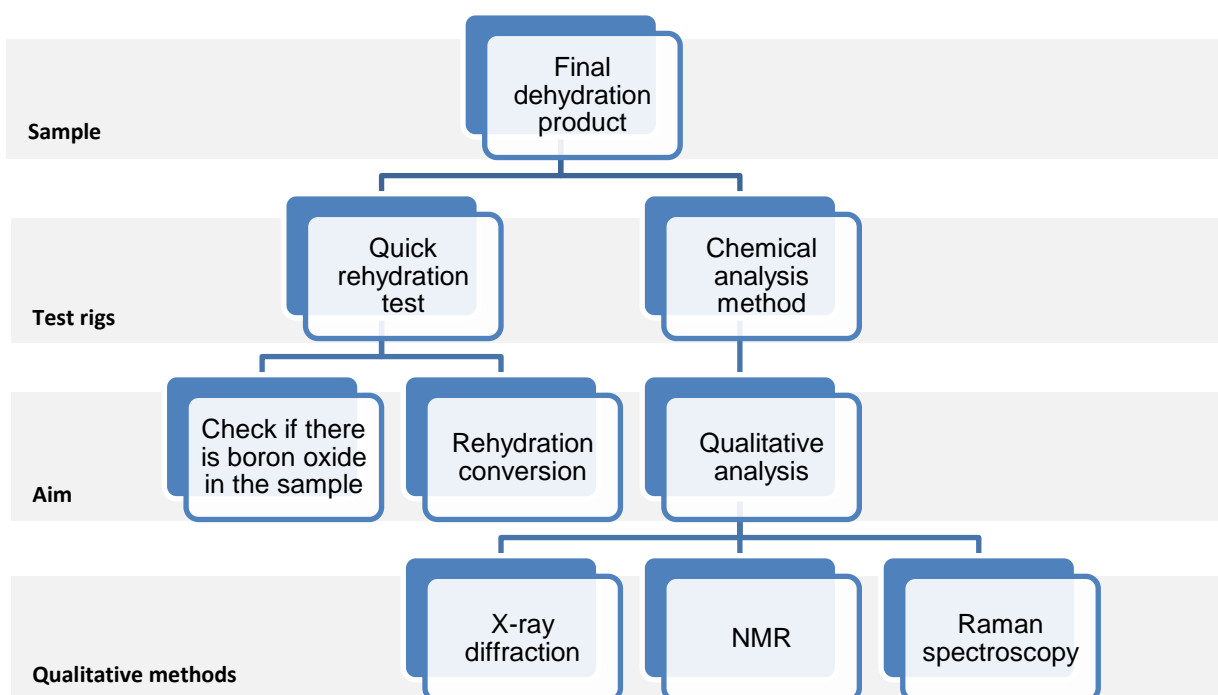


Figure 5.1: Methodology used for the analysis methods.

5.1.1 Rehydration tests

To have an immediate response to the content of the dehydration product and to know what is the difference of performing the rehydration step of the reaction with boron oxide produced with pure or generated boric acid, the final product was rehydrated in a very simple test rig, that can be seen in Figure 5.2. Since the rehydration reaction is exothermic, it is known that if the temperature increases, there will be boron oxide in the dehydration product, which is converted again into boric acid. The test rig includes a thermometer (PCE-T390) with two thermocouples (one to measure the water temperature and the other one to measure the temperature increase during the experiment) and a flask.

That way, if the temperature increases, the sample should be analysed with a suitable chemical analytical method.

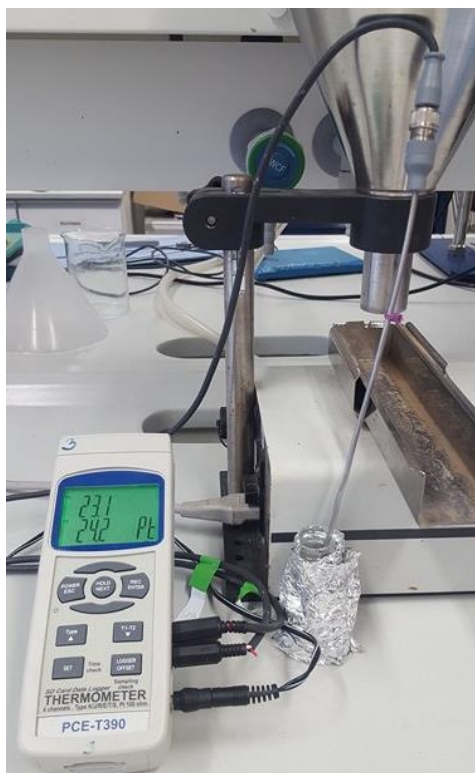


Figure 5.2: Rehydration test rig.

First, according to solubility data of pure boron oxide and boric acid, it was possible to narrow the water volume used in these tests and see the variation of ΔT . This way, 3 mL and 7 mL of water at room temperature (23,8°C) and at 30°C were added to the final product. The results can be seen in Table 5.1.

Table 5.1: Rehydration tests of pure boron oxide.

| V_{H_2O} added [mL] | ΔT | |
|--------------------------|---------------------------------|-------------------------------|
| | $T_{H_2O} = 23,9^\circ\text{C}$ | $T_{H_2O} = 30^\circ\text{C}$ |
| 3 | 9,8 | 3,6 |
| 7 | 4,6 | 1,3 |

From this information, it is possible to conclude that for the same water temperature, with less water the ΔT will be higher. However, using the same amount of water but with different water temperature, with less temperature, the ΔT will be higher.

Therefore, the following experiments were done with 7 mL of water at room temperature (23,9°C). The water was added and mixed to 0,2000±0,0050 g of final dehydration product that was already inside of the insulated flask, and the temperature increase was recorded. To be noted that all the rehydration

tests made had an average duration of 60 seconds.

From the experience data, a calibration line was made based on the conversion of the reaction and the heat released during the experiment (Figure 5.3). The three points, from left to right, represent the experiment made with pure boric acid, pure metaboric acid and pure boron oxide. With this, it is possible to have an idea of the sample's content, that is, if there is only boron oxide in the sample or if there is boric acid or metaboric acid too.

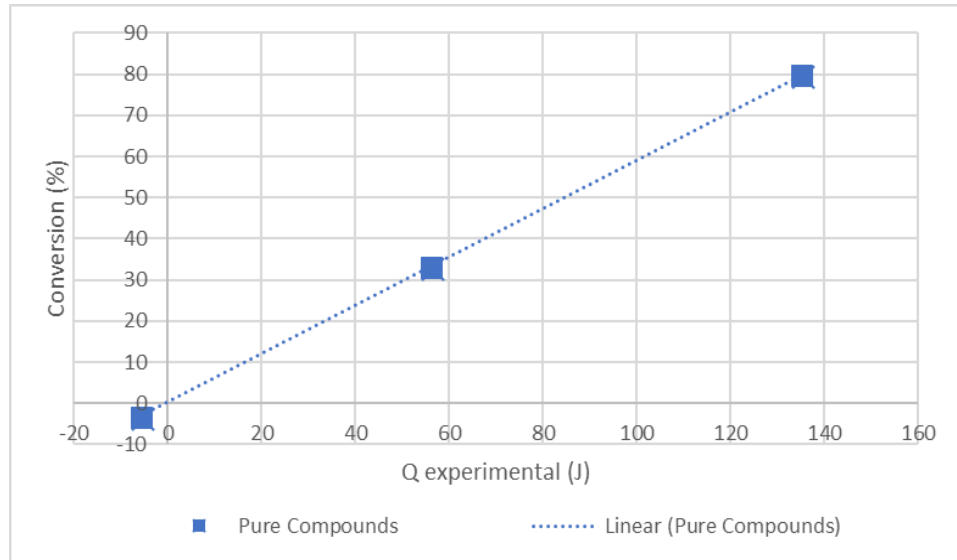


Figure 5.3: Calibration line for 7 mL of water, at 23,9°C ($\alpha(\%) = 0,5876Q + 0,3780$, $R^2 = 1$).

For the calibration lines, rehydration conversion, α , was calculated based on the ratio of heat released on the reaction ($Q_{experimental}$) and the theoretical one that is supposed to be released ($Q_{theoretical}$).

$$\alpha = \frac{(n_{H_2O} [\text{mol}] + n_{B_2O_3} [\text{mol}]) \cdot cp_{mix} [\text{kJ/mol}\cdot\text{K}] \cdot (T_{[K]} - T_{H_2O} [K]) - \text{heat loss} [\text{kJ}]}{n_{B_2O_3} [\text{mol}] \cdot \Delta H_r [\text{kJ/mol}]} \quad (5.1)$$

Where:

- T - Temperature after the rehydration test;
- T_{H_2O} - Water temperature used for the rehydration test (23,9°C);
- ΔH_r - Enthalpy of the rehydration reaction (23,9°C) using liquid water (58,59 kJ/mol);
- cp_{mix} - Heat capacity of the mixture calculated through equation 5.2;

$$cp_{mix} [\text{kJ/mol}\cdot\text{K}] = \left(\frac{n_{B_2O_3}}{n_{B_2O_3} + n_{H_2O}} \right) \cdot cp_{B_2O_3} [\text{kJ/mol}\cdot\text{K}] + \left(\frac{n_{H_2O}}{n_{B_2O_3} + n_{H_2O}} \right) \cdot cp_{H_2O} [\text{kJ/mol}\cdot\text{K}] \quad (5.2)$$

- $cp_{B_2O_3}$ - Heat capacity of boron oxide at 23,9°C (75,24 J/mol.K)
- cp_{H_2O} - Heat capacity of liquid water at 23,9°C (62,54 J/mol.K)
- $n_{B_2O_3}$ - Number of moles of the dehydration final product. It is supposed to be boron oxide, but

it can be boron oxide and boric acid or metaboric acid, reason why " B_2O_3 " is written in quotation marks.

The equation used to calculate the rehydration conversion (equation 5.1) considers the heat loss to the surroundings. With the aim of measuring the temperature decrease, an experience was performed with water between 28,5°C (maximum temperature achieved in the experiments) and 23,9°C (initial temperature of the water) over time, to know if the heat loss to surroundings has a significant influence on the conversion calculations. For this experiment, the same conditions as the rehydration test were used and in Figure 5.4 and Figure 5.5 it is possible to analyse the results. According to the graphics temperature decrease about 0,3°C during the 60 seconds of the experiment. So, the heat loss is close to zero and for this reason, can be neglected.

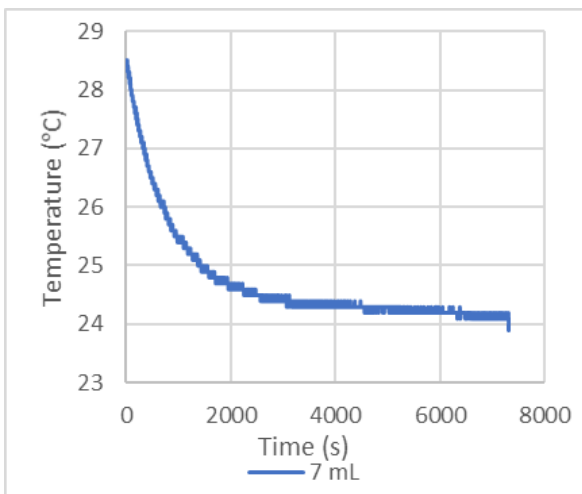


Figure 5.4: Water temperature variation over time.

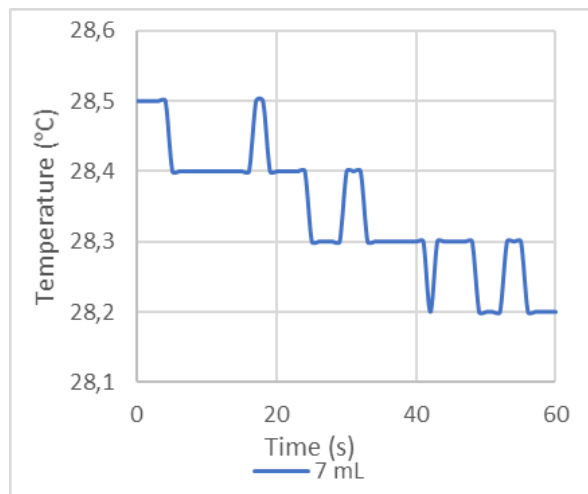


Figure 5.5: Water temperature variation during the 60 seconds of the experiment.

Concerning the experiments performed using muffle furnace final product (Figure 5.6, left), the results were similar for all the experiments done with different temperature and time conditions. In all, the final product did not dissolve properly in water, and the water stayed transparent, but a part of the hard flakes was at the bottom of the flask. However, there was a temperature increase, which proves that there is boron oxide in the samples.

For the experiments performed using the evaporation device final product (Figure 5.6, right) the samples were a hard powder instead of a glassy solid and when one tried to dissolve the dehydration product in water, everything was dissolved and the ΔT obtained in these experiments were higher than in the muffle furnace experiments.



Figure 5.6: Rehydration of boron oxide produced in the muffle furnace (left) and in the evaporation device (right) using 7 mL of water.

In Figure 5.7 and Figure 5.8 it is possible to compare the calibration line for the rehydration of boron oxide produced with pure boric acid and with generated boric acid, respectively. To be noted that only the optimum temperature and time conditions determined in 4.1.3 and 4.1.4, were shown.

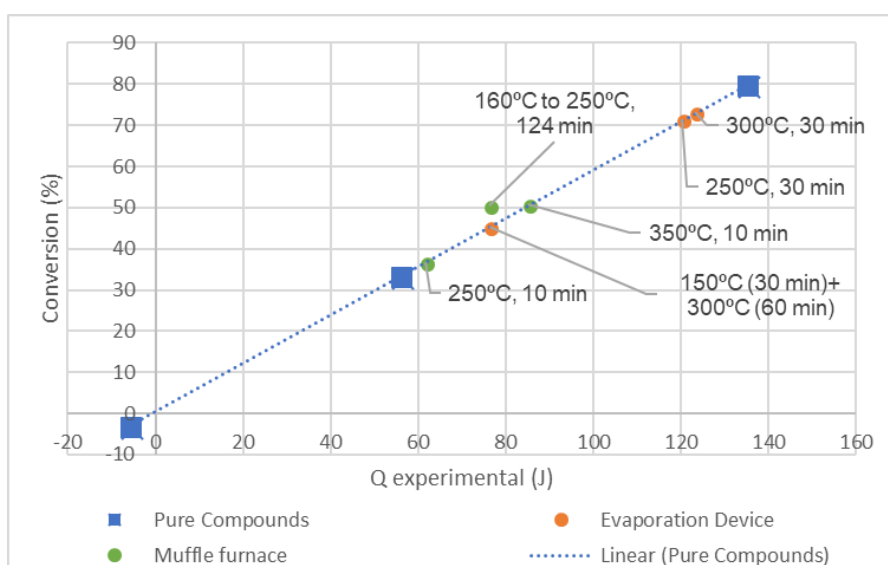


Figure 5.7: Rehydration of boron oxide produced with pure boric acid.

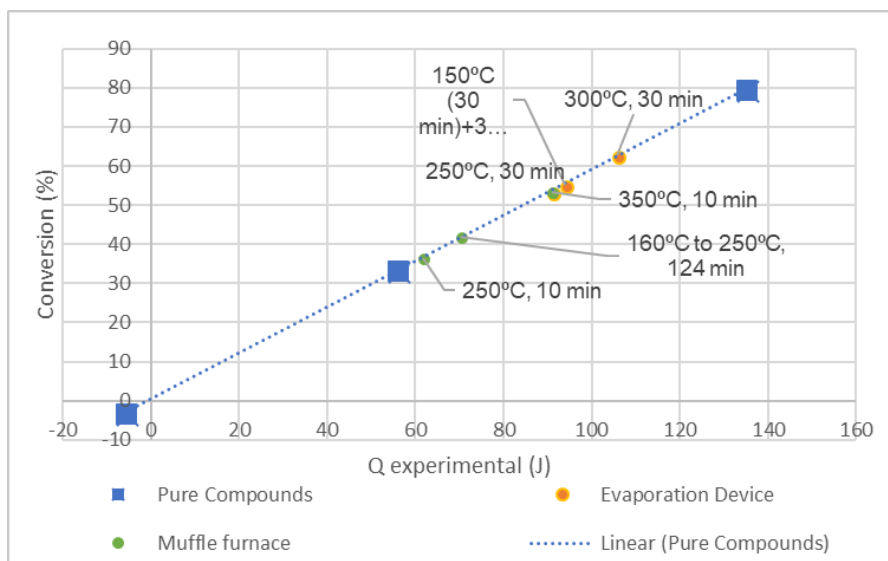


Figure 5.8: Rehydration of boron oxide produced with generated boric acid.

In general, looking at the graphics, it is possible to conclude that the results obtained using the samples produced in the evaporation device are better than using the ones produced in the muffle furnace, mostly because of the powder appearance of the boron oxide, which is easy to dissolve in water. The best rehydration conversion was obtained with the samples of the evaporation device at 300°C for 30 minutes followed by 250°C for 30 minutes. The other conclusion is that there is boron oxide in the final dehydration product of both test rigs, which is concordant with the dehydration conversion presented in 4.1.3 and 4.1.4. Nevertheless, it is not 100% boron oxide otherwise the conversion will be just like pure boron oxide, but a mixture of metaboric acid, boron oxide and probably boric acid residues.

Through this method, it is only possible to know that there are other compounds in the sample, but it is not possible to know if it is metaboric acid or boric acid. Therefore, a chemical analysis was performed to know the qualitative composition of the final dehydration product and to see if the dehydration of boric acid was successfully done.

5.1.2 Chemical analysis methods

Analytical chemistry techniques can be split into two main types:

- Qualitative - the aim is to establish the presence of a given element, compound, or phase in a sample;
- Quantitative - pursues to establish the amount of a given element, compound, or some other component in a sample.

Some qualitative/quantitative analysis methods can be used, like X-ray diffraction, NMR or Raman spectroscopy.

X-ray diffraction (XRD) [49],[50]

X-ray diffraction is a non-destructive technique used quantitatively to recognise the crystallinity, orientation and the composition of a compound, in which the crystalline atoms make an incident X-ray beam and diffract in many specific directions. Besides that, this technique is used to determine structural properties of a compound like its grain size, phase composition, strain and its atomic arrangement.

By analysing the scattered intensity of an X-ray beam when it hits a sample as a function of incident and scattered angle, polarisation, and wavelength or energy, it is possible to determine the structure of that sample.

Although XRD is used for chemical analysis of boric oxide by a few researchers, this is not a proper technique because the generated boron oxide obtained is an amorphous solid. Moreover, boron is a light compound and the results obtained are not reliable.

Nuclear Magnetic Resonance (NMR) [70]–[72]

NMR is a quantitative and qualitative analysis used to determine the structure of many compounds by studying the bands of nuclear magnetic resonance spectra. These compounds can be previously known or not. For unknown compounds, NMR can either be used to match against spectral libraries or to infer the primary structure directly.

In this analysis, the nuclei absorb and emit electromagnetic radiation. This energy is at a specific resonance frequency which depends on the strength of the magnetic field and the magnetic properties of the isotope of the atoms. It was performed a proton NMR, that is, the application of nuclear magnetic resonance in NMR spectroscopy concerning hydrogen-1 nuclei within the molecules of a substance (^1H NMR) and ^{11}B NMR.

The final dehydration product must be dissolved in methanol, water or glycerol, to use this technique. However, on the one hand, it is not possible to use water to dissolve the final product because it will react with the boron oxide to form boric acid. On the other hand, if one uses methanol or glycerol to dissolve the final product, it is also not possible because the boron oxide will also react with these alcohols forming esters and boric acid [27]. Thereby, NMR analysis is not a suitable method to analyse boron oxide obtained from dehydration of boric acid.

Raman spectroscopy [68],[72],[73]

Incident laser light in the UV, visible or NIR, is scattered inelastically from molecular vibrational modes. When molecules scatter monochromatic radiation, a small fraction of the scattered radiation is absorbed because it has different frequency when compared to the incident radiation; this is known as Raman effect.

Raman analysis is a non-destructive light scattering technique suitable for qualitative and quantitative analysis. It can be used for the explanation of molecular structures, locating functional groups and chemical bonds in complex mixtures and unknown materials.

Although the Raman spectra are related to the infrared absorption spectra, they are produced by an entirely different mechanism thus providing complementary information. It is important to refer that the

relative intensities of the Raman stripes and absorption bands in the infrared spectra are often different and some transitions may be weak or absent in one of the spectra. This technique is often superior to infrared for spectroscopy investigating inorganic systems because aqueous solutions can be employed.

The Raman spectra are composed of a group of stripes located on the side of the largest wavelengths about a very intense excitatory line. The distances between the Raman stripes are related to the vibrational-rotational distances of this absorption spectrum. Raman stripes are characteristic of the vibration modes of the irradiated substance and constitute a fingerprint of the substance. However, it is important to consider that the energy of the excitation radiation must be less than the minimum necessary for the molecule go to the lower excited state. Otherwise, the absorption may be followed by fluorescence (emission of light by a substance that has absorbed light or other electromagnetic radiation) and the Raman spectrum is not produced.

Of all the methods tested, Raman spectroscopy proved to be the best technique to analyse glassy boron oxide, and the results contribute to confirm the optimum temperatures and time conditions found during the experiments, which need to be used in dehydration reaction for obtaining practically 100% of boron oxide, and the conversion results.

First, it is necessary to analyse pure boric acid, pure metaboric acid and pure boron oxide samples and compare the results with literature values. According to literature, on the one hand, pure amorphous boron oxide spectrum has two distinct bands: one intense band at 808 cm^{-1} (due to boroxol rings that create the boron oxide structure) and another one, weaker, at 1260 cm^{-1} [74],[75]. On the other hand, pure boric acid has four important bands around 213 cm^{-1} , 499 cm^{-1} (strong band), 884 cm^{-1} (very strong band) and 1172 cm^{-1} (weak band) [76]. Once before the boron oxide formation, boric acid transforms into metaboric acid; it is important to know how the metaboric acid spectra are. Even though one could not find any references to metaboric acid Raman spectrum, the Raman spectroscopies for the three pure compounds were done, and it is possible to see the important bands in Figure 5.9. Comparing the information taken by the three pure spectra with the spectra obtained with final dehydration product from muffle furnace and evaporation device, it is possible to understand if the product produced by the different methods used is 100% boron oxide or if there is still boric acid or metaboric acid in the final product.

It is needed to know that this technique was only applied as a qualitative method, so the YY axis is not essential once there is no reference to compare.

Figure 5.9 confirms the data found in the literature, although the boron oxide spectrum has, in addition to the band of 808 cm^{-1} , one at 500 cm^{-1} and another at 884 cm^{-1} probably because the boron oxide used was crystalline instead of amorphous. Since these two bands do not exist in the spectrum of the amorphous boron oxide and the boron oxide produced by the dehydration will always be amorphous, these bands will not be considered for any decision. For the metaboric acid spectrum, it is possible to see that there is an important region between 400 cm^{-1} and 550 cm^{-1} , a band at 592 cm^{-1} and another at 800 cm^{-1} . However, this spectrum appears to have fluorescence that can appear due to the type of laser used, the amount of shine or even the physical properties of the sample surface but it is impossible to point out a possible reason with certainties.

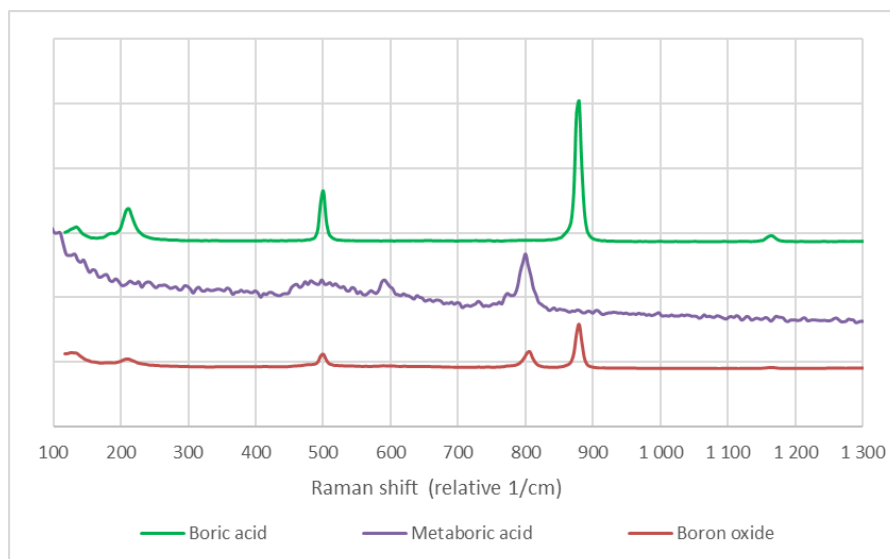


Figure 5.9: Comparison between pure boric acid, pure metaboric acid and pure boron oxide.

In all, the significant difference between boric acid and boron oxide spectra is the 808 cm^{-1} band that can only be found in boron oxide, and for this reason, it will be the decisive factor.

As referred before, after the rehydration, one has boric acid with water that must be separated and stored in different places before the dehydration reaction occurs. Figure 5.10 presents three different ways tested to dry the generated boric acid produced by Joana Reis: the first one using vacuum filtration at 400 mbar and the second and third test using a muffle furnace at 75°C for one day and 65°C for two days, respectively.

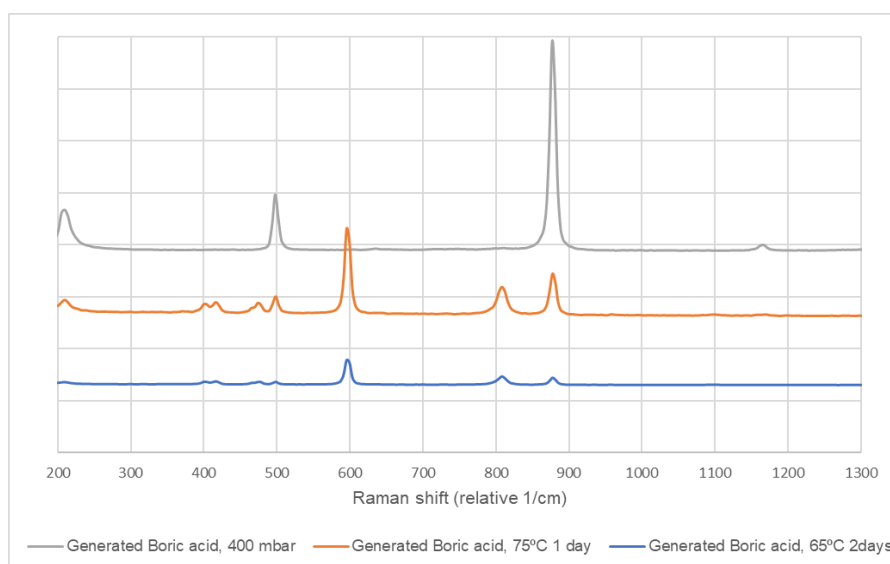


Figure 5.10: Generated boric acid dried under different drying conditions.

On the one hand, both samples, dried using the muffle furnace, present a 592 cm^{-1} band, characteristic of metaboric acid, one at 808 cm^{-1} , found in boron oxide and another band at 884 cm^{-1} , found in boric acid. This way it is possible to conclude that the drying process to remove the excess of water from the boric acid using the muffle furnace produced a mixture of boric acid, metaboric acid and boron oxide.

On the other hand, the boric acid dried using a vacuum filtration apparatus presents a graphic with a 499 cm^{-1} , 884 cm^{-1} and 1172 cm^{-1} bands, both characteristics of pure boric acid. Since in an energy storage context, the product resulting from rehydration (boric acid and water) will be stored separately, it is preferred to use the vacuum filtration to dry and separate the water and the boric acid.

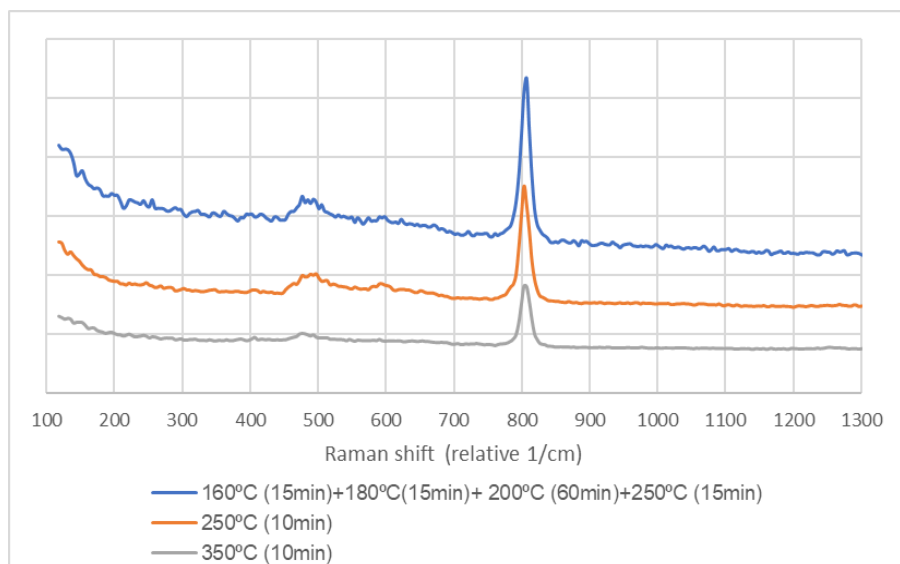


Figure 5.11: Final product from muffle furnace, produced with pure boric acid.

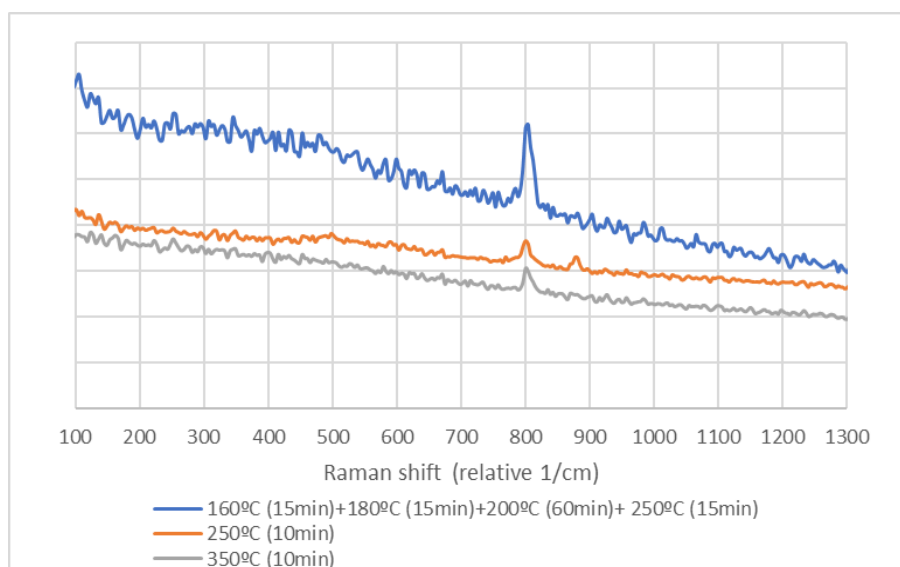


Figure 5.12: Final product from muffle furnace, produced with generated boric acid.

Figure 5.11 and Figure 5.12 show the Raman spectra of the muffle furnace final product using the best temperature and time conditions selected. Both graphics resulting from the dehydration using a temperature range between 160°C and 250°C present a band at 808 cm^{-1} , characteristic of BO, and a band between 400 and 550 cm^{-1} with fluorescence, that means that there is metaboric acid too in the samples. Concerning the final product produced using 250°C for 10 minutes, there is a difference between using sheer or generated boric acid. On the one hand, the spectrum of the final product produced with sheer BA presents a band between 450 - 550 cm^{-1} and a peak at 592 cm^{-1} , both characteristics of metaboric acid and an 808 cm^{-1} band characteristic of BO. On the other hand, in

addition to having the same bands as the previous spectrum, the spectrum produced with generated BA still has one band at 884 cm^{-1} , which means that BA still exists in the sample. Finally, for the spectrum produced at $350\text{ }^{\circ}\text{C}$ for 10 minutes both graphics present an 808 cm^{-1} band, characteristic of boron oxide, although the spectrum produced with generated BA also presents fluorescence that may mean the presence of metaboric acid too. A possible justification for having better results with pure boric acid instead of generated boric acid is the different particle sizes and shapes of the BA sample used, as mentioned in 4.1.3. One can conclude that, according to this spectroscopy, produce BO at 350°C for 10 minutes is the better option. However, once possible evaporation of the boric acid can influence the conversion results at 350°C for 10 minutes, in section 4.1.3 it was concluded that it was best to use “ $250\text{ }^{\circ}\text{C}$ for 10 minutes”. Comparing the spectra of 250°C for 10 minutes and 350°C for 10 minutes using either sheer or generated BA, it is possible to see that both results are similar, but better results were obtained for higher temperatures (because of the 884 cm^{-1} band presented in the BO spectrum produced with generated BA at 250°C). However, it is necessary to carry out further tests to see if there is a loss of BA and to estimate this loss or if the boric acid was completely converted to metaboric acid and boron oxide. Since this spectroscopy is not a quantitative analysis, it is not possible to know how much boron oxide exists in the sample comparatively the option of 250°C for 10 minutes and how much was lost. Thus, for future tests, it is necessary also to perform a quantitative analysis from this spectroscopy. In all, it is concluded that the safest option is to use “ 250°C for 10 minutes” when working with a muffle furnace.

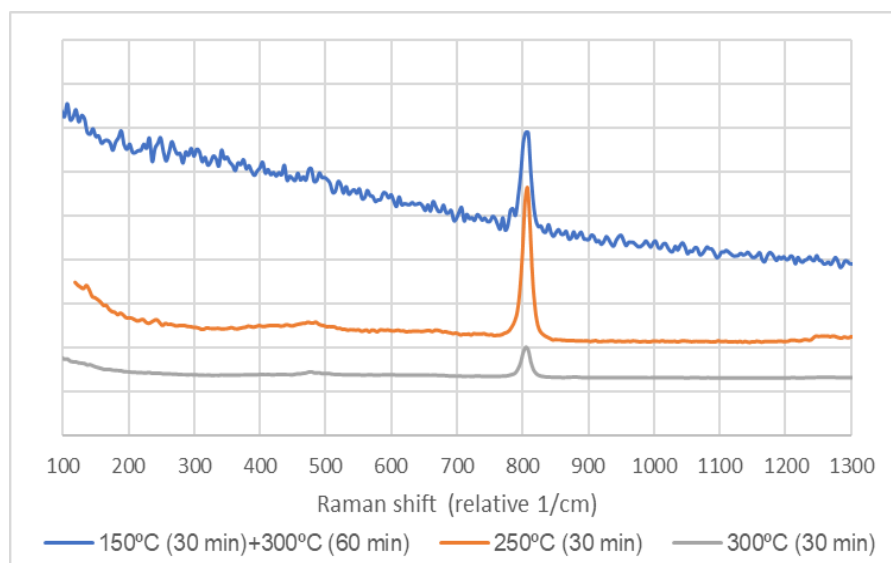


Figure 5.13: Final product from evaporation device, produced with pure boric acid.

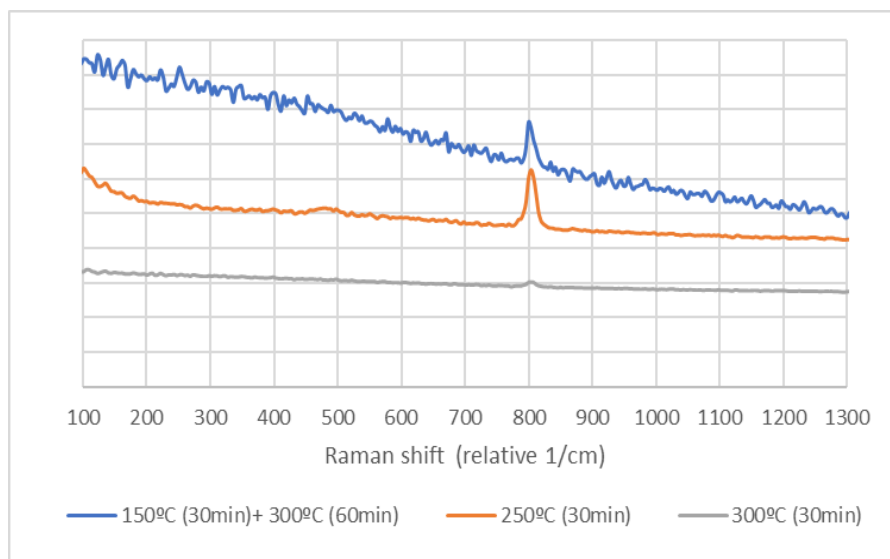


Figure 5.14: Final product from evaporation device, produced with generated boric acid.

Figure 5.13 and Figure 5.14 present the final product produced in the evaporation device using pure and generated boric acid. Both final products produced at “150°C+300°C” present a $\sim 808\text{ cm}^{-1}$ band and fluorescence, once again that it is not possible to precisely know the origin, present in the pure metaboric acid spectrum too. However, this could mean that the spectra produced at its temperature range are mostly metaboric acid. Regarding the final product produced at 250°C for 30 minutes, both graphics present one band at 808 cm^{-1} , characteristic of BO spectra. However, the dehydration product produced with generated BA presents a protuberance between $450\text{-}500\text{ cm}^{-1}$ which means that the sample is BO with a little of metaboric acid. At last, the spectra of the product produced at 300°C for 30 minutes, are also practically equal in both figures and correspond to BO because of the 808 cm^{-1} band. In conclusion, since “250°C for 30 minutes” and “300°C for 30 minutes” spectra are remarkably similar, Raman spectroscopy confirms what was stated in 4.1.4, that is, the optimum temperature and time conditions to perform the dehydration of boric acid is “250°C for 30 minutes”.

Chapter 6

Conclusions

This chapter finalises this work, summarising conclusions and pointing out aspects to be developed in future work.

6.1 Conclusions

Investigations for thermochemical energy storage systems using H_3BO_3/B_2O_3 reaction were started for the first time in TU Wien by Thomas Karel, Markus Deutsch and Kimiasadat Hashemi. The aim of this master thesis is to continue the study of this reverse system regarding its potential as a TCES, following Karel's work [19] but focused mostly on the dehydration step of the reaction.

The work presented in this master thesis was divided into two parts:

First, the mass variation with temperature was studied to see if it was concordant with the ones found in the literature, and a kinetic analysis was performed using a macro TGA and an STA, respectively. In TGA two experiments were made using 12 A of electric current and 4 L/min and 6 L/min of nitrogen flow, respectively. It was possible to note that the mass loss in these experiments were higher (experiment at 4 L/min, mass loss of $-50,84 \pm 0,08\%$ and 6 L/min, mass loss of $-46,27 \pm 0,07\%$) than the theoretical one ($-43,70\%$). This proves that there is evaporation of boric acid besides water because once the reaction occurs very rapidly, there is not enough time for the boric acid to be converted to metaboric acid. So, if the boiling point of the boric acid is reached, the boric acid remaining in the sample will evaporate. From the experiments in the macro TGA, it was concluded that the reaction starts around $90-100^\circ\text{C}$ and stops at around 400°C , which is concordant to the values given by Aghili et al. in [33].

In the STA, to determine the steps of the reaction and respective temperatures and the kinetic parameters, three isokinetic experimental runs have been conducted, using different heating rates: 2 K/min, 4 K/min and 8 K/min. Through DSC and TGA-DTG, it was possible to see that although in TGA three steps of reaction (looking at a mass loss over temperature) are observed, in DSC and DTG one can only see two endothermic steps: step-I between 90°C and $121,9^\circ\text{C}$ and step-II between $121,9^\circ\text{C}$ and $346,3^\circ\text{C}$. This situation had already occurred in Sevim et al. and Balci et al. work [32],[36] but they assume that only two steps of reaction were occurred due to the poor quality of DTA measurements. The kinetic results for the two regions observed were analysed with the C-R model-fitting method. Once the activation energy for the second region is negative, this means that there is no activation energy at all, so only the values for the first region have meaning. For the first region, using a heating rate of 2 K/min, the best r-square was obtained at a partial order reaction of $\frac{3}{4}$. The activation energy and frequency factor obtained is $132,2 \text{ kJ/mol}$ and $1,89 \times 10^{15} \text{ s}^{-1}$, respectively. These values are a little bit higher compared to the ones found in literature (for example $79,85 \text{ kJ/mol}$ at 3 K/min [36], 45 kJ/mol at 5 K/min [32] or $57,55 \text{ kJ/mol}$ at 3 K/min [33]) but the parameters were determined using different conditions so it is not possible to compare them properly.

Using the temperature range found in the macro TGA, it was possible to start the experiments in two different test rigs, with the aim of obtaining the best possible conversion (always above 90%) using the lowest temperature and dehydration time allowed, that is, the optimum temperature and time conditions. These experiments were made at atmospheric pressure, in a muffle furnace, and below atmospheric pressure, in an evaporation device, to understand how the pressure can influence the temperature and dehydration time used, the final appearance of the product and, consequently, the conversion and the energy density of the reaction.

All these experiments were done using pure boric acid from *Carl Roth* and generated boric acid from Joana Reis's experiments [67], and the results (conversion values and Raman spectroscopy) were compared. The generated boric acid, before use in the dehydration reaction, was dried by vacuum filtration at a pressure of 400 mbar, obtaining a powder with larger dimension particles than the pure one. In the end, only boric acid was obtained, and the results were confirmed by Raman spectroscopy.

The optimum conditions to work at atmospheric pressure, in the muffle furnace, found by the intentions above, are at 250°C for 10 min, obtaining a conversion of 94,08±0,02% and 91,57±0,02% for pure and generated boric acid, respectively. These conditions are the best ones because one can use a lower temperature and less time (comparing to the other temperature and time conditions presented in 4.1.3) and obtain a conversion value above 90%, reducing the financial cost. Comparing the Raman spectra of BO produced at 250°C for 10 minutes and 350°C for 10 minutes using either sheer or generated BA, it is concluded that the results at higher temperature are better since at 250°C the spectrum still presents boric acid (884cm⁻¹) when using generated BA or metaboric acid (450-550cm⁻¹) when using pure BA. However, at 350°C the boiling point of BA was exceeded, so is necessary to carry out further tests to see if there is a loss of boric acid and to estimate this loss. For this reason, it is concluded that the safest option is to use 250°C even if the conversion is 6-7% lower than at 350°C, using pure and generated BA. Energy density values are also calculated for pure and generated boric acid, obtaining values of 1769 MJ/m³_{H₃BO₃} and 1713 MJ/m³_{H₃BO₃}. The energy density values are lower than the theoretical one, once the theoretical value is calculated at equilibrium temperature (157,5°C) and the experimental values are calculated at 250°C which means that at this temperature the enthalpy of fusion of the boric acid needs to be added, decreasing the enthalpy of reaction.

In the evaporation device, at ~175 mbar, since it is crucial to make a compromise between temperature, dehydration time and conversion, it was concluded that using 250°C for 30 minutes is the best option below atmospheric pressure. Using a lower temperature, for the same time as the 300°C experiment, it is possible to obtain a conversion over 90%, even though the conversion is a bit lower (2,7% and 8,3% considering the use of pure BA or generated BA) than at 300°C. The conversion values calculated for pure boric acid or generated boric acid are 96,2% and 90,2%, respectively. Raman spectroscopy confirms the choice of the temperature/time conditions, since "250°C for 30 minutes" and "300°C for 30 minutes" spectra are remarkably similar, with a distinguish band at 808cm⁻¹. So, the lower temperature is preferentially chosen.

In this case, the dehydration time used to obtain the same range of conversion values as in atmospheric pressure is higher, but since the temperature gradient between the muffle and the evaporation device is different, it is not possible to compare. Energy density values are also calculated for pure and generated boric acid, obtaining values of 1800 MJ/m³_{H₃BO₃} and 1688 MJ/m³_{H₃BO₃}. The energy density values are lower than the theoretical values for the same reason as in muffle furnace.

After the dehydration experiments, the other goal of this master thesis was to find out if only boron oxide exists in the dehydration product or if there is boric acid or metaboric acid in the final sample. For that, two different tests were made: a quick rehydration test and a chemical analysis test.

Rehydration tests were made using the dehydration products obtained at the best temperature and time conditions achieved in the muffle furnace and the evaporation device. In all the tests, the temperature at the end of the experiment was higher (maximum temperature of 28,5°C) than at the beginning, because the reaction was exothermic, which means that boron oxide exists in the sample. These tests show that the final appearance of the product does influence the rehydration conversion once better results were obtained with the hard powder:

- $\alpha_{final\ dehydration\ product\ produced\ with\ pure\ BA}^{(250^\circ C, 30\ min)} = 71,4 \pm 3,5\%$;
- $\alpha_{final\ dehydration\ product\ produced\ with\ generated\ BA}^{(250^\circ C, 30\ min)} = 53,5 \pm 4,6\%$

instead of the glassy solid obtained in the muffle:

- $\alpha_{final\ dehydration\ product\ produced\ with\ pure\ BA}^{(250^\circ C, 10\ min)} = 36,8 \pm 6,8\%$;
- $\alpha_{final\ dehydration\ product\ produced\ with\ generated\ BA}^{(250^\circ C, 10\ min)} = 36,5 \pm 6,8\%$.

For this reason, one can conclude that is better to perform the dehydration reaction below atmospheric pressure, mostly because of the final appearance of the product. The product, instead of a glassy solid is a hard powder that is easier to dissolve in water, reason why this is considered the main advantage in working below atmospheric pressure. However, these rehydration conversion values are not very precise, and for more precise results one must follow Joana Reis's experiments and join the discoveries that Joana made in her master thesis with those that were made in this thesis to build the whole TCES system for boric acid/boron oxide reaction.

Final dehydration product was analysed too with a chemical analysis method, as referred before. In this thesis three qualitative/quantitative analysis methods were investigated for boric acid/boron oxide reaction: XRD, NMR and Raman Spectroscopy. Of all the methods tested only with Raman spectroscopy was possible to analyse the final product since the generated boron oxide obtained is in an amorphous, vitreous solid that cannot be dissolved in water or alcohols because it reacts with them, and because boron is a light compound. These facts make the results obtained non-reliable with other techniques. The best samples obtained at and below atmospheric pressure were analysed with this method, verifying the conversion results found in the muffle furnace and in the evaporation device, and consequently, the best conditions selected for each device.

As a final point, the conversions values obtained below or at atmospheric pressure are always above 90% using pure and generated boric acid which means that the fact that the product undergoes a pasty melting state, at atmospheric pressure, does not influence the dehydration conversion, so it is not necessary to avoid it. However, as proved in the rehydration test, the final appearance of the dehydration product influences the reverse reaction, and since for TCES the two reactions must occur with good results, it is concluded that for dehydration purposes "below atmospheric pressure" should be used.

6.2 Future work

For future work, some topics can be suggested: From the results obtained in this thesis a more detailed study, below atmospheric pressure, can be made in a lab-scale reactor, such a reactor with a stirrer or a rotary kiln using a vacuum pump. In fact, during the experiments performed in this master thesis a lab scale rotary kiln was used. However, the reactor was not adapted for TCES conditions, and it must be left for future work. So, the following conditions must be changed in the rotary kiln: The reactor needs a better and more detailed temperature software with at least on more thermocouple to measure the air temperature. A large crucible with the same shape of the reactor with a system to remove it when the time of the reaction stops needs to be incorporated in the reactor (so that the product does not stick to the inside of the reactor and it is possible to measure the final mass) as well as a vacuum pump and a suitable system to exhaust the reaction gases.

Another essential factor to be studied is to understand if the grinding of the glassy boron oxide obtained at atmospheric pressure (for example in a ball mill instead of manually) improve the rehydration conversion values (In this master thesis the grinding of glassy boron oxide was made manually because the amount of product produced was not enough to put in a ball mill).

To finish the suggestions for future work, instead of dehydrating boric acid with heat, try the possibility to perform the dehydration reaction using an acid like sulphuric acid or aluminium oxide.

Annex A

This Annex presents more information about the work developed.

A.1 Enthalpy of reaction at different temperatures

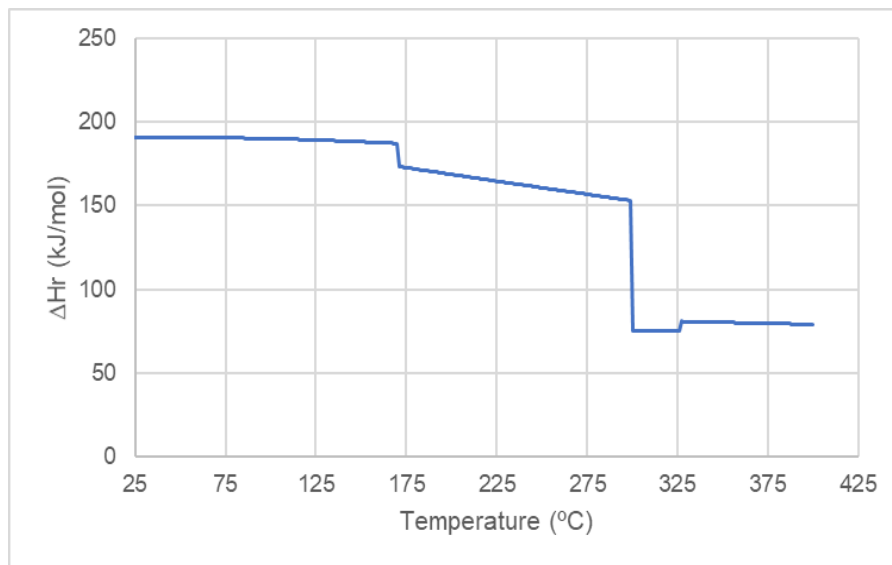


Figure 7.1: Boric acid/boron oxide enthalpy of reaction at atmospheric pressure.

Correction to use in enthalpy of reaction when pressure is below atmospheric pressure

When working below atmospheric pressure, the enthalpy of reaction needs to be corrected because it was calculated at atmospheric pressure. Table 7.1 depicts the enthalpy correction for each temperature needed.

Table 7.1: Enthalpy variation from atmospheric pressure to 175 mbar. [77]

| | h_{H_2O} (kJ/mol) P_{atm} (1013,2 mbar) | h_{H_2O} (kJ/mol) P_{final} (175 mbar) | Δh_{H_2O} (kJ/mol) |
|-------------------------|--|---|----------------------------|
| $T = 225^\circ\text{C}$ | 2925,0 | 2928,5 | 0,063 |
| $T = 250^\circ\text{C}$ | 2974,5 | 2977,2 | 0,048 |
| $T = 300^\circ\text{C}$ | 3074,5 | 3076,6 | 0,039 |

A.2 Propagation of uncertainty

There are two types of errors: systematic or random. Systematic errors are determinable and correctable and can be instrumental errors (calibration) or due to impurities in the compounds whereas the random errors cannot be eliminated but minimised (for example always making measurements with the same operator and the same apparatus).

All calculations performed have an associated error. In this work, the mass of boric acid is weighed in two electronic scales with the readability of 0,1 mg and 10 mg. The scale with the readability of 0,1 mg (type ABJ 220-4M), belongs to the fine class (I) and has an error of 0,1 mg. For the rehydration experiments, a one mL graduated pipette was used with an error of 0,05 mL.

Thus, the value is present in the form of

$$R = Xx \pm dx \quad (7.1)$$

Where Xx is the probable value e dx the uncertainty associated, in this case, with the measuring instrument.

One wants to calculate the error associated with the equation of the conversion (equation 4.2). For this, the following formulas of uncertainty are used.

Table 7.2: Propagation of uncertainty.

| | |
|--|--|
| $z = x \pm y$ | $\Delta Z = \sqrt{[(\Delta x)^2 + (\Delta y)^2]}$ |
| $z = \frac{x}{y}$ | $\Delta z = \left(\frac{\Delta z}{z}\right)^2 = \left(\frac{\Delta x}{x}\right)^2 + \left(\frac{\Delta y}{y}\right)^2$ |
| $z = c \cdot x$ c= constant | $\Delta z = \left \frac{\Delta z}{z}\right = \left \frac{\Delta x}{x}\right $ |
| $z = c \cdot x \cdot y$ c= constant | $\Delta z = \left(\frac{\Delta z}{z}\right)^2 = \left(\frac{\Delta x}{x}\right)^2 + \left(\frac{\Delta y}{y}\right)^2$ |

The error propagation was calculated for the best values of conversion can be found in Table 7.3.

Table 7.3: Dehydration conversion relative error, calculated for the best temperature and time conditions found.

| Muffle furnace | Type of BA used | 160°C, 15 min | 250°C | 350°C |
|--------------------|-----------------|--|--------|---------|
| | | + 180°C, 15 min + 200°C 60 min + 250°C 15 min. | 10 min | 10 min. |
| Relative error [%] | Pure | 0,018 | 0,017 | 0,018 |
| | Generated | 0,018 | 0,018 | 0,017 |

| Evaporation device | Type of BA used | 250°C 30 min | 300°C 30 min | 150°C (30 min) + 300°C (60 min) |
|---------------------------|------------------------|-------------------------|-------------------------|--|
| Relative error [%] | Pure | 0,007 | 0,007 | 0,007 |
| | Generated | 0,007 | 0,007 | 0,007 |

Regarding the relative error of rehydration conversion, the values can be found in Table 7.4.

Table 7.4: Rehydration conversion relative error, calculated for the best temperature and time conditions found.

| Muffle furnace | Type of BA used | 160°C, 15 min + 180°C, 15 min + 200°C 60 min + 250°C 15 min. | 250°C 10 min | 350°C 10 min. |
|-----------------------|------------------------|---|-------------------------|--------------------------|
| Relative error [%] | Pure | 5,49 | 6,78 | 4,93 |
| | Generated | 5,94 | 6,78 | 4,62 |

| Evaporation device | Type of BA used | 250°C 30 min | 300°C 30 min | 150°C (30 min) + 300°C (60 min) |
|---------------------------|------------------------|-------------------------|-------------------------|--|
| Relative error [%] | Pure | 3,52 | 3,44 | 5,49 |
| | Generated | 4,61 | 3,99 | 4,62 |

A.3 Thermogravimetric analysis

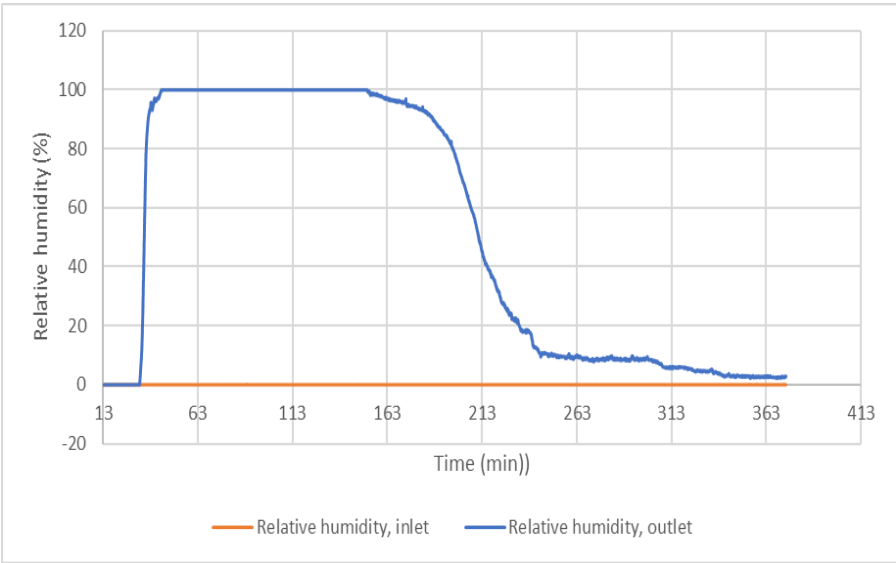


Figure 7.2: Relative humidity at the inlet and outlet over time for experiment 1.

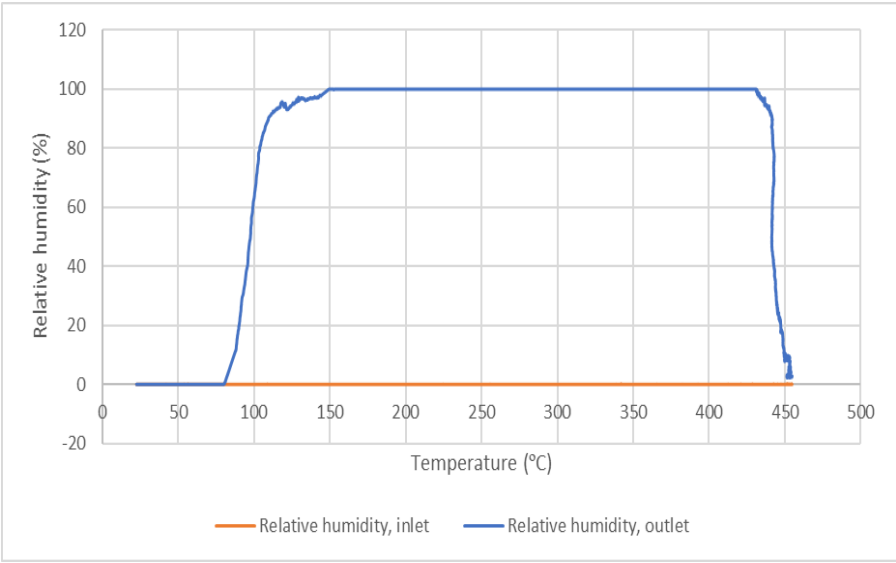


Figure 7.3: Relative humidity at the inlet and outlet over temperature for experiment 1.

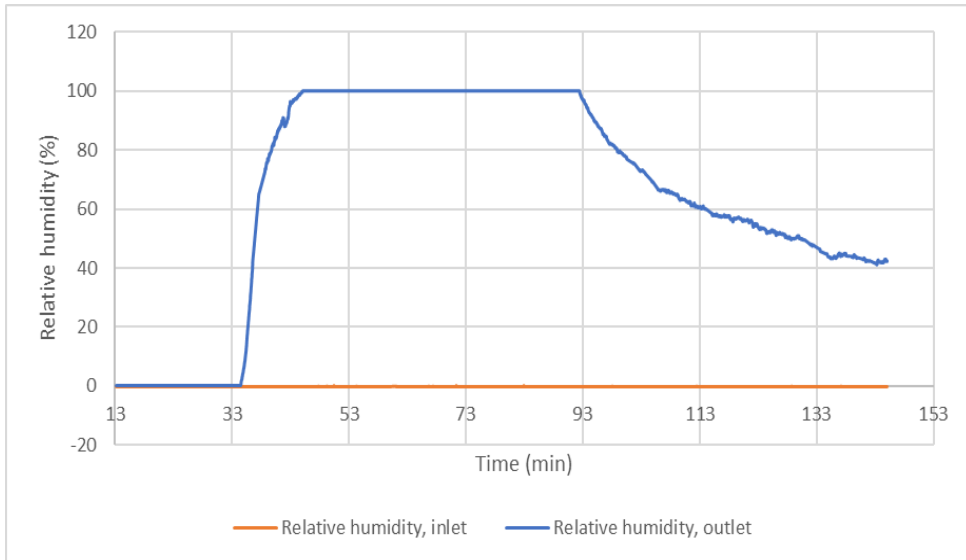


Figure 7.4: Relative humidity at the inlet and outlet over time for experiment 2.

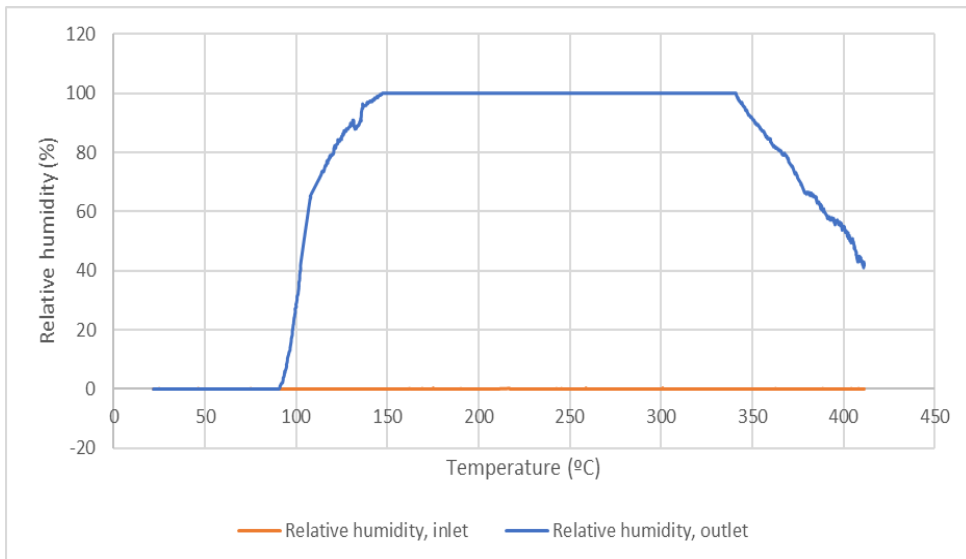


Figure 7.5: Relative humidity at the inlet and outlet over temperature for experiment 2.

A.4 Simultaneous Thermal Analysis

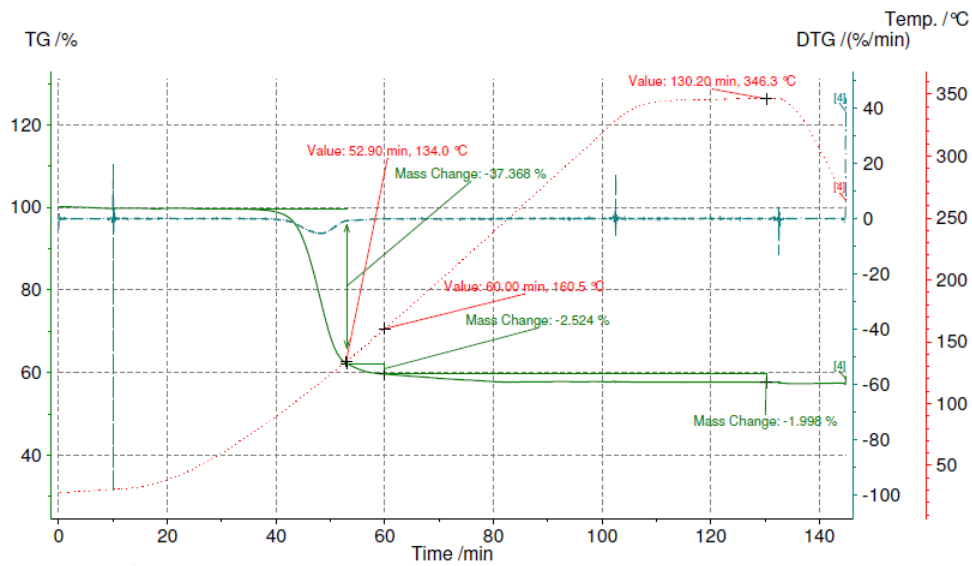


Figure 7.6: TG and DTG for a heating rate of 4 K/min (mass loss of -41,89%).

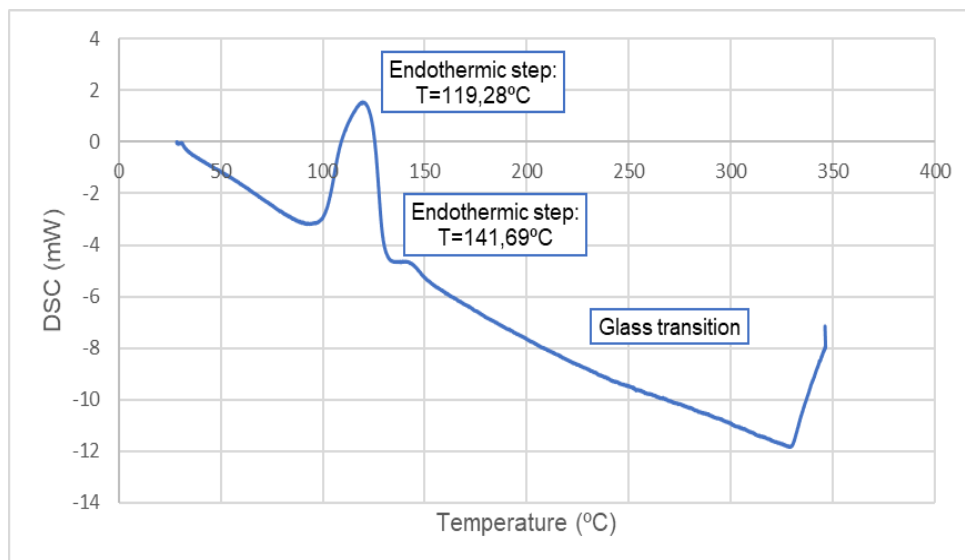


Figure 7.7: DSC signal for a heating rate of 4 K/min.

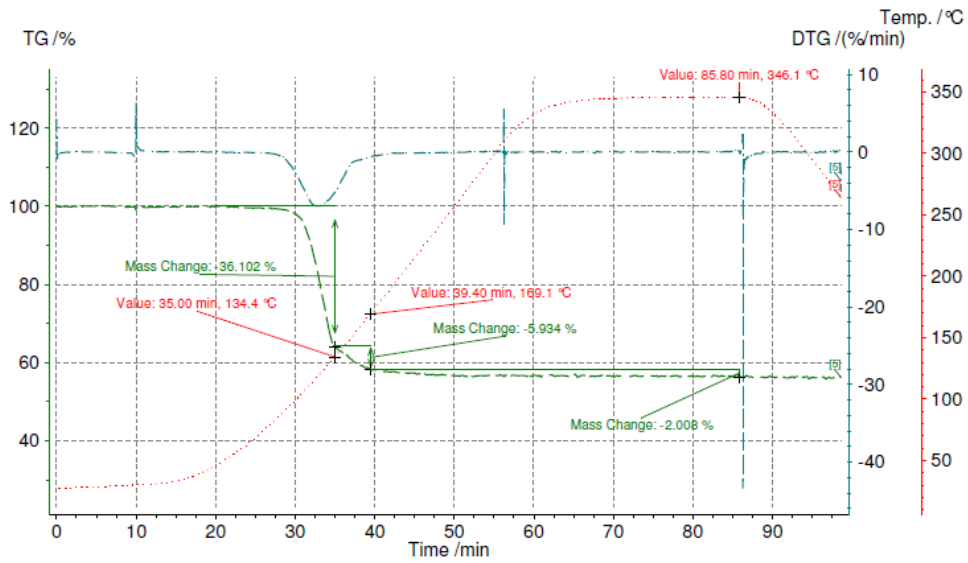


Figure 7.8: TG and DTG for a heating rate of 8K/min (mass loss of -44,04%).

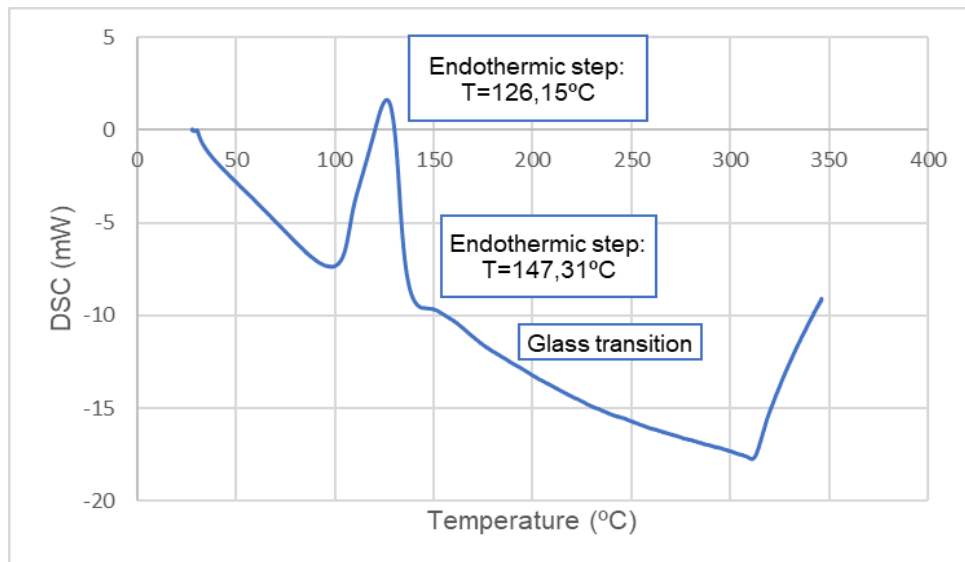


Figure 7.9: DSC signal for a heating rate of 8 K/min.

A.5 Dehydration results

A.5.1 Muffle furnace

Dehydration conversion

Table 7.5 Values to calculate dehydration conversion in experiments of 10 minutes.

| T [°C] | $m_{H_3BO_3\ initial}$ [g] | m_{final} [g] | Δm [g] | W_{H_2O} [g] | Dehydration x [%] |
|----------|----------------------------|-----------------|----------------|----------------|---------------------|
| 160 | 2,0001 | 1,3770 | 0,6231 | 0,8734 | 71,34 |

| | | | | | |
|-----|--------|--------|--------|--------|-------|
| 200 | 2,0004 | 1,3432 | 0,6572 | 0,8735 | 75,23 |
| 230 | 2,0002 | 1,2383 | 0,7619 | 0,8735 | 87,23 |
| 250 | 2,0003 | 1,1785 | 0,8218 | 0,8735 | 94,08 |
| 300 | 2,0021 | 1,1202 | 0,8819 | 0,8743 | 100,9 |
| 350 | 2,0010 | 1,1201 | 0,8809 | 0,8738 | 100,8 |
| 400 | 2,0000 | 1,0910 | 0,9036 | 0,8733 | 103,5 |

Table 7.6: Values to calculate dehydration conversion.

| T [°C] | Time [min] | $m_{H_3BO_3}$ initial [g] | m_{final} [g] | Δm [g] | W_{H_2O} [g] | Dehydration x [%] |
|-----------------|-------------|---------------------------|-----------------|----------------|----------------|---------------------|
| 160 | 30 | 2,0010 | 1,2618 | 0,7392 | 0,8738 | 84,60 |
| 250 | 2 | 2,0003 | 1,6364 | 0,3639 | 0,8735 | 41,66 |
| 250 | 4 | 2,0000 | 1,3661 | 0,6339 | 0,8734 | 72,58 |
| 250 | 6 | 2,0003 | 1,2806 | 0,7197 | 0,8735 | 82,39 |
| 250 | 8 | 2,0004 | 1,2150 | 0,7854 | 0,8735 | 89,91 |
| 250 | 15 | 2,0001 | 1,1844 | 0,8157 | 0,8734 | 93,39 |
| 250 | 20 | 2,0003 | 1,1805 | 0,8198 | 0,8735 | 93,85 |
| 250 | 60 | 2,0009 | 1,1675 | 0,8334 | 0,8738 | 97,31 |
| 250 | 120 | 2,0004 | 1,1504 | 0,8500 | 0,8735 | 97,31 |
| 150+250 | 30+15 | 2,0008 | 1,1721 | 0,8287 | 0,8737 | 94,85 |
| 160+180+200+250 | 15+15+60+15 | 2,0010 | 1,1700 | 0,8310 | 0,8738 | 95,10 |
| 150+250+350 | 60+30+15 | 2,0031 | 1,0966 | 0,9065 | 0,8747 | 103,63 |
| 300 | 40 | 2,0021 | 1,0492 | 0,9529 | 0,8743 | 108,99 |
| 350 | 2 | 2,0000 | 1,1795 | 0,8205 | 0,8734 | 93,94 |
| 350 | 4 | 2,0002 | 1,1015 | 0,8987 | 0,8734 | 102,9 |
| 350 | 6 | 2,0002 | 1,1248 | 0,8754 | 0,8734 | 100,2 |
| 350 | 8 | 2,0010 | 1,1017 | 0,8993 | 0,8738 | 102,9 |
| 350 | 15 | 2,0004 | 1,1228 | 0,8776 | 0,8735 | 100,5 |
| 350 | 20 | 2,0007 | 1,0975 | 0,9032 | 0,8737 | 103,4 |
| 350 | 60 | 2,0003 | 1,0861 | 0,9142 | 0,8735 | 104,7 |
| 350 | 120 | 2,0000 | 1,0870 | 0,9130 | 0,8734 | 104,5 |
| 400 | 2 | 2,0002 | 1,1370 | 0,8632 | 0,8734 | 98,83 |
| 400 | 4 | 2,0000 | 1,0990 | 0,9010 | 0,8734 | 103,2 |
| 400 | 6 | 2,0001 | 1,1004 | 0,8997 | 0,8734 | 103,0 |
| 400 | 8 | 2,0004 | 1,0961 | 0,9043 | 0,8735 | 103,5 |
| 400 | 15 | 2,0007 | 1,0956 | 0,9051 | 0,8737 | 103,6 |
| 400 | 20 | 2,0004 | 1,0922 | 0,9082 | 0,8735 | 104,0 |
| 400 | 60 | 2,0008 | 1,0910 | 0,9098 | 0,8737 | 104,1 |
| 400 | 120 | 2,0003 | 1,0930 | 0,9073 | 0,8735 | 103,9 |

Rehydration conversion

The initial temperature of the water was 23,9°C, and 7 mL of water was used.

Table 7.7: Values to calculate rehydration conversion.

| T [°C] | Time [min] | $m_{"B_2O_3"}$ [g] | ΔT [°C] | α [%] |
|----------|------------|--------------------|-----------------|--------------|
|----------|------------|--------------------|-----------------|--------------|

| | | | | |
|-----------------|-------------|--------|------|------|
| 160 | 10 | 0,2000 | 2,20 | 38,5 |
| 200 | 10 | 0,2000 | 2,60 | 41,4 |
| 230 | 10 | 0,2010 | 1,80 | 31,4 |
| 250 | 2 | 0,2000 | 0,50 | 8,8 |
| 250 | 4 | 0,2000 | 1,80 | 31,5 |
| 250 | 6 | 0,2000 | 2,30 | 40,3 |
| 250 | 8 | 0,2000 | 2,10 | 36,8 |
| 250 | 10 | 0,2000 | 2,10 | 36,8 |
| 250 | 15 | 0,2007 | 3,30 | 57,6 |
| 250 | 20 | 0,2005 | 3,50 | 61,1 |
| 250 | 120 | 0,2017 | 2,80 | 49,0 |
| 150+250 | 30+15 | 0,1900 | 2,60 | 47,9 |
| 160+180+200+250 | 15+15+60+15 | 0,1800 | 2,60 | 50,5 |
| 150+250+350 | 60+30+15 | 0,1800 | 3,10 | 60,3 |
| 300 | 40 | 0,2000 | 3,40 | 56,7 |
| 350 | 2 | 0,2000 | 2,60 | 45,5 |
| 350 | 4 | 0,2000 | 2,60 | 45,5 |
| 350 | 6 | 0,2000 | 3,90 | 68,3 |
| 350 | 8 | 0,2000 | 3,20 | 56,0 |
| 350 | 10 | 0,2000 | 2,90 | 50,8 |

Particle size influence

Table 7.8: Particle size influence on conversion.

| <i>T</i> (°C)=160+180+200+250 | | | | | | | | |
|---|--------|--------|--------|--------|--------|--------|--------|--------|
| <i>Time</i> (min)=15+15+60+15 | | | | | | | | |
| <i>Particle size</i> [mm] | 630 | 400 | 315 | 280 | 160 | 125 | 80 | 50 |
| <i>m</i> _{H₃BO₃} initial [g] | 2,0000 | 2,0004 | 2,0009 | 2,0005 | 2,0009 | 2,0007 | 2,0006 | 2,0007 |
| <i>m</i> _{final} [g] | 1,1718 | 1,1758 | 1,1668 | 1,1619 | 1,1776 | 1,1714 | 1,1638 | 1,1632 |
| Δm [g] | 0,8282 | 0,8246 | 0,8341 | 0,8386 | 0,8233 | 0,8293 | 0,8368 | 0,8375 |
| <i>W</i> _{H₂O} | 0,8734 | 0,8735 | 0,8738 | 0,8736 | 0,8738 | 0,8737 | 0,8736 | 0,8737 |
| <i>x</i> [%] | 94,83 | 94,40 | 95,46 | 96,00 | 94,23 | 94,92 | 95,78 | 95,86 |
| <i>T</i> (°C)= 250 | | | | | | | | |
| <i>Time</i> (min)=10 | | | | | | | | |
| <i>Particle size</i> [mm] | 630 | 400 | 315 | 280 | 160 | 125 | 80 | 50 |
| <i>m</i> _{H₃BO₃} initial [g] | 2,0007 | 2,0005 | 2,0005 | 2,0003 | 2,0000 | 2,0005 | 2,0001 | 2,0006 |
| <i>m</i> _{final} [g] | 1,1695 | 1,1530 | 1,1688 | 1,2061 | 1,2069 | 1,1942 | 1,1904 | 1,2134 |
| Δm [g] | 0,8312 | 0,8475 | 0,8317 | 0,7942 | 0,7931 | 0,8063 | 0,8097 | 0,7872 |
| <i>W</i> _{H₂O} | 0,8737 | 0,8736 | 0,8736 | 0,8735 | 0,8734 | 0,8736 | 0,8734 | 0,8736 |
| <i>x</i> [%] | 95,14 | 97,01 | 95,21 | 90,92 | 90,81 | 92,30 | 92,71 | 90,11 |

A.5.2 Evaporation device

Dehydration Conversion

Table 7.9: Values to calculate dehydration conversion below atmospheric pressure.

| T [°C] | Time [min] | P [mbar] | $m_{H_3BO_3}^{initial}$ [g] | m_{final} [g] | Δm [g] | W_{H_2O} [g] | Dehydration x [%] |
|-------------------------|-------------------|------------|-----------------------------|-----------------|----------------|----------------|---------------------|
| 150 | 30 | 171-174 | 5,00 | 4,00 | 1,00 | 2,18 | 45,80 |
| 200 | 30 | 173-174 | 5,00 | 3,27 | 1,73 | 2,18 | 79,2 |
| 230 | 10 | 172-175 | 5,00 | 4,38 | 0,62 | 2,18 | 28,4 |
| 230 ¹ | 30 | 170 | 4,85 | 3,53 | 1,32 | 2,12 | 62,3 |
| 250 | 10 | 171-174 | 5,00 | 3,54 | 1,46 | 2,18 | 66,9 |
| 250 | 30 | 170-173 | 5,00 | 2,90 | 2,10 | 2,18 | 96,2 |
| 250 | 120 | 170-172 | 5,00 | 2,96 | 2,04 | 2,18 | 93,4 |
| 160+180+200+250 | 15+15+60+15 | 170-176 | 5,00 | 3,41 | 1,59 | 2,18 | 78,3 |
| 150+250 | 30+30 | 170-172 | 5,00 | 3,24 | 1,76 | 2,18 | 80,6 |
| 150+300 | 30+60 | 171-174 | 5,00 | 2,97 | 2,03 | 2,18 | 93,0 |
| 150+300 | 60+60 | 171-172 | 5,00 | 2,92 | 2,08 | 2,18 | 95,3 |
| 300 | 10 | 170-172 | 5,00 | 3,35 | 1,65 | 2,18 | 75,6 |
| 300 | 30 | 170-174 | 5,00 | 2,84 | 2,16 | 2,18 | 98,9 |
| 100+150+180+200+250+300 | 30+30+30+30+15+10 | 170-175 | 5,00 | 3,28 | 1,72 | 2,18 | 78,8 |

¹ I took a sample at 230°C (10 min) to analyse and the rest continuous in the apparatus for more 20 min.

Rehydration Conversion

The rehydration conversion shown in the table below was obtained with 7 mL of water at room temperature (23,9°C).

Table 7.10: Values to calculate rehydration conversion.

| T [°C] | Time [min] | $m_{B_2O_3}$ [g] | ΔT [°C] | α [%] |
|-----------------|-------------|------------------|-----------------|--------------|
| 150 | 30 | 0,2003 | 1,90 | 33,2 |
| 200 | 30 | 0,2000 | 2,90 | 50,8 |
| 230 | 30 | 0,2006 | 2,40 | 41,9 |
| 250 | 10 | 0,2000 | 2,40 | 42,0 |
| 250 | 30 | 0,2010 | 4,10 | 71,4 |
| 250 | 120 | 0,2010 | 3,70 | 64,4 |
| 160+180+200+250 | 15+15+60+15 | 0,2006 | 3,20 | 55,8 |

| | | | | |
|-------------------------|-------------------|--------|------|------|
| 150+250 | 30+30 | 0,2003 | 4,00 | 69,9 |
| 150+300 | 30+60 | 0,2010 | 2,60 | 45,3 |
| 150+300 | 60+60 | 0,2003 | 3,90 | 68,2 |
| 300 | 10 | 0,2020 | 3,20 | 55,5 |
| 300 | 30 | 0,2011 | 4,20 | 73,1 |
| 100+150+180+200+250+300 | 30+30+30+30+15+10 | 0,2020 | 4,10 | 71,1 |

Particle size influence (P between 170 and 180mbar)

Table 7.11: Particle size influence in evaporation device.

| | | $T [^{\circ}\text{C}]=250^{\circ}\text{C}$ | | | | | | | |
|---|--|--|-------|-------|-------|-------|-------|-------|-------|
| | | $\text{Time [min]}=30$ | | | | | | | |
| Particle size [mm] | | 630 | 400 | 315 | 280 | 160 | 125 | 80 | 50 |
| $m_{\text{H}_3\text{BO}_3 \text{ initial [g]}}$ | | 4,96 | 5,00 | 5,01 | 5,03 | 5,00 | 5,00 | 5,00 | 5,00 |
| $m_{\text{final [g]}}$ | | 2,84 | 3,1 | 2,95 | 2,89 | 2,92 | 2,87 | 2,97 | 3,15 |
| $\Delta m [g]$ | | 2,12 | 1,9 | 2,06 | 2,14 | 2,08 | 2,13 | 2,03 | 1,85 |
| $W_{\text{H}_2\text{O}}$ | | 2,17 | 2,18 | 2,19 | 2,20 | 2,18 | 2,18 | 2,18 | 2,18 |
| $x[\%]$ | | 97,88 | 87,02 | 94,16 | 97,43 | 95,26 | 97,55 | 92,97 | 84,73 |
| | | $T [^{\circ}\text{C}]=300^{\circ}\text{C}$ | | | | | | | |
| | | $\text{Time [min]}=30$ | | | | | | | |
| Particle size [mm] | | 630 | 400 | 315 | 280 | 160 | 125 | 80 | 50 |
| $m_{\text{H}_3\text{BO}_3 \text{ initial [g]}}$ | | 5,00 | 5,00 | 5,00 | 5,00 | 5,00 | 5,01 | 5,00 | 5,01 |
| $m_{\text{final [g]}}$ | | 2,84 | 2,82 | 2,89 | 2,95 | 2,85 | 2,85 | 2,85 | 2,92 |
| $\Delta m [g]$ | | 2,16 | 2,18 | 2,11 | 2,05 | 2,15 | 2,16 | 2,15 | 2,09 |
| $W_{\text{H}_2\text{O}}$ | | 2,18 | 2,18 | 2,18 | 2,18 | 2,18 | 2,19 | 2,18 | 2,18 |
| $x[\%]$ | | 98,93 | 99,84 | 96,64 | 93,89 | 98,47 | 98,73 | 98,47 | 95,53 |

A.6 Particle size influence

To understand how the boric acid particle size can influence the conversion rate, some tests with different particle ranges were done. First, boric acid from Carl Roth was sieved for 2 hours, using the sieve shaker with 9 sieve trays, from RETSCH company at 30 rpm.

The particle size ranges which have been tested are:

- 630 mm
- 630-400 mm
- 400-315 mm
- 315-280 mm
- 280-160 mm
- 160-125 mm
- 125-80 mm
- 80-50 mm

- 50-0 mm

The mass fraction retained in each sieve is calculated with equation

$$\text{Mass fraction retained} = \frac{W_i \text{ [mm]}}{W_{\text{total}} \text{ [mm]}} \quad (7.2)$$

- W_i - Weight of a sieve tray i after sieving analysis;
- W_{total} - Total weight of all sieves trays after sieving analysis.

Figure 7.10 shows the differential granulometric composition curve, where the sieve equivalent diameter is the average of mesh sizes.

$$\text{Sieve equivalent diameter}_{\text{[mm]}} = \frac{\text{mesh size}_i \text{ [mm]} + \text{mesh size}_{i+1} \text{ [mm]}}{2} \quad (7.3)$$

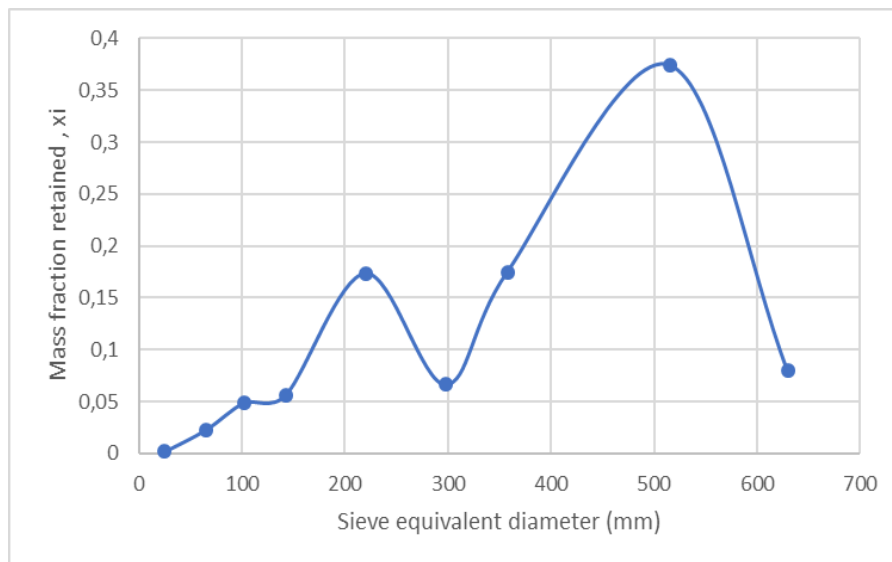


Figure 7.10: Differential granulometric composition curve.

References

- [1] "U.S. Energy Information Administration." [Online]. Available: <https://www.eia.gov/beta/international/data/browser/#/?c=4100000020000600000000000000g000200000000000000001&vs=-----INTL.44-2-WORLD-QBTU.A&vo=0&v=C&end=2015>. [Accessed: 15-Oct-2017].
- [2] Enerdata, "Global energy statistical yearbook." [Online]. Available: <https://yearbook.enerdata.net/total-energy/world-consumption-statistics.html>. [Accessed: 08-Nov-2017].
- [3] T. Yan, R. Z. Wang, T. X. Li, L. W. Wang, and I. T. Fred, "A review of promising candidate reactions for chemical heat storage," *Renew. Sustain. Energy Rev.*, vol. 43, no. November, pp. 13–31, 2015.
- [4] P. Pardo, A. Deydier, Z. Anxionnaz-Minvielle, S. Rougé, M. Cabassud, and P. Cognet, "A review on high-temperature thermochemical heat energy storage," *Renew. Sustain. Energy Rev.*, vol. 32, pp. 591–610, 2014.
- [5] J. Yan and C. Y. Zhao, "Thermodynamic and kinetic study of the dehydration process of CaO/Ca(OH)₂ thermochemical heat storage system with Li doping," *Chem. Eng. Sci.*, vol. 138, pp. 86–92, 2015.
- [6] D. Aydin, S. P. Casey, and S. Riffat, "The latest advancements on thermochemical heat storage systems," *Renew. Sustain. Energy Rev.*, vol. 41, pp. 356–367, 2015.
- [7] A. Abedin and M. Rosen, "A Critical Review of Thermochemical Energy Storage Systems.," *Open Renew. Energy J.*, vol. 4, pp. 42–46, 2011.
- [8] G. Li, "Sensible heat thermal storage energy and exergy performance evaluations," *Renew. Sustain. Energy Rev.*, vol. 53, pp. 897–923, 2016.
- [9] A. Solé, I. Martorell, and L. F. Cabeza, "State of the art on gas-solid thermochemical energy storage systems and reactors for building applications," *Renew. Sustain. Energy Rev.*, vol. 47, pp. 386–398, 2016.
- [10] T. M. Letcher, *Storing energy - with special reference to renewable energy sources*, 2016th ed. Elsevier, 2013.
- [11] N. Pflieger, T. Bauer, C. Martin, M. Eck, and A. Wörner, "Thermal energy storage – overview and specific insight into nitrate salts for sensible and latent heat storage," pp. 1487–1497, 2015.
- [12] G. Li, "Sensible heat thermal storage energy and exergy performance evaluations," *Renew.*

- Sustain. Energy Rev.*, vol. 53, pp. 897–923, 2016.
- [13] M. Deutsch, “A systematic approach to identify new thermochemical energy storage systems,” PhD thesis, TU Wien, 2017.
- [14] Global CCS Institute, “Latent heat storage.” [Online]. Available: <https://hub.globalccsinstitute.com/publications/strategic-research-priorities-cross-cutting-technology/33-latent-heat-storage>.
- [15] J. Cot-Gores, A. Castell, and L. F. Cabeza, “Thermochemical energy storage and conversion: A state-of-the-art review of the experimental research under practical conditions,” *Renew. Sustain. Energy Rev.*, vol. 16, no. 7, pp. 5207–5224, 2012.
- [16] Z. H. Pan and C. Y. Zhao, “Gas–solid thermochemical heat storage reactors for high-temperature applications,” Elsevier Ltd, 2017.
- [17] A. Werner, F. Winter, C. Jordan, M. Deutsch, T. Karel, and H. Sieberth, “Technology offer Boric Acid,” 2015, p. 1.
- [18] G. Vettermark, “Thermochemical Energy Storage,” in *Energy Storage Systems*, B. Killas; S. Kakaç, Ed. 1989, pp. 673–674.
- [19] T. Karel, “Development of an innovative process for thermochemical energy storage on the basis of boric acid / boron oxide,” MSc thesis, TU Wien, 2015.
- [20] S. Kiyabu, J. S. Lowe, A. Ahmed, and D. J. Siegel, “Computational Screening of Hydration Reactions for Thermal Energy Storage,” *Chem. Mater.*, pp. 2006–2017, 2018.
- [21] M. Deutsch, C. Aumeyr, P. Weinberger, and F. Winter, “Kinetic analysis of the decomposition of H_3BO_3 and $FeSO_4 \cdot 7H_2O$ for thermochemical energy storage.”
- [22] Y. A. Criado, A. Huille, S. Rougé, and J. C. Abanades, “Experimental investigation and model validation of a $CaO/Ca(OH)_2$ fluidized bed reactor for thermochemical energy storage applications,” *Chem. Eng. J.*, vol. 313, pp. 1194–1205, 2014.
- [23] E. Alonso, C. Pérez-Rábago, J. Licurgo, A. Gallo, E. Fuentealba, and C. A. Estrada, “Experimental aspects of CuO reduction in solar-driven reactors: Comparative performance of a rotary kiln and a packed-bed,” *Renew. Energy*, vol. 105, pp. 665–673, 2017.
- [24] K. Hashemi, “Investigation of the reaction of boron oxide with liquid water for thermochemical energy storage,” MSc thesis, TU Wien, 2016.
- [25] S. Christian and W. Antje, “Thermochemical Energy Storage Systems,” *Storing Energy*, no. January, pp. 345–372, 2010.
- [26] F. Schaube, A. Wörner, and R. Tamme, “High Temperature Thermochemical Heat Storage for Concentrated Solar Power Using Gas–Solid Reactions,” *J. Sol. Energy Eng.*, vol. 133, no. 3, p. 31006, 2011.
- [27] K. Wagner and M. Nr, “Analysing the hydration reaction of boron oxide in selected solvents by,”

MSc Thesis, TU Wien, 2016.

- [28] A. Roine, "HSC Chemistry 6." Outotec Research oy Antti Roine, 2007.
- [29] B. E. Poling, M. Prausnitz, and J. P. O'Connell, *The properties of gases and loquids*, 5th ed., vol. 23, no. 3. 2006.
- [30] J. O. Maloney, *Perry's Chemical Engineers Handbook*, 8 edition. 2007.
- [31] P. Patnaik, *Handbook of Inorganic Chemicals*. 2003.
- [32] S. Balci, N. A. Sezgi, and E. Eren, "Boron oxide production kinetics using boric acid as raw material," *Ind. Eng. Chem. Res.*, vol. 51, no. 34, pp. 11091–11096, 2012.
- [33] S. Aghili, M. Panjepour, and M. Meratian, "Kinetic analysis of formation of boron trioxide from thermal decomposition of boric acid under non-isothermal conditions," *J. Therm. Anal. Calorim.*, vol. 131, no. 3, pp. 2443–2455, 2018.
- [34] F. C. Kracek, G. W. Morey, and H. E. Merwin, "The System Water-Boron Oxide," *Am. J. Sci.*, vol. A 35, pp. 143–171, 1938.
- [35] S. Kocakuşak *et al.*, "Production of anhydrous, crystalline boron oxide in fluidized bed reactor," *Chem. Eng. Process. Process Intensif.*, vol. 35, no. 4, pp. 311–317, 1996.
- [36] F. Sevim, F. Demir, M. Bilen, and H. Okur, "Kinetic analysis of thermal decomposition of boric acid from thermogravimetric data," *Korean J. Chem. Eng.*, vol. 23, no. 5, pp. 736–740, 2006.
- [37] G. Brauer, *Handbook of preparative inorganic chemistry*. 1963.
- [38] W. H. Zachariasen, "The crystal structure of monoclinic metaboric acid," *Acta Crystallogr.*, vol. 16, no. 5, pp. 385–389, 1963.
- [39] D. Schubert, *Boron Oxides, Boric Acid, and Borates: Kirk-Othmer Encyclopedia of Chemical Technology*. 2011.
- [40] A. Rotaru, "Thermal and kinetic study of hexagonal boric acid versus triclinic boric acid in air flow," *J. Therm. Anal. Calorim.*, vol. 127, no. 1, pp. 755–763, 2017.
- [41] J. W. Anthony, R. A. Bideaux, K. W. Bladh, and M. C. Nichols, "Sassolite," in *Handbook of mineralogy*, vol. 5, no. 4, Mineral Data publishing, Ed. .
- [42] PubChem, "PubChem Boric acid." [Online]. Available: https://pubchem.ncbi.nlm.nih.gov/compound/boric_acid#section=Experimental-Properties. [Accessed: 03-Nov-2017].
- [43] Mollard;Paul, "Fluidized bed process for obtaining granulated boric oxide," 1971.
- [44] A. Harabor, P. Rotaru, R. I. Scorei, and N. A. Harabor, "Non-conventional hexagonal structure for boric acid," *J. Therm. Anal. Calorim.*, vol. 118, no. 2, pp. 1375–1384, 2014.
- [45] ROTH, "Safety data sheet of boric acid," no. 1. ROTH, 2016.
- [46] Carl Roth, "SAFETY DATA SHEET CARL ROTH," 2014.

- [47] PubChem, "PubChem Boron Oxide," 2005, 2005. [Online]. Available: https://pubchem.ncbi.nlm.nih.gov/compound/Boric_oxide#section=Formulations-Preparations. [Accessed: 03-Nov-2017].
- [48] Royal Society of Chemistry, "The Merck Index online." [Online]. Available: <https://www.rsc.org/merck-index>. [Accessed: 20-Nov-2017].
- [49] J. Michael, E. Nygren, J. F. Hays, and D. Turnbull, "Crystal Growth Kinetics of Boron Oxide Under Pressure," Massachusetts, 1984.
- [50] K. P. Crapse and E. A. Kyser, "Literature Review of Boric Acid Solubility Data," *Srnl*, vol. 578, no. 1, pp. 1–26, 2011.
- [51] ETIMADEN, "Safety data sheet boron oxide," 2016.
- [52] 20 mule team borax, "Boric Oxide," 2014. [Online]. Available: <https://www.borax.com/wp-content/uploads/2016/07/pds-borates-boricoxide-us.pdf>.
- [53] Alfa Aesar, "Safety Data Sheet Boron Oxide." pp. 2–5, 2016.
- [54] A. Vasconi and P. Mazzinghi, "Boron oxide preparation method," 1990.
- [55] A. Gallo, M. I. Roldán, E. Alonso, and E. Fuentealba, "Considerations for using a rotary kiln for high temperature industrial processes with and without thermal storage," *ISES EuroSun Conf.*, no. October, 2016.
- [56] A. Meier, E. Bonaldi, G. M. Cella, W. Lipinski, D. Wuillemin, and R. Palumbo, "Design and experimental investigation of a horizontal rotary reactor for the solar thermal production of lime," *Energy*, vol. 29, no. 5–6, pp. 811–821, 2004.
- [57] D. Kunii and O. Levenspiel, *Fluidization Engineering*. 2013.
- [58] C. Schlägner, "Diplomarbeit Aufbau einer Makro-Thermowaage zur Untersuchung von Diplom-Ingenieurs Diplomarbeit," MSc thesis, TU Wien, 2018.
- [59] "Buoyancy effect of TGA experiment." [Online]. Available: <https://www.cementscience.com/2013/04/buoyancy-effect-of-tga-experiment.html>. [Accessed: 25-Feb-2018].
- [60] Thermal Analysis & Surface Solutions, "Buoyancy Phenomenon in TGA Systems." [Online]. Available: http://www.thass.org/DOWN/applications/TGA_Applications/pdfthass/chn206_Buoancy.pdf. [Accessed: 25-Feb-2018].
- [61] V.-G. V. und Chemieingenieurwesen, *VDI Heat Atlas*, 2nd ed. 2010.
- [62] S. Vyazovkin *et al.*, "ICTAC Kinetics Committee recommendations for collecting experimental thermal analysis data for kinetic computations," *Thermochim. Acta*, vol. 590, pp. 1–23, 2014.
- [63] "Linseis Thermal analysis." [Online]. Available: <https://www.linseis.com/en/our-products/simultaneous-thermogravimetry/>. [Accessed: 15-Mar-2018].
- [64] "cmfurnaces." [Online]. Available: <https://cmfurnaces.com/muffle-furnaces/>. [Accessed: 01-Dec-

- 2017].
- [65] "Nabertherm." [Online]. Available: <http://www.nabertherm.com/produkte/labor/en>. [Accessed: 02-Dec-2017].
- [66] A. Khawam, "Application of solid-state kinetics to desolvation reactions," PhD Thesis, University of Iowa, 2007.
- [67] J. Reis, "Hydration of boron oxide for thermochemical energy storage," MSc Thesis, TU Wien, 2018.
- [68] H. Willar, L. Merrit Jr, and J. Dean, "Análise Instrumental," in *Análise instrumental*, Fundação Caloust Gulbenkian, Ed. Lisboa.
- [69] B. Borie, "X-Ray Diffraction in Crystals, Imperfect Crystals, and Amorphous Bodies," *Journal of the American Chemical Society*, vol. 87, no. 1. pp. 140–141, 1965.
- [70] "NMR." [Online]. Available: <https://www2.chemistry.msu.edu/faculty/reusch/virttxtjml/spectrpy/nmr/nmr1.htm>. [Accessed: 10-Oct-2017].
- [71] "NMR." [Online]. Available: <http://chem.ch.huji.ac.il/nmr/whatisnmr/whatisnmr.html>. [Accessed: 12-Oct-2017].
- [72] D. A. Skoog, F. J. Holler, and S. R. Crouch, *Principles of Instrumental Analysis, 5th edition*. .
- [73] "Princeton Instruments- General Raman." [Online]. Available: <https://www.princetoninstruments.com/applications/raman-gen>. [Accessed: 29-Jan-2018].
- [74] B. N. Meera and J. Ramakrishna, "Raman spectral studies of borate glasses," *J. Non. Cryst. Solids*, vol. 159, pp. 1–21, 1993.
- [75] Z. Xing-Le Ding, a, b Yong-Ning Zhou, b Yin Yang, b Qian Sun, b Fang Lu, a and Zheng-Wen Fub, "Electrochemical Mechanism of Amorphous Boron Oxide Thin Film with Lithium," in *Electrochem. Solid-State Lett.* 2011 14(12): A177-A179;, 2011.
- [76] K. Krishnan, "Section A: The Raman spectrum of boric acid," in *Proceedings of the Indian Academy of Sciences* -, vol. 57, 1963, pp. 103–108.
- [77] G. de Azevedo and Edmundo, "Tabelas de Vapor," in *Termodinâmica Aplicada*, Lisbon: Escolar Editora, 2011.